

A BLOCK COORDINATE DESCENT METHOD FOR NONSMOOTH COMPOSITE OPTIMIZATION UNDER ORTHOGONALITY CONSTRAINTS

006 **Anonymous authors**

007 Paper under double-blind review

ABSTRACT

010 Nonsmooth composite optimization with orthogonality constraints has a wide
 011 range of applications in statistical learning and data science. However, this prob-
 012 lem is challenging due to its nonsmooth objective and computationally expensive,
 013 non-convex constraints. In this paper, we propose a new approach called **OBCD**,
 014 which leverages Block Coordinate Descent to address these challenges. **OBCD**
 015 is a feasible method with a small computational footprint. In each iteration, it
 016 updates k rows of the solution matrix, where $k \geq 2$, by globally solving a small
 017 nonsmooth optimization problem under orthogonality constraints. We prove that
 018 the limiting points of **OBCD**, referred to as (global) block- k stationary points, of-
 019 fer stronger optimality than standard critical points. Furthermore, we show that
 020 **OBCD** converges to ϵ -block- k stationary points with an iteration complexity of
 021 $\mathcal{O}(1/\epsilon)$. Additionally, under the Kurdyka-Łojasiewicz (KL) inequality, we estab-
 022 lish the non-ergodic convergence rate of **OBCD**. We also demonstrate how novel
 023 breakpoint search methods can be used to solve the subproblem in **OBCD**. Em-
 024 pirical results show that our approach consistently outperforms existing methods.

1 INTRODUCTION

We consider the following nonsmooth composite optimization problem under orthogonality constraints (' \triangleq ' means define):

$$\min_{\mathbf{X} \in \mathbb{R}^{n \times r}} F(\mathbf{X}) \triangleq f(\mathbf{X}) + h(\mathbf{X}), \text{ s.t. } \mathbf{X}^\top \mathbf{X} = \mathbf{I}_r. \quad (1)$$

Here, $n \geq r$, $n \geq 2$, and \mathbf{I}_r is a $r \times r$ identity matrix. We do not assume convexity of $f(\mathbf{X})$ and $h(\mathbf{X})$. For brevity, the orthogonality constraints $\mathbf{X}^\top \mathbf{X} = \mathbf{I}_r$ in Problem (1) is rewritten as $\mathbf{X} \in \text{St}(n, r) \triangleq \{\mathbf{X} \in \mathbb{R}^{n \times r} \mid \mathbf{X}^\top \mathbf{X} = \mathbf{I}_r\}$, where $\mathcal{M} \triangleq \text{St}(n, r)$ is the Stiefel manifold in the literature (Edelman et al., 1998; Absil et al., 2008; Wen & Yin, 2013; Hu et al., 2020). We impose the following assumptions on Problem (1) throughout this paper. (Asm-i) For any \mathbf{X} and \mathbf{X}^+ , where \mathbf{X} and \mathbf{X}^+ only differ at most by k rows with $k \geq 2$, we assume $f : \mathbb{R}^{n \times r} \mapsto \mathbb{R}$ is differentiable and \mathbf{H} -smooth with $\mathbf{H} \in \mathbb{R}^{nr \times nr}$ such that:

$$f(\mathbf{X}^+) \leq \mathcal{Q}(\mathbf{X}^+; \mathbf{X}) \triangleq f(\mathbf{X}) + \langle \mathbf{X}^+ - \mathbf{X}, \nabla f(\mathbf{X}) \rangle + \frac{1}{2} \|\mathbf{X}^+ - \mathbf{X}\|_{\mathbf{H}}^2, \quad (2)$$

where $\|\mathbf{H}\|_{\text{sp}} \leq L_f$ for some constant $L_f > 0$ and $\|\mathbf{X}\|_{\mathbf{H}}^2 \triangleq \text{vec}(\mathbf{X})^\top \mathbf{H} \text{vec}(\mathbf{X})$ ¹. Here, $\|\mathbf{H}\|_{\text{sp}}$ is the spectral norm of \mathbf{H} . Notably, when $\mathbf{H} = L_f \cdot \mathbf{I}_{nr}$, this condition simplifies to the standard L_f -smoothness (Nesterov, 2003). (Asm-ii) The function $h(\mathbf{X}) : \mathbb{R}^{n \times r} \mapsto \mathbb{R}$ is proper, lower semicontinuous, and potentially non-smooth. Additionally, it is coordinate-wise separable, such that $h(\mathbf{X}) = \sum_{i,j} h(\mathbf{X}_{ij})$. Typical examples of $h(\mathbf{X})$ include the ℓ_p norm $h(\mathbf{X}) = \|\mathbf{X}\|_p$ with $p \in \{0, 1\}$, the capped- ℓ_1 function $h(\mathbf{X}) = \sum_{i,j} \max(|\mathbf{X}_{ij}|, \tau)$ with $\tau > 0$, and the indicator function for non-negativity constraints $h(\mathbf{X}) = \iota_{\geq 0}(\mathbf{X})$. (Asm-iii) The following small-sized subproblem can be solved exactly and efficiently:

$$\min_{\mathbf{V} \in \text{St}(k, k)} \mathcal{P}(\mathbf{V}) \triangleq \frac{1}{2} \|\mathbf{V}\|_{\tilde{\mathbf{Q}}}^2 + \langle \mathbf{V}, \mathbf{P} \rangle + h(\mathbf{VZ}) \quad (3)$$

for any given $\mathbf{Z} \in \mathbb{R}^{k \times r}$, $\mathbf{P} \in \mathbb{R}^{k \times k}$, and $\tilde{\mathbf{Q}} \in \mathbb{R}^{k^2 \times k^2}$. Here, we employ a notational simplification by defining $h(\mathbf{VZ}) \triangleq \sum_{i,j} h([\mathbf{VZ}]_{ij})$, given the coordinate-wise separability of $h(\cdot)$. This assumption is analogous to the "prox-friendly" condition in (variable-metric) proximal gradient methods

¹Consider $f(\mathbf{X}) = \frac{1}{2} \text{tr}(\mathbf{X}^\top \mathbf{C} \mathbf{X}) = \frac{1}{2} \|\mathbf{X}\|_{\mathbf{H}}^2$, where $\mathbf{H} = \mathbf{C} \otimes \mathbf{I}_r$, and $\mathbf{C} \in \mathbb{R}^{n \times n}$, $\mathbf{D} \in \mathbb{R}^{r \times r}$ are symmetric. Clearly, $f(\mathbf{X})$ satisfies (2) with equality, i.e., $f(\mathbf{X}^+) = \mathcal{Q}(\mathbf{X}^+; \mathbf{X})$ for all \mathbf{X} and \mathbf{X}^+ .

(Beck & Teboulle, 2009; Raguet et al., 2013), but instead of a standard proximal operator for a single nonsmooth term in the full space, our subproblem jointly handles two nonsmooth components (the function $h(\cdot)$ and the orthogonality constraint) in a low-dimensional $k \times k$ space.

Problem (1) is an optimization framework that plays a crucial role in a variety of statistical learning and data science models, such as sparse Principal Component Analysis (PCA) (Journée et al., 2010; Shalit & Chechik, 2014), nonnegative PCA (Zass & Shashua, 2006; Qian et al., 2021), deep neural networks (Cogswell et al., 2016; Cho & Lee, 2017; Xie et al., 2017; Bansal et al., 2018; Massart & Abrol, 2022; Huang & Gao, 2023), electronic structure calculation (Zhang et al., 2014; Liu et al., 2014), Fourier transforms approximation (Frerix & Bruna, 2019), phase synchronization (Liu et al., 2017), orthogonal nonnegative matrix factorization (Jiang et al., 2022), K -indicators clustering (Jiang et al., 2016), and dictionary learning (Zhai et al., 2020).

1.1 MOTIVATING APPLICATIONS

Many machine learning and data science models can be cast as instances of Problem (1). Below, we present two representative examples: L_0 -regularized sparse PCA and L_1 -regularized sparse PCA. An additional example on nonnegative PCA is provided in Appendix Section G.1.

► **L_0 -Regularized Sparse PCA.** L_0 -regularized Sparse PCA (SPCA) is a method that uses ℓ_0 norm to produce modified principal components with sparse loadings, which helps reduce model complexity and increase model interpretability (d'Aspremont et al., 2008; Chen et al., 2016). It can be formulated as: $\min_{\mathbf{X} \in \text{St}(n,r)} -\langle \mathbf{X}, \mathbf{C}\mathbf{X} \rangle + \lambda \|\mathbf{X}\|_0$, where $\mathbf{C} = \mathbf{A}^\top \mathbf{A} \in \mathbb{R}^{n \times n}$ is the covariance of the data matrix $\mathbf{A} \in \mathbb{R}^{m \times n}$ and $\lambda > 0$.

► **L_1 -Regularized Sparse PCA.** As the L_1 norm provides the tightest convex relaxation for the L_0 -norm over the unit ball in the sense of L_∞ -norm, some researchers replace the non-convex and discontinuous L_0 norm function with a convex but non-smooth function (Chen et al., 2016; Vu et al., 2013; Lu & Zhang, 2012). This leads to the following optimization problem of L_1 -regularized SPCA: $\min_{\mathbf{X} \in \text{St}(n,r)} -\langle \mathbf{X}, \mathbf{C}\mathbf{X} \rangle + \lambda \|\mathbf{X}\|_1$, where $\mathbf{C} \in \mathbb{R}^{n \times n}$ is the covariance matrix of the data, and $\lambda > 0$.

1.2 RELATED WORK

We now present some related algorithms in the literature.

► **Minimizing Smooth Functions under Orthogonality Constraints.** One of the main challenges in solving Problem (1) stems from the nonconvexity of the orthogonality constraints. Existing approaches for addressing this difficulty can be broadly grouped into four classes: (i) Geodesic-like methods (Abrudan et al., 2008; Edelman et al., 1998; Absil et al., 2008). Computing exact geodesics typically involves solving ordinary differential equations, which can be computationally expensive. To avoid this, geodesic-like methods approximate the geodesic path by computing the geodesic logarithm using simpler linear algebraic operations. (ii) Projection-like methods (Absil et al., 2008; Golub & Van Loan, 2013; Jiang & Dai, 2015). These include techniques such as projection onto the nearest orthogonal matrix, polar decomposition, and QR-based projection. At each iteration, these methods descend along the Euclidean or Riemannian gradient direction and subsequently apply a projection step to enforce orthogonality. (iii) Multiplier correction methods (Gao et al., 2018; 2019; Xiao et al., 2022). These methods exploit the fact that the Lagrange multiplier associated with the orthogonality constraint is symmetric and admits a closed-form expression at first-order stationarity. They update the multiplier after achieving sufficient decrease in the objective, resulting in efficient feasible or infeasible first-order methods. (iv) Landing methods (Ablin & Peyré, 2022; Vary et al.; Ablin et al., 2024). These methods avoid explicit retractions by working in the ambient Euclidean space while adding a penalty that attracts iterates toward the orthogonal manifold. Each update combines a descent direction for the objective with a corrective term that reduces constraint violation, and, with appropriate step sizes, the iterates converge to points that are nearly orthogonal and nearly stationary for the original problem.

► **Minimizing Nonsmooth Functions under Orthogonality Constraints.** Another major challenge in solving Problem (1) arises from the nonsmoothness of the objective function. Existing approaches for handling this issue can be broadly categorized into four classes: (i) Subgradient methods (Hwang et al., 2015; Li et al., 2021; Cheung et al., 2024). These methods generalize gradient descent to nonsmooth settings. Many of the previously mentioned geodesic-like and projection-based strategies can be incorporated into subgradient frameworks on manifolds. (ii) Proximal gradient methods (Chen et al., 2020; Li et al., 2024b; Lyu & Li, 2025). These methods compute a descent direction by solving a strongly convex subproblem over the tangent space, often using a semi-smooth Newton method.

108 The resulting point is then mapped back onto the manifold via a retraction to preserve orthogonality.
 109 **(iii)** Block Majorization Minimization (BMM) on Riemannian manifolds (Li et al., 2024b; 2023;
 110 Breloy et al., 2021; Gutman & Ho-Nguyen, 2023). This class of methods iteratively constructs a
 111 tangential majorizing surrogate for a block of the objective, takes an approximate descent step in
 112 the corresponding tangent space, and retracts the iterate back to the manifold. **(iv)** Operator splitting
 113 methods (Lai & Osher, 2014; Chen et al., 2016; Zhang et al., 2019). These methods reformulate
 114 the original problem by introducing auxiliary variables and linear constraints, decomposing it into
 115 simpler subproblems that can be solved separately and often exactly. Prominent examples include
 116 the Alternating Direction Method of Multipliers (ADMM) (He & Yuan, 2012), Riemannian ADMM
 117 (RADMM) (Li et al., 2024a), and Penalty-based Splitting Method (PSM) (Yuan, 2024; Chen, 2012).

118 **► Block Coordinate Descent Methods.** (Block) coordinate descent is a classical and powerful
 119 algorithm that solves optimization problems by iteratively performing minimization along (block)
 120 coordinate directions (Tseng & Yun, 2009; Xu & Yin, 2013). The BCD methods have recently
 121 gained attention in solving nonconvex optimization problems, including sparse optimization (Yuan,
 122 2024), k -means clustering (Nie et al., 2022), recurrent neural network (Massart & Abrol, 2022), and
 123 multi-layer convolutional networks (Bibi et al., 2019; Zeng et al., 2019). BCD methods have also
 124 been used in (Shalit & Chechik, 2014; Massart & Abrol, 2022) for solving optimization problems
 125 with orthogonal group constraints. However, their column-wise BCD methods are limited only to
 126 solve smooth minimization problems with $k = 2$ and $r = n$ (Refer to Section 4.2 in (Shalit &
 127 Chechik, 2014)). Our row-wise BCD methods can solve coordinate-wise nonsmooth problems with
 128 $k \geq 2$ and $r \leq n$. The work of (Gao et al., 2019) proposes a parallelizable column-wise BCD
 129 scheme for solving the subproblems of their proximal linearized augmented Lagrangian algorithm.
 130 Impressive parallel scalability in a parallel environment of their algorithm is demonstrated. We stress
 131 that our **row-wise** BCD methods differ from the two **column-wise** counterparts.

132 **► Summary.** Existing methods typically suffer from one or more of the following limitations: **(i)** they
 133 rely on full gradient information, incurring high computational costs per iteration; **(ii)** **they**
 134 **do not accommodate coordinate-wise nonsmooth composite objectives**; **(iii)** they lack true descent
 135 properties and are often infeasible methods what only attain feasibility only at the limit; **(iv)** **they**
 136 **often lack rigorous last-iterate convergence guarantees**; **(v)** they provide only weak optimality results
 137 at critical points. ★ In contrast, our methods overcome these limitations by using a tailored block
 138 coordinate descent framework for efficient composite optimization on the Stiefel manifold, with
 139 strong optimality and convergence guarantees.

139 1.3 CONTRIBUTIONS AND NOTATIONS

140 This paper makes the following contributions. **(i)** Algorithmically: We propose a Block Coor-
 141 dinate Descent (BCD) algorithm tailored for nonsmooth composite optimization under orthogonality
 142 constraints (Section 2). **(ii)** Theoretically: We provide comprehensive optimality and convergence
 143 analyses of our methods (Sections 3 and 4). **(iii)** Empirically: Extensive experiments demonstrate
 144 that our methods surpass existing solutions in terms of accuracy and/or efficiency (Section 5).

145 We define $[n] \triangleq \{1, 2, \dots, n\}$, and denote the Stiefel manifold as $\mathcal{M} \triangleq \text{St}(n, r)$. Matlab-style colon
 146 notation is used to describe submatrices. For a matrix $\mathbf{X} \in \mathbb{R}^{n \times r}$, let $\text{vec}(\mathbf{X}) \in \mathbb{R}^{nr \times 1}$ denote
 147 the vector formed by stacking its columns, and let $\text{mat}(\mathbf{x}) \in \mathbb{R}^{n \times r}$ denote the inverse operator,
 148 such that $\text{mat}(\text{vec}(\mathbf{X})) = \mathbf{X}$. We use $\mathbb{A} + \mathbb{B}$ and $\mathbb{A} - \mathbb{B}$ to denote standard Minkowski addition
 149 and subtraction between sets \mathbb{A} and \mathbb{B} , and $\mathbb{A} \oplus \mathbb{B}$ and $\mathbb{A} \ominus \mathbb{B}$ to denote element-wise addition and
 150 subtraction, respectively. Additional notations are summarized in Appendix A.1.

151 2 THE PROPOSED OBCD ALGORITHM

152 In this section, we introduce **OBCD**, a Block Coordinate Descent algorithm for solving coordinate-
 153 wise nonsmooth composite problems under Orthogonality constraints, as defined in Problem (1).

154 We start by presenting a new update scheme designed to maintain the orthogonality constraint.

155 **► A New Constraint-Preserving Update Scheme.** For any partition of the index vector $[1, 2, \dots, n]$
 156 into $[\mathbf{B}, \mathbf{B}^c]$ with $\mathbf{B} \in \mathbb{N}^k$, $\mathbf{B}^c \in \mathbb{N}^{n-k}$, we define $\mathbf{U}_{\mathbf{B}} \in \mathbb{R}^{n \times k}$ and $\mathbf{U}_{\mathbf{B}^c} \in \mathbb{R}^{n \times (n-k)}$ as:
 157 $(\mathbf{U}_{\mathbf{B}})_{ji} = \begin{cases} 1, & \mathbf{B}_i = j; \\ 0, & \text{else.} \end{cases}$, $(\mathbf{U}_{\mathbf{B}^c})_{ji} = \begin{cases} 1, & \mathbf{B}^c_i = j; \\ 0, & \text{else.} \end{cases}$. Therefore, we have the following variable
 158 splitting for any $\mathbf{X} \in \mathbb{R}^{n \times r}$: $\mathbf{X} = \mathbf{I}_n \mathbf{X} = (\mathbf{U}_{\mathbf{B}} \mathbf{U}_{\mathbf{B}}^T + \mathbf{U}_{\mathbf{B}^c} \mathbf{U}_{\mathbf{B}^c}^T) \mathbf{X} = \mathbf{U}_{\mathbf{B}} \mathbf{X}(\mathbf{B}, :) + \mathbf{U}_{\mathbf{B}^c} \mathbf{X}(\mathbf{B}^c, :)$,
 159 where $\mathbf{X}(\mathbf{B}, :) = \mathbf{U}_{\mathbf{B}}^T \mathbf{X} \in \mathbb{R}^{k \times r}$ and $\mathbf{X}(\mathbf{B}^c, :) = \mathbf{U}_{\mathbf{B}^c}^T \mathbf{X} \in \mathbb{R}^{(n-k) \times r}$.

162 In each iteration t , the indices $\{1, 2, \dots, n\}$ of the rows of decision variable $\mathbf{X} \in \text{St}(n, r)$ are separated to two sets \mathbb{B} and \mathbb{B}^c , where \mathbb{B} is the working set with $|\mathbb{B}| = k$ and $\mathbb{B}^c = \{1, 2, \dots, n\} \setminus \mathbb{B}$. To simplify notation, we use \mathbb{B} instead of \mathbb{B}^t , as t can be inferred from the context. We only update k rows of the variable \mathbf{X} via $\mathbf{X}^{t+1}(\mathbb{B}, :) \Leftarrow \mathbf{V}\mathbf{X}^t(\mathbb{B}, :)$ for some appropriate matrix $\mathbf{V} \in \mathbb{R}^{k \times k}$. The following equivalent expressions hold:

$$\mathbf{X}^{t+1}(\mathbb{B}, :) = \mathbf{V}\mathbf{X}^t(\mathbb{B}, :) \Leftrightarrow \mathbf{X}^{t+1} = (\mathbf{U}_{\mathbb{B}}\mathbf{V}\mathbf{U}_{\mathbb{B}}^T + \mathbf{U}_{\mathbb{B}^c}\mathbf{U}_{\mathbb{B}^c}^T)\mathbf{X}^t \quad (4)$$

$$\Leftrightarrow \mathbf{X}^{t+1} = \mathbf{X}^t + \mathbf{U}_{\mathbb{B}}(\mathbf{V} - \mathbf{I}_k)\mathbf{U}_{\mathbb{B}}^T\mathbf{X}^t. \quad (5)$$

170 We consider the following minimization procedure to iteratively solve Problem (1):

$$\min_{\mathbf{V}} F(\mathcal{X}_{\mathbb{B}}^t(\mathbf{V})), \text{ s.t. } \mathcal{X}_{\mathbb{B}}^t(\mathbf{V}) \in \text{St}(n, r), \text{ where } \mathcal{X}_{\mathbb{B}}^t(\mathbf{V}) \triangleq \mathbf{X}^t + \mathbf{U}_{\mathbb{B}}(\mathbf{V} - \mathbf{I}_k)\mathbf{U}_{\mathbb{B}}^T\mathbf{X}^t. \quad (6)$$

173 The following lemma shows that the orthogonality constraint for $\mathbf{X}^+ = \mathbf{X} + \mathbf{U}_{\mathbb{B}}(\mathbf{V} - \mathbf{I}_k)\mathbf{U}_{\mathbb{B}}^T\mathbf{X}$ can be preserved by choosing suitable \mathbf{V} and \mathbf{X} .

175 **Lemma 2.1.** (Proof in Appendix D.1) We let $\mathbb{B} \in \{\mathcal{B}_i\}_{i=1}^{C_n^k}$, where the set $\{\mathcal{B}_1, \mathcal{B}_2, \dots, \mathcal{B}_{C_n^k}\}$ denotes all possible combinations of the index vectors choosing k items from n without repetition. We let $177 \mathbf{V} \in \text{St}(k, k)$. We define $\mathbf{X}^+ \triangleq \mathcal{X}_{\mathbb{B}}(\mathbf{V}) \triangleq \mathbf{X} + \mathbf{U}_{\mathbb{B}}(\mathbf{V} - \mathbf{I}_k)\mathbf{U}_{\mathbb{B}}^T\mathbf{X}$. (a) For any $\mathbf{X} \in \mathbb{R}^{n \times r}$, we have $[\mathbf{X}^+]^T\mathbf{X}^+ = \mathbf{X}^T\mathbf{X}$. (b) If $\mathbf{X} \in \text{St}(n, r)$, then $\mathbf{X}^+ \in \text{St}(n, r)$.

180 Thanks to Lemma 2.1, we can now explore the following alternative formulation for Problem (6).

$$\bar{\mathbf{V}}^t \in \arg \min_{\mathbf{V}} F(\mathcal{X}_{\mathbb{B}}^t(\mathbf{V})), \text{ s.t. } \mathbf{V} \in \text{St}(k, k). \quad (7)$$

183 Then the solution matrix is updated via: $\mathbf{X}^{t+1} = \mathcal{X}_{\mathbb{B}}^t(\bar{\mathbf{V}}^t)$.

185 The following lemma offers important properties for the update rule $\mathbf{X}^+ = \mathbf{X} + \mathbf{U}_{\mathbb{B}}(\mathbf{V} - \mathbf{I}_k)\mathbf{U}_{\mathbb{B}}^T\mathbf{X}$.

186 **Lemma 2.2.** (Proof in Appendix D.2) We define $\mathbf{X}^+ = \mathbf{X} + \mathbf{U}_{\mathbb{B}}(\mathbf{V} - \mathbf{I}_k)\mathbf{U}_{\mathbb{B}}^T\mathbf{X}$. For any $\mathbf{X} \in \text{St}(n, r)$, $187 \mathbf{V} \in \text{St}(k, k)$, $\mathbb{B} \in \{\mathcal{B}_i\}_{i=1}^{C_n^k}$, and symmetric matrix $\mathbf{H} \in \mathbb{R}^{nr \times nr}$, we have: (a) $\frac{1}{2}\|\mathbf{X}^+ - \mathbf{X}\|_{\mathbf{H}}^2 = \frac{1}{2}\|\mathbf{V} - \mathbf{I}_k\|_{\underline{\mathbf{Q}}}^2$, where $\underline{\mathbf{Q}} \triangleq (\mathbf{Z}^T \otimes \mathbf{U}_{\mathbb{B}})^T \mathbf{H} (\mathbf{Z}^T \otimes \mathbf{U}_{\mathbb{B}})$, $\mathbf{Z} \triangleq \mathbf{U}_{\mathbb{B}}^T \mathbf{X} \in \mathbb{R}^{k \times r}$, and $\mathbf{X} \otimes \mathbf{Y}$ is the Kronecker product of \mathbf{X} and \mathbf{Y} . (b) $\frac{1}{2}\|\mathbf{X}^+ - \mathbf{X}\|_{\mathbf{F}}^2 = \langle \mathbf{I}_k - \mathbf{V}, \mathbf{U}_{\mathbb{B}}^T \mathbf{X} \mathbf{X}^T \mathbf{U}_{\mathbb{B}} \rangle$. (c) $\frac{1}{2}\|\mathbf{X}^+ - \mathbf{X}\|_{\mathbf{F}}^2 \leq \frac{1}{2}\|\mathbf{V} - \mathbf{I}_k\|_{\mathbf{F}}^2 = \langle \mathbf{I}_k, \mathbf{I}_k - \mathbf{V} \rangle$.

192 **► The Main Algorithm.** The proposed algorithm **OB**CD is an iterative procedure that sequentially minimizes the objective function along block coordinate directions within a sub-manifold of \mathcal{M} .

194 Starting with an initial feasible solution, **OB**CD iteratively determines a working set \mathbb{B}^t using specific strategies. It then solves the small-sized subproblem in Problem (7) through successive Majorization Minimization (MM). This method iteratively constructs a surrogate function that majorizes the objective function, driving it to decrease as expected (Mairal, 2013; Razavyayn et al., 195 2013; Sun et al., 2016; Breloy et al., 2021), and it has proven effective for minimizing complex 196 functions.

200 We now demonstrate how to derive the majorization function for $F(\mathcal{X}_{\mathbb{B}}^t(\mathbf{V}))$ in Problem (7). Initially, 201 for any $\mathbf{X}^t \in \text{St}(n, r)$ and $\mathbf{V} \in \text{St}(k, k)$, we establish following inequalities: $f(\mathcal{X}_{\mathbb{B}}^t(\mathbf{V})) - f(\mathbf{X}^t) \stackrel{\textcircled{1}}{\leq} 202 \langle \mathcal{X}_{\mathbb{B}}^t(\mathbf{V}) - \mathbf{X}^t, \nabla f(\mathbf{X}^t) \rangle + \frac{1}{2}\|\mathcal{X}_{\mathbb{B}}^t(\mathbf{V}) - \mathbf{X}^t\|_{\mathbf{H}}^2 \stackrel{\textcircled{2}}{=} \langle \mathbf{U}_{\mathbb{B}}(\mathbf{V} - \mathbf{I}_k)\mathbf{U}_{\mathbb{B}}^T\mathbf{X}^t, \nabla f(\mathbf{X}^t) \rangle + \frac{1}{2}\|\mathbf{V} - \mathbf{I}_k\|_{\underline{\mathbf{Q}}}^2 \stackrel{\textcircled{3}}{\leq} 203 \langle \mathbf{V} - \mathbf{I}_k, [\nabla f(\mathbf{X}^t)(\mathbf{X}^t)^T]_{\mathbb{B}\mathbb{B}} \rangle + \frac{1}{2}\|\mathbf{V} - \mathbf{I}_k\|_{\underline{\mathbf{Q}} + \alpha \mathbf{I}}^2$, where step ① uses Inequality (2); step ② uses 204 Lemma 2.2(a); step ③ uses $\alpha > 0$ and $\underline{\mathbf{Q}} \preceq \mathbf{Q}$, which can be ensured by choosing \mathbf{Q} using one of 205 the following methods:

$$\mathbf{Q} = \underline{\mathbf{Q}} \triangleq (\mathbf{Z}^T \otimes \mathbf{U}_{\mathbb{B}})^T \mathbf{H} (\mathbf{Z}^T \otimes \mathbf{U}_{\mathbb{B}}), \quad (8)$$

$$\mathbf{Q} = \varsigma \mathbf{I}, \text{ with } \|\underline{\mathbf{Q}}\|_{\text{sp}} \leq \varsigma \leq L_f. \quad (9)$$

211 where $\mathbf{Z} \triangleq \mathbf{U}_{\mathbb{B}}^T \mathbf{X}^t$. Then, we apply the MM technique to the smooth function $f(\mathbf{X})$, while keeping 212 the nonsmooth component $h(\mathbf{X})$ unchanged, leading to a function $\mathcal{K}(\mathbf{V}; \mathbf{X}^t, \mathbb{B})$ that majorizes 213 $F(\mathcal{X}_{\mathbb{B}}^t(\mathbf{V})) = f(\mathcal{X}_{\mathbb{B}}^t(\mathbf{V})) + h(\mathcal{X}_{\mathbb{B}}^t(\mathbf{V}))$:

$$\begin{aligned} 214 F(\mathcal{X}_{\mathbb{B}}^t(\mathbf{V})) &\leq f(\mathbf{X}^t) + \langle \mathbf{V} - \mathbf{I}_k, [\nabla f(\mathbf{X}^t)(\mathbf{X}^t)^T]_{\mathbb{B}\mathbb{B}} \rangle + \frac{1}{2}\|\mathbf{V} - \mathbf{I}_k\|_{\underline{\mathbf{Q}} + \alpha \mathbf{I}}^2 + h(\mathbf{V}\mathbf{U}_{\mathbb{B}}^T\mathbf{X}^t) \\ 215 &\leq \mathcal{K}(\mathbf{V}; \mathbf{X}^t, \mathbb{B}) \triangleq \frac{1}{2}\|\mathbf{V} - \mathbf{I}_k\|_{\underline{\mathbf{Q}} + \alpha \mathbf{I}}^2 + \langle \mathbf{V}, [\nabla f(\mathbf{X}^t)(\mathbf{X}^t)^T]_{\mathbb{B}\mathbb{B}} \rangle + h(\mathbf{V}\mathbf{U}_{\mathbb{B}}^T\mathbf{X}^t) + \bar{c}, \end{aligned} \quad (10)$$

216 **Algorithm 1 OBCD:** Block Coordinate Descent for Problem (1)

217
 218 1: **Input:** proximal parameter $\alpha > 0$, initial feasible point \mathbf{X}^0 , block size $k \geq 2$, $t = 0$.
 219 2: **for** $t = 0$ to T **do**
 220 3: (S1) Select working set $\mathbf{B}^t \in \{1, \dots, n\}^k$. Let $\mathbf{B} = \mathbf{B}^t$ and $\mathbf{B}^c = \{1, \dots, n\} \setminus \mathbf{B}$.
 221 4: (S2) Choose $\mathbf{Q} \in \mathbb{R}^{k^2 \times k^2}$ using (8) or (9).
 222 5: (S3) Define $\mathcal{K}(\cdot, \cdot, \cdot)$ as in Equation (10). Compute $\bar{\mathbf{V}}^t$ as the global minimizer

$$\bar{\mathbf{V}}^t \in \arg \min_{\mathbf{V} \in \text{St}(k, k)} \mathcal{K}(\mathbf{V}; \mathbf{X}^t, \mathbf{B}). \quad (11)$$

223 Alternatively, find a local solution $\bar{\mathbf{V}}^t$ such that $\mathcal{K}(\bar{\mathbf{V}}^t; \mathbf{X}^t, \mathbf{B}) \leq \mathcal{K}(\mathbf{I}_k; \mathbf{X}^t, \mathbf{B})$.
 224 6: (S4) $\mathbf{X}^{t+1}(\mathbf{B}, :) \leftarrow \bar{\mathbf{V}}^t \mathbf{X}^t(\mathbf{B}, :)$
 225 7: **end for**

226 where $\ddot{c} = f(\mathbf{X}^t) + h(\mathbf{U}_{\mathbf{B}^c}^T \mathbf{X}^t) - \langle \mathbf{I}_k, [\nabla f(\mathbf{X}^t)(\mathbf{X}^t)^T]_{\mathbf{B}^c} \rangle$ is a constant. Here, we use the
 227 coordinate-wise separable property of $h(\cdot)$ as follows: $h(\mathcal{X}_{\mathbf{B}}^t(\mathbf{V})) = h(\mathbf{U}_{\mathbf{B}^c} \mathbf{U}_{\mathbf{B}^c}^T \mathbf{X}^t + \mathbf{U}_{\mathbf{B}} \mathbf{V} \mathbf{U}_{\mathbf{B}}^T \mathbf{X}^t) =$
 228 $h(\mathbf{U}_{\mathbf{B}^c}^T \mathbf{X}^t) + h(\mathbf{V} \mathbf{U}_{\mathbf{B}}^T \mathbf{X}^t)$. We minimize the upper bound of the right-hand side of Inequality (10),
 229 resulting in the minimization problem that $\bar{\mathbf{V}}^t \in \arg \min_{\mathbf{V} \in \text{St}(k, k)} \mathcal{K}(\mathbf{V}; \mathbf{X}^t, \mathbf{B})$, which can be effi-
 230 ciently and exactly solved due to our assumption.
 231

232 Two simple strategies to find the working set \mathbf{B} with $|\mathbf{B}| = k$ can be considered. (i) Random strategy: \mathbf{B} is randomly selected from $\{\mathcal{B}_1, \mathcal{B}_2, \dots, \mathcal{B}_{C_n^k}\}$ with equal probability $1/C_n^k$. (ii) Cyclic strategy: \mathbf{B}^t
 233 takes all possible combinations in cyclic order, such as $\mathcal{B}_1 \rightarrow \mathcal{B}_2 \rightarrow \dots \rightarrow \mathcal{B}_{C_n^k} \rightarrow \mathcal{B}_1 \rightarrow \dots$.
 234

235 The proposed **OBCD** algorithm is summarized in Algorithm 1. Importantly, **OBCD** is a partial
 236 gradient method with low iterative computational complexity as it only assesses k rows of the Euclidean
 237 gradient of $\nabla f(\mathbf{X}^t)$ and the solution \mathbf{X}^t to compute the linear term $\langle [\nabla f(\mathbf{X}^t)(\mathbf{X}^t)^T]_{\mathbf{B}^c}, \mathbf{V} \rangle =$
 238 $\langle [\nabla f(\mathbf{X}^t)]_{\mathbf{B}, :}^T [\mathbf{X}^t]_{\mathbf{B}, :}, \mathbf{V} \rangle$, as shown in Equation (10). Appendix C.3 details the complexity compari-
 239 son between **OBCD** and full gradient methods for some quadratic function $f(\mathbf{X})$.
 240

241 **► Solving the General OBCD Subproblems.** The following lemma outlines key properties of the
 242 **OBCD** subproblems.
 243

244 **Lemma 2.3.** (Proof in Appendix D.3) We define $\mathbf{Z} = \mathbf{U}_{\mathbf{B}}^T \mathbf{X}^t$ and $\mathbf{P} \triangleq [\nabla f(\mathbf{X}^t)(\mathbf{X}^t)^T]_{\mathbf{B}^c} -$
 245 $\text{mat}(\mathbf{Q}\text{vec}(\mathbf{I}_k)) - \alpha \mathbf{I}_k$. We have:

246 (a) The subproblem in Equation (11) is equivalent to Problem (3) with $\tilde{\mathbf{Q}} = \mathbf{Q} + \alpha \mathbf{I}$.
 247 (b) Assume that Formula (9) is used to choose \mathbf{Q} . Problem (3) further reduces to the following
 248 problem: $\bar{\mathbf{V}}^t \in \arg \min_{\mathbf{V} \in \text{St}(k, k)} \mathcal{P}(\mathbf{V}) \triangleq \langle \mathbf{V}, \mathbf{P} \rangle + h(\mathbf{VZ})$. In particular, when $h(\mathbf{X}) \triangleq 0$,
 249 we obtain: $\bar{\mathbf{V}}^t = -\mathbb{P}_{\mathcal{M}}(\mathbf{P})$. Here, $\mathbb{P}_{\mathcal{M}}(\mathbf{P})$ is the nearest orthogonality matrix to \mathbf{P} .
 250

251 **Remark 2.4.** (a) By Lemma 2.3(b), when $k > 2$, $h(\mathbf{X}) = 0$, and \mathbf{Q} is chosen to be a diagonal
 252 matrix as in Equation (9), the subproblem $\bar{\mathbf{V}}^t \in \arg \min_{\mathbf{V} \in \text{St}(k, k)} \mathcal{K}(\mathbf{V}; \mathbf{X}^t, \mathbf{B})$ in Algorithm 1 can
 253 be solved exactly and efficiently due to our assumption, see Remark 2.6. (b) For general k and
 254 $h(\cdot)$, the subproblem may not admit a global solution. However, if a **local** stationary solution $\bar{\mathbf{V}}^t$
 255 satisfying $(\bar{\mathbf{V}}^t; \mathbf{X}^t, \mathbf{B}) \leq \mathcal{K}(\mathbf{I}_k; \mathbf{X}^t, \mathbf{B})$ can be found, then the sufficient descent condition remains
 256 valid, and convergence to a weaker optimality condition for the final solution \mathbf{X}^∞ is still achievable
 257 (see Inequalities (42), (44)).
 258

259 **► Smallest Possible Subproblems When $k = 2$.** We now discuss how to solve the subproblems
 260 exactly when $k = 2$. The following lemma reveals an equivalent expression for any $\mathbf{V} \in \text{St}(2, 2)$.
 261

262 **Lemma 2.5.** (Proof in Appendix D.4) Any orthogonal matrix $\mathbf{V} \in \text{St}(2, 2)$ can be expressed as
 263 $\mathbf{V} = \mathbf{V}_\theta^{\text{rot}}$ or $\mathbf{V} = \mathbf{V}_\theta^{\text{ref}}$ for some $\theta \in \mathbb{R}$, where $\mathbf{V}_\theta^{\text{rot}} \triangleq \begin{pmatrix} \cos(\theta) & \sin(\theta) \\ -\sin(\theta) & \cos(\theta) \end{pmatrix}$, $\mathbf{V}_\theta^{\text{ref}} \triangleq \begin{pmatrix} -\cos(\theta) & \sin(\theta) \\ \sin(\theta) & \cos(\theta) \end{pmatrix}$.
 264 We have $\det(\mathbf{V}_\theta^{\text{rot}}) = 1$ and $\det(\mathbf{V}_\theta^{\text{ref}}) = -1$ for any θ .
 265

266 Using Lemma 2.5, we can reformulate Problem (3) as the following one-dimensional problem:

$$\bar{\theta} \in \arg \min_{\theta} \mathcal{P}(\mathbf{V}), \text{ s.t. } \mathbf{V} \in \{\mathbf{V}_\theta^{\text{rot}}, \mathbf{V}_\theta^{\text{ref}}\}.$$

267 The optimal solution $\bar{\theta}$ can be identified even if $h(\cdot) \neq 0$ using a novel breakpoint searching method,
 268 which is discussed later in Section B in the Appendix.
 269

270 **Remark 2.6.** (i) $\mathbf{V}_\theta^{\text{rot}}$ and $\mathbf{V}_\theta^{\text{ref}}$ are called Givens rotation matrix and Jacobi reflection matrix
 271 respectively in the literature (Sun & Bischof, 1995). Previous research only considered $\{\mathbf{V}_\theta^{\text{rot}}\}$ for
 272 solving symmetric linear eigenvalue problems (Golub & Van Loan, 2013) and sparse PCA problems
 273 (Shalit & Chechik, 2014), while we use $\{\mathbf{V}_\theta^{\text{ref}}, \mathbf{V}_\theta^{\text{rot}}\}$ for solving Problem (1). (ii) We show the
 274 necessity of using $\{\mathbf{V}_\theta^{\text{ref}}, \mathbf{V}_\theta^{\text{rot}}\}$ in the following two examples of 2×2 optimization problems with
 275 orthogonality constraints: $\min_{\mathbf{V} \in \text{St}(2,2)} F(\mathbf{V}) \triangleq \|\mathbf{V} - \mathbf{A}\|_F^2$, and $\min_{\mathbf{V} \in \text{St}(2,2)} F(\mathbf{V}) \triangleq \|\mathbf{V} -$
 276 $\mathbf{B}\|_F^2 + 5\|\mathbf{V}\|_1$, where $\mathbf{A} = \begin{pmatrix} 1 & 0 \\ -1 & -1 \end{pmatrix}$ and $\mathbf{B} = \begin{pmatrix} 1 & 0 \\ 1 & 2 \end{pmatrix}$. The use of the reflection matrix $\mathbf{V}_\theta^{\text{ref}}$ is
 277 essential in these examples because it results in lower objective values. See Section C.1 in the
 278 Appendix for more details.

280 3 OPTIMALITY ANALYSIS

281 This section provides the optimality analysis for **OB****CD**. First, we establish the completeness of
 282 the proposed update scheme, showing that **OB****CD** can reach any feasible point from an arbitrary
 283 initialization. Second, we analyze the optimality conditions of both Problem (1) and the associated
 284 subproblems of **OB****CD**. Finally, by comparing these two sets of conditions, we derive a hierarchy
 285 of optimality, illustrating how the algorithm's stationarity relates to that of Problem (1).

286 ▶ **Basis Representation of Orthogonal Matrices.** The following theorem shows that any orthog-
 287 onal matrix $\mathbf{D} \in \text{St}(n, n)$ and any point $\mathbf{X} \in \text{St}(n, r)$ can be generated by composing simple
 288 2-dimensional updates.

289 **Theorem 3.1** (Basis Representation of Orthogonal Matrices). *(Proof in Appendix E.1) Assume $k =$*
 290 *2. For all $i \in [C_n^k]$, define $\mathcal{W}_i \triangleq \mathbf{I}_n + \mathbf{U}_{\mathcal{B}_i}(\mathcal{V}_i - \mathbf{I}_k)\mathbf{U}_{\mathcal{B}_i}^T = \mathbf{U}_{\mathcal{B}_i}\mathcal{V}_i\mathbf{U}_{\mathcal{B}_i}^T + \mathbf{U}_{\mathcal{B}_i^c}\mathbf{U}_{\mathcal{B}_i^c}^T$, where*
 291 *$\mathcal{V}_i \in \text{St}(k, k)$. Then:*

292 (a) *Any matrix $\mathbf{D} \in \text{St}(n, n)$ can be expressed as $\mathbf{D} = \mathcal{W}_{C_n^k} \dots \mathcal{W}_2\mathcal{W}_1$ for suitable choice of \mathcal{W}_i*
 293 *(equivalently, of \mathcal{V}_i). Furthermore, if $\forall i, \mathcal{V}_i = \mathbf{I}_2$, then $\mathbf{D} = \mathbf{I}_n$.*
 294 (b) *For any fixed reference point $\mathbf{X}^0 \in \text{St}(n, r)$, every $\mathbf{X} \in \text{St}(n, r)$ can be expressed as $\mathbf{X} =$*
 295 *$\mathcal{W}_{C_n^k} \dots \mathcal{W}_2\mathcal{W}_1\mathbf{X}^0$ for suitable \mathcal{W}_i .*

296 The above representation for $k = 2$ can in fact be extended to any block size $k \geq 2$, as stated next.

297 **Corollary 3.2.** *(Proof in Appendix E.2) The conclusion of Theorem 3.1 extends to all $k \geq 2$.* □

298 **Remark 3.3.** (i) We use both Givens rotation and Jacobi reflection matrices to compute $\mathbf{D} \in$
 299 $\text{St}(n, n)$. This is necessary since a reflection matrix cannot be represented through a sequence
 300 of rotations. (ii) The result of Corollary 3.2 indicates that the proposed update scheme $\mathbf{X}^+ \Leftarrow$
 301 $\mathbf{X} + \mathbf{U}_B(\mathbf{V} - \mathbf{I}_k)\mathbf{U}_B^T\mathbf{X}$ with $\mathbf{V} \in \text{St}(k, k)$ as shown in Formula (5) can reach any orthogonal matrix
 302 $\mathbf{X} \in \text{St}(n, r)$ for any starting solution $\mathbf{X}^0 \in \text{St}(n, r)$.

303 ▶ **First-Order Optimality Conditions for Problem (1).** We provide the first-order optimality con-
 304 dition of Problem (1) (Wen & Yin, 2013; Chen et al., 2020). We use $\partial F(\mathbf{X})$ to denote the limiting
 305 subdifferential of $F(\mathbf{X})$ (Mordukhovich, 2006; Rockafellar & Wets., 2009), which is always non-
 306 empty since $F(\mathbf{X})$ is closed, proper, and lower semicontinuous. Given $f(\mathbf{X})$ is differentiable, we
 307 have $\partial F(\mathbf{X}) = \partial(f + h)(\mathbf{X}) = \nabla f(\mathbf{X}) + \partial h(\mathbf{X})$ (Rockafellar & Wets., 2009). We extend the def-
 308 inition of *limiting subdifferential* to introduce $\partial_{\mathcal{M}} F(\mathbf{X})$ as the *Riemannian limiting subdifferential*
 309 of $F(\mathbf{X})$ at \mathbf{X} , defined as $\partial_{\mathcal{M}} F(\mathbf{X}) \triangleq \partial F(\mathbf{X}) \ominus (\mathbf{X}[\partial F(\mathbf{X})]^T\mathbf{X})$, where \ominus is the element-wise
 310 subtraction between sets.

311 Introducing a Lagrangian multiplier matrix $\mathbf{\Lambda} \in \mathbb{R}^{r \times r}$ for the orthogonality constraint, we define
 312 the following Lagrangian function of Problem (1): $\mathcal{L}(\mathbf{X}, \mathbf{\Lambda}) = F(\mathbf{X}) + \frac{1}{2}\langle \mathbf{I}_r - \mathbf{X}^T\mathbf{X}, \mathbf{\Lambda} \rangle$. Notably,
 313 the matrix $\mathbf{\Lambda}$ is symmetric, as $\mathbf{X}^T\mathbf{X}$ is symmetric. We state the following definition of first-order
 314 optimality condition.

315 **Definition 3.4.** *Critical Point* (Wen & Yin, 2013; Chen et al., 2020). A solution $\check{\mathbf{X}} \in \text{St}(n, r)$ is
 316 a critical point of Problem (1) if: $\mathbf{0} \in \partial_{\mathcal{M}} F(\check{\mathbf{X}}) \triangleq \partial F(\check{\mathbf{X}}) \ominus (\check{\mathbf{X}}[\partial F(\check{\mathbf{X}})]^T\check{\mathbf{X}})$, where $(\partial F(\check{\mathbf{X}}) \ominus$
 317 $\check{\mathbf{X}}[\partial F(\check{\mathbf{X}})]^T\check{\mathbf{X}}) \triangleq \{\mathbf{G} - \check{\mathbf{X}}\mathbf{G}^T\check{\mathbf{X}} \mid \mathbf{G} \in \partial F(\check{\mathbf{X}})\}$. Moreover, the corresponding multiplier satisfies
 318 $\mathbf{\Lambda} \in [\partial F(\check{\mathbf{X}})]^T\check{\mathbf{X}}$.

319 **Remark 3.5.** The critical point condition in Lemma 3.4 can be equivalently expressed as (Absil
 320 et al., 2008; Jiang & Dai, 2015; Liu et al., 2016): $\mathbf{0} \in \mathbb{P}_{T_{\check{\mathbf{X}}} \mathcal{M}}(\partial F(\check{\mathbf{X}}))$. Here, $T_{\check{\mathbf{X}}} \mathcal{M}$ is the tangent
 321 space to \mathcal{M} at $\mathbf{X} \in \mathcal{M}$ with $T_{\mathbf{X}} \mathcal{M} = \{\mathbf{Y} \in \mathbb{R}^{n \times r} \mid \mathbf{X}^T \mathbf{Y} + \mathbf{Y}^T \mathbf{X} = \mathbf{0}\}$.

324 **► Optimality Conditions for the Subproblems.** The Euclidean subdifferential of $\mathcal{K}(\mathbf{V}; \mathbf{X}^t, \mathbf{B}^t)$
 325 w.r.t. \mathbf{V} is given by $\tilde{\mathbf{G}}(\mathbf{V}) \triangleq \tilde{\Delta}(\mathbf{V}) + \mathbf{U}_B^\top [\nabla f(\mathbf{X}^t) + \partial h(\mathbf{X}^{t+1})](\mathbf{X}^t)^\top \mathbf{U}_B$, where $\tilde{\Delta}(\mathbf{V}) =$
 326 $\text{mat}((\mathbf{Q} + \alpha \mathbf{I}_k) \text{vec}(\mathbf{V} - \mathbf{I}_k))$ and $\mathbf{X}^{t+1} = \mathbf{X}^t + \mathbf{U}_B(\mathbf{V} - \mathbf{I}_k)\mathbf{U}_B^\top \mathbf{X}^t$. Using Lemma 3.4, we set
 327 the Riemannian subdifferential of $\mathcal{K}(\mathbf{V}; \mathbf{X}^t, \mathbf{B}^t)$ w.r.t. \mathbf{V} to zero and obtain the following first-order
 328 optimality condition for $\bar{\mathbf{V}}^t$: $\mathbf{0} \in \partial_{\mathcal{M}} \mathcal{K}(\bar{\mathbf{V}}^t; \mathbf{X}^t, \mathbf{B}^t) \triangleq \tilde{\mathbf{G}}(\bar{\mathbf{V}}^t) \ominus \bar{\mathbf{V}}^t \tilde{\mathbf{G}}(\bar{\mathbf{V}}^t)^\top \bar{\mathbf{V}}^t$. This inclusion
 329 is a key ingredient in establishing the optimality hierarchy in Theorem 3.7(a) and the Riemannian
 330 subgradient lower bound in Lemma 4.4(a).

331 **► Optimality Conditions and Their Hierarchy.** We introduce the following new optimality con-
 332 dition of block- k stationary points.

333 **Definition 3.6.** (Global) Block- k Stationary Point, abbreviated as BS_k -point. Let $\alpha > 0$ and
 334 $k \geq 2$. A solution $\ddot{\mathbf{X}} \in \text{St}(n, r)$ is called a block- k stationary point if: $\forall \mathbf{B} \in \{\mathcal{B}_i\}_{i=1}^{C_n^k}$, $\mathbf{I}_k \in$
 335 $\arg \min_{\mathbf{V} \in \text{St}(k, k)} \mathcal{K}(\mathbf{V}; \ddot{\mathbf{X}}, \mathbf{B})$, where $\mathcal{K}(\cdot; \cdot, \cdot)$ is defined in Equation (10).

336 **Remarks.** BS_k -point states that if we *globally* minimize the majorization function $\mathcal{K}(\mathbf{V}; \ddot{\mathbf{X}}, \mathbf{B})$,
 337 there is no possibility of improving the objective function value for $\mathcal{K}(\mathbf{V}; \ddot{\mathbf{X}}, \mathbf{B})$ across all $\mathbf{B} \in$
 338 $\{\mathcal{B}_i\}_{i=1}^{C_n^k}$.

339 The following theorem establishes the relation between BS_k -points, standard critical points, and
 340 global optimal points.

341 **Theorem 3.7.** (Proof in Appendix E.3) We establish the following relationships:

- 342 (a) {critical points $\ddot{\mathbf{X}}$ } \supseteq {BS₂-points $\ddot{\mathbf{X}}$ }.
- 343 (b) {BS_k-points $\ddot{\mathbf{X}}$ } \supseteq {global optimal points $\ddot{\mathbf{X}}$ }, where $k \in \{2, 3, \dots, n\}$.
- 344 (c) {BS_k-points $\ddot{\mathbf{X}}$ } \supseteq {BS_{k+1}-points $\ddot{\mathbf{X}}$ }, where $k \in \{2, 3, \dots, n-1\}$.
- 345 (d) The reverse of the above three inclusions may not always hold true.

346 **Remark 3.8.** (i) The optimality of BS₂-points is stronger than that of standard critical points
 347 (Wen & Yin, 2013; Chen et al., 2020; Absil et al., 2008). (ii) Testing whether a solution $\ddot{\mathbf{X}}$ is a
 348 BS_k-points deterministically requires solving all C_n^k subproblems. However, by randomly selecting
 349 the working set \mathbf{B} from the C_n^k possible combinations $\{\mathcal{B}_i\}_{i=1}^{C_n^k}$, one can test whether $\ddot{\mathbf{X}}$ is a BS_k-point
 350 in expectation.

351 4 CONVERGENCE ANALYSIS

352 This section establishes the iteration complexity and non-ergodic (last-iterate) convergence rates of
 353 the proposed **OBCD** algorithm. We first prove a sufficient descent property, followed by an ergodic
 354 convergence rate typical in nonconvex optimization. We then analyze iteration complexity under
 355 the Riemannian subgradient condition, commonly used in nonsmooth manifold settings. Finally, we
 356 derive a last-iterate convergence rate based on the KL inequality.

357 Throughout this section, we assume that the working set is determined by a random strategy and that
 358 the global minimizer $\bar{\mathbf{V}}^t \in \arg \min_{\mathbf{V} \in \text{St}(k, k)} \mathcal{K}(\mathbf{V}; \mathbf{X}^t, \mathbf{B}^t)$ can be computed. The algorithm **OBCD**
 359 then generates a random output $(\bar{\mathbf{V}}^t, \mathbf{X}^{t+1})$ for $t = 0, 1, \dots, \infty$, depending on the realization of the
 360 random variable $\xi^t \triangleq (\mathbf{B}^1, \mathbf{B}^2, \dots, \mathbf{B}^t)$. We denote \mathbf{X}^∞ as an arbitrary limit point of **OBCD**.

361 4.1 ITERATION COMPLEXITY

362 Initially, we introduce the notation of ϵ -BS_k-point as follows.

363 **Definition 4.1.** (ϵ -BS_k-point) Given any constant $\epsilon > 0$, a point $\ddot{\mathbf{X}}$ is called an ϵ -BS_k-point if:
 364 $\frac{1}{C_n^k} \sum_{i=1}^{C_n^k} \text{dist}(\mathbf{I}_k, \arg \min_{\mathbf{V}} \mathcal{K}(\mathbf{V}; \ddot{\mathbf{X}}, \mathcal{B}_i))^2 \leq \epsilon$, where $\mathcal{K}(\cdot; \cdot, \cdot)$ is defined in Equation (10). Here,
 365 the set $\{\mathcal{B}_1, \mathcal{B}_2, \dots, \mathcal{B}_{C_n^k}\}$ denotes all possible combinations of the index vectors choosing k items
 366 from n without repetition, and $\text{dist}(\Xi, \Xi')$ denotes the distance between two sets Ξ and Ξ' .

367 Using the optimality measure from Definition 4.1, we establish the iteration complexity of **OBCD**.

368 **Theorem 4.2.** (Proof in Appendix F.1) We define $\tilde{c} \triangleq \frac{2}{\alpha} \cdot (F(\mathbf{X}^0) - F(\mathbf{X}^\infty)) \geq 0$. We have:

- 369 (a) The following sufficient decrease condition holds for all $t \geq 0$:

$$370 \frac{\alpha}{2} \|\mathbf{X}^{t+1} - \mathbf{X}^t\|_F^2 \leq \frac{\alpha}{2} \|\bar{\mathbf{V}}^t - \mathbf{I}_k\|_F^2 \leq F(\mathbf{X}^t) - F(\mathbf{X}^{t+1}).$$

378 (b) If the \mathbf{B}^t is selected from $\{\mathcal{B}_i\}_{i=1}^{C_n^k}$ randomly and uniformly, **OBCD** finds an ϵ -BS_k-point of
 379 Problem (1) in at most T iterations in the sense of expectation, where $T \geq \lceil \frac{\bar{c}}{\epsilon} \rceil$.
 380

381 **Remark 4.3.** Theorem 4.2 shows that **OBCD** converges to ϵ -block- k stationary points with an iteration
 382 complexity of $\mathcal{O}(1/\epsilon)$, which is typical for general nonconvex optimization.
 383

384 Apart from Definition 4.1, another common optimality measure relies on the Riemannian subgradient.
 385 At the point $\mathbf{V} = \mathbf{I}_k$, the Riemannian subdifferential of $\mathcal{K}(\mathbf{V}; \mathbf{X}^t, \mathbf{B}^t)$ is $\partial_{\mathcal{M}}\mathcal{K}(\mathbf{I}_k; \mathbf{X}^t, \mathbf{B}^t) =$
 386 $\mathbf{U}_{\mathbf{B}^t}^T (\mathbb{D} \ominus \mathbb{D}^T) \mathbf{U}_{\mathbf{B}^t}$, where $\mathbb{D} = [\nabla f(\mathbf{X}^t) + \partial h(\mathbf{X}^t)][\mathbf{X}^t]^T$. We next derive a Riemannian subgradient
 387 lower bound in terms of the iterate gap.
 388

389 **Lemma 4.4.** (Proof in Appendix F.2, Riemannian Subgradient Lower Bound for the Iterates
 390 Gap) Assume that $F(\cdot)$ is C_F -Lipschitz continuous on $\text{St}(n, r)$, i.e., $\|\mathbf{G}\|_F \leq C_F$ for all $\mathbf{X} \in$
 391 $\text{St}(n, r)$ and all $\mathbf{G} \in \partial F(\mathbf{X})$. We have:

392 (a) $\mathbb{E}_{\xi^{t+1}}[\text{dist}(\mathbf{0}, \partial_{\mathcal{M}}\mathcal{K}(\mathbf{I}_k; \mathbf{X}^{t+1}, \mathbf{B}^{t+1}))] \leq \phi \cdot \mathbb{E}_{\xi^t}[\|\bar{\mathbf{V}}^t - \mathbf{I}_k\|_F]$, where $\phi \triangleq 4(C_F + L_f) + 2\alpha$.
 393 (b) $\mathbb{E}_{\xi^t}[\text{dist}(\mathbf{0}, \partial_{\mathcal{M}}F(\mathbf{X}^t))] \leq \gamma \cdot \mathbb{E}_{\xi^t}[\text{dist}(\mathbf{0}, \partial_{\mathcal{M}}\mathcal{K}(\mathbf{I}_k; \mathbf{X}^t, \mathbf{B}^t))]$, where $\gamma \triangleq (C_n^k / C_{n-2}^{k-2})^{1/2}$.

394 **Remark 4.5.** The important class of nonsmooth ℓ_1 norm function $h(\mathbf{X}) = \|\mathbf{X}\|_1$ (Chen et al., 2020;
 395 2024) satisfies the assumption made in Lemma 4.4.

396 We establish the iteration complexity of **OBCD** using the optimality measure of Riemannian sub-
 397 gradient (Chen et al., 2020; Cheung et al., 2024; Li et al., 2024b).

398 **Theorem 4.6.** (Proof in Appendix F.3) We define \tilde{c} as in Theorem 4.2 and $\{\phi, \gamma\}$ as in Lemma 4.4.
 399 **OBCD** finds an ϵ -critical point of Problem (1), i.e., $\mathbb{E}_{\xi^{\bar{t}}}[\text{dist}^2(\mathbf{0}, \partial_{\mathcal{M}}F(\mathbf{X}^{\bar{t}+1}))] \leq \epsilon$, in at most
 400 $T + 1$ iterations in expectation, where $\bar{t} \in [T]$ and $T \geq \lceil \frac{\gamma^2 \phi^2 \tilde{c}}{\epsilon} \rceil$.
 401

4.2 CONVERGENCE RATE UNDER KL INEQUALITY

402 We establish the non-ergodic convergence rate of **OBCD** using the Kurdyka-Łojasiewicz inequality,
 403 a key tool in non-convex analysis (Attouch et al., 2010; Bolte et al., 2014; Liu et al., 2016).
 404

405 Initially, we make the following additional assumption.

406 **Assumption 4.7.** The function $F_t(\mathbf{X}) = F(\mathbf{X}) + \iota_{\mathcal{M}}(\mathbf{X})$ is a Kurdyka-Łojasiewicz (KL) function.

407 **Remark 4.8.** Semi-algebraic functions constitute a broad class of KL functions, including real
 408 polynomials, norm functions $\|\mathbf{x}\|_p$ with $p \geq 0$, rank functions, and indicator functions of sets such
 409 as the Stiefel manifold and the positive semidefinite cone (Attouch et al., 2010).

410 We present the following useful proposition regarding to the KL function.

411 **Proposition 4.9. (Kurdyka-Łojasiewicz Property)**, see, e.g., (Attouch et al., 2010; Bolte et al.,
 412 2014). Let $F_t : \mathbb{R}^{m \times n} \rightarrow (-\infty, +\infty]$ be a KL function and $\mathbf{X}^\infty \in \text{dom } F_t$. Then there exist $\sigma \in [0, 1)$,
 413 $\eta \in (0, +\infty]$, a neighborhood Υ of \mathbf{X}^∞ , and a concave continuous function $\varphi(t) = ct^{1-\sigma}$
 414 with $c > 0$ and $t \in [0, \eta]$ such that for all $\mathbf{X}' \in \Upsilon$ satisfying $F_t(\mathbf{X}') \in (F_t(\mathbf{X}^\infty), F_t(\mathbf{X}^\infty) + \eta)$, it
 415 holds that $\text{dist}(\mathbf{0}, \partial F_t(\mathbf{X}')) \varphi'(F_t(\mathbf{X}') - F_t(\mathbf{X}^\infty)) \geq 1$.
 416

417 Utilizing the Kurdyka-Łojasiewicz property, one can establish a finite-length property of **OBCD**, a
 418 result considerably stronger than that of Theorem 4.2.
 419

420 **Theorem 4.10. (Proof in Appendix F.4, A Finite Length Property).** We define $E_{t+1} \triangleq \mathbb{E}_{\xi^t}[\|\bar{\mathbf{V}}^t -$
 421 $\mathbf{I}_k\|_F]$, and $D_i = \sum_{j=i}^{\infty} E_{j+1}$. Under the continuity assumption in Lemma 4.4, there exists a suffi-
 422 ciently large t_* such that, for all $t \geq t_*$, we have

423 (a) It holds that $(E_{t+1})^2 \leq \kappa E_t(\varphi_t - \varphi_{t+1})$, where $\varphi_t \triangleq \varphi(F(\mathbf{X}^t) - F(\mathbf{X}^\infty))$, $\kappa \triangleq \frac{2\gamma\phi}{\alpha}$ is a pos-
 424 tive constant, $\gamma \triangleq (C_n^k / C_{n-2}^{k-2})^{1/2}$, ϕ is defined in Lemma 4.4, and $\varphi(\cdot)$ is the desingularization
 425 function defined in Proposition 4.9.

426 (b) It holds that $\sum_{j=t}^{\infty} E_{j+1} \leq E_t + 2\kappa\varphi_t$. The sequence $\{E_t\}_{t=1}^{\infty}$ has the finite length property
 427 that $D_t \triangleq \sum_{j=t}^{\infty} E_{j+1}$ is always upper-bounded by a certain constant for all $t \geq t_*$.
 428

429 Finally, we establish the last-iterate convergence rate for **OBCD**.
 430

431 **Theorem 4.11. (Proof in Appendix F.5).** Based on the continuity assumption made in Lemma 4.4,
 432 for all $t \geq t_*$, we have:

432	data-m-n	LADMM (id)	RADMM (id)	SPM (id)	LADMM (rnd)	RADMM (rnd)	SPM (rnd)	OBCD-R (id)	data-m-n	LADMM (id)	RADMM (id)	SPM (id)	LADMM (rnd)	RADMM (rnd)	SPM (rnd)	OBCD-R (id)		
$r = 20, \lambda = 10, \text{time limit}=40$																		
433	w1a-2477-300	199.897	219.698	199.897	259.825	239.717	259.672	199.667	TDT2-500-1000	199.997	359.382	199.997	389.376	269.292	389.260	199.258		
434	20News-8000-1000	199.995	219.673	199.995	239.301	219.243	349.228	199.222	sector-6412-1000	199.980	349.793	199.980	479.996	249.813	369.651	199.649		
435	E2006-2000-1000	199.999	239.115	199.999	269.128	219.084	709.095	199.077	E2006-2000-1000	199.999	239.115	199.999	269.128	219.084	709.095	199.077		
436	MNIST-60000-784	199.985	339.970	199.985	289.917	339.910	1339.774	199.896	Gisette-3000-1000	199.980	339.970	199.980	539.979	369.981	1639.952	199.979		
437	CnnCal-3000-1000	199.981	429.979	199.981	689.970	379.979	909.931	199.946	Cifar-1000-1000	199.979	449.982	429.975	2169.934	199.974	3149.974	4349.972	199.974	
438	randn-500-1000	199.980	469.980	199.980	389.980	1349.975	199.977											
$r = 20, \lambda = 50, \text{time limit}=40$																		
439	w1a-2477-300	2499.912	2799.713	2199.819	2399.723	2499.708	3299.662	1999.667	TDT2-500-1000	2499.912	2199.802	1999.812	8799.310	2699.278	2499.257	1999.257		
440	20News-8000-1000	2699.480	2199.262	1999.440	2099.242	1999.230	3999.224	1999.222	sector-6412-1000	7799.995	4399.971	3009.998	4399.966	2199.952	3139.966	10149.964		
441	E2006-2000-1000	2099.977	3199.983	1999.284	2599.966	2599.905	4399.081	1999.077	E2006-2000-1000	1999.984	1199.984	11799.715	3199.922	3599.907	2799.981	1999.979		
442	MNIST-60000-784	1999.984	2199.980	4299.979	1999.980	4299.982	1449.982	1999.982	Gisette-3000-1000	1999.981	3399.997	3399.983	6799.938	1999.946	Cifar-1000-1000	1999.979	4999.979	1999.974
443	CnnCal-3000-1000	1999.981	2499.981	1999.982	11499.997	3399.975	14499.978	1999.974	Cifar-1000-1000	1999.979	14499.978	1999.979	14499.978	14499.978	14499.978	1999.977		
$r = 100, \text{time limit}=40$																		
444	w1a-2477-300	2499.912	2799.713	2199.819	2399.723	2499.708	3299.662	1999.667	TDT2-500-1000	2499.912	2199.802	1999.812	8799.310	2699.278	2499.257	1999.257		
445	20News-8000-1000	2699.480	2199.262	1999.440	2099.242	1999.230	3999.224	1999.222	sector-6412-1000	7799.995	4399.971	3009.998	4399.966	2199.952	3139.966	10149.964		
446	E2006-2000-1000	2099.977	3199.983	1999.284	2599.966	2599.905	4399.081	1999.077	E2006-2000-1000	1999.984	1199.984	11799.715	3199.922	3599.907	2799.981	1999.979		
447	MNIST-60000-784	1999.984	2199.980	4299.979	1999.980	4299.982	1449.982	1999.982	Gisette-3000-1000	1999.981	3399.997	3399.983	6799.938	1999.946	Cifar-1000-1000	1999.979	4999.979	1999.974
448	CnnCal-3000-1000	1999.981	2499.981	1999.982	11499.997	3399.975	14499.978	1999.974	Cifar-1000-1000	1999.979	14499.978	1999.979	14499.978	14499.978	14499.978	1999.977		
449	randn-500-1000	6699.980	4099.980	7899.977	2599.980	3299.980	9099.976	1999.977										
450	$r = 100, \text{time limit}=40$																	
451	w1a-2477-300	2499.912	2799.713	2199.819	2399.723	2499.708	3299.662	1999.667	TDT2-500-1000	2499.912	2199.802	1999.812	8799.310	2699.278	2499.257	1999.257		
452	20News-8000-1000	2699.480	2199.262	1999.440	2099.242	1999.230	3999.224	1999.222	sector-6412-1000	7799.995	4399.971	3009.998	4399.966	2199.952	3139.966	10149.964		
453	E2006-2000-1000	2099.977	3199.983	1999.284	2599.966	2599.905	4399.081	1999.077	E2006-2000-1000	1999.984	1199.984	11799.715	3199.922	3599.907	2799.981	1999.979		
454	MNIST-60000-784	1999.984	2199.980	4299.979	1999.980	4299.982	1449.982	1999.982	Gisette-3000-1000	1999.981	3399.997	3399.983	6799.938	1999.946	Cifar-1000-1000	1999.979	4999.979	1999.974
455	CnnCal-3000-1000	1999.981	2499.981	1999.982	11499.997	3399.975	14499.978	1999.974	Cifar-1000-1000	1999.979	14499.978	1999.979	14499.978	14499.978	14499.978	1999.977		
456	randn-500-1000	6699.980	4099.980	7899.977	2599.980	3299.980	9099.976	1999.977										

Table 1: Comparisons of objective values for L_0 -regularized SPCA. The 1st, 2nd, and 3rd best results are colored with red, green and blue, respectively.

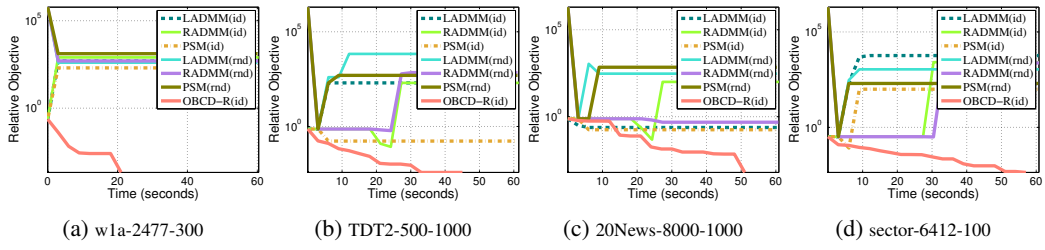


Figure 1: The convergence curve for solving L_0 -regularized SPCA with $\lambda = 100$. No matter how long the algorithms run, the other methods remain trapped in poor local minima.

- (a) If $\sigma = 0$, then the sequence \mathbf{X}^t converges in a finite number of steps in expectation.
- (b) If $\sigma \in (0, \frac{1}{2}]$, then there exist $\dot{c} > 0$ and $\dot{\tau} \in [0, 1)$ such that $\mathbb{E}_{\xi^{t-1}}[\|\mathbf{X}^t - \mathbf{X}^\infty\|_F] \leq \dot{c}\dot{\tau}^t$.
- (c) If $\sigma \in (\frac{1}{2}, 1)$, then there exist $\dot{c} > 0$ such that $\mathbb{E}_{\xi^{t-1}}[\|\mathbf{X}^t - \mathbf{X}^\infty\|_F] \leq \frac{\dot{c}}{t^\dot{\tau}}$, where $\dot{\tau} \triangleq \frac{1-\sigma}{2\sigma-1} > 0$.

Remark 4.12. When $F(\mathbf{X})$ is a semi-algebraic function and the desingularising function is $\varphi(t) = ct^{1-\sigma}$ for some $c > 0$ and $\sigma \in [0, 1)$, Theorem 4.11 shows that **OBCD** converges in finite iterations when $\sigma = 0$, with linear convergence when $\sigma \in (0, \frac{1}{2}]$, and sublinear convergence when $\sigma \in (\frac{1}{2}, 1)$ for the gap $\|\mathbf{X}^t - \mathbf{X}^\infty\|_F$ in expectation. These results are consistent with those in (Attouch et al., 2010).

5 EXPERIMENTS

This section presents numerical comparisons between **OBCD** and state-of-the-art methods on both real-world and synthetic data. We describe the application of L_0 -regularized SPCA in the sequel, while additional applications for L_1 -regularized SPCA and nonnegative PCA can be found in Appendix Section G.2.

► **Compared Methods on L_0 -Regularized SPCA.** We compare against three operator splitting methods: Linearized ADMM (LADMM) (Lai & Osher, 2014; He & Yuan, 2012), Riemannian ADMM (RADMM) (Li et al., 2024a), and the Penalty-based Splitting Method (PSM) (Yuan, 2024; Chen, 2012). Each method is initialized with either a random or identity matrix, yielding six variants: LADMM(id), RADMM(id), SPM(id), LADMM(rnd), RADMM(rnd), and PSM(rnd). For **OBCD**, we adopt a random working set strategy with identity initialization, denoted as **OBCD-R(id)**.

► **Implementations.** All methods are implemented in MATLAB on an Intel 2.6 GHz CPU with 32 GB RAM. However, our breakpoint searching procedure is developed in C++ and integrated into the MATLAB environment ², as it requires inefficient element-wise loops in native MATLAB. The code for all three applications used to reproduce the experiments can be found in the **supplemental material**.

²Although we prioritize accuracy over speed, the comparisons remain fair, as the other methods based on matrix multiplication and SVD rely on highly optimized BLAS and LAPACK libraries.

486 ▶ **Experiment Settings.** We compare objective values $F(\mathbf{X})$ for different methods after running for
 487 30 seconds. For numerical stability in reporting the objectives, we use the count of elements with
 488 absolute values greater than a threshold of 10^{-6} instead of the original ℓ_0 norm function $\|\mathbf{X}\|_0$. We
 489 set $\alpha = 10^{-5}$ for **OBCD**. Full-gradient methods have higher per-iteration complexity but require
 490 fewer iterations, while **OBCD**, as a partial-gradient method, has lower per-iteration costs but needs
 491 more iterations. Thus, we compare based on CPU time rather than iteration count.

492 ▶ **Experiment Results.** Table 1 and Figure 1 display accuracy and computational efficiency results
 493 for L_0 -regularized PCA, yielding the following observations: *(i)* **OBCD-R** delivers the best per-
 494 formance. *(ii)* Unlike other methods where objectives fluctuate during iterations, **OBCD-R** mono-
 495 tonically decreases the objective function while maintaining the orthogonality constraint. This is
 496 because **OBCD** is a greedy descent method for this problem class. *(iii)* While other methods of-
 497 ten get stuck in poor local minima, **OBCD-R** escapes from such minima and generally finds lower
 498 objectives, aligning with our theory that our methods locate *stronger stationary points*.

499 6 CONCLUSIONS

500 In this paper, we introduced **OBCD**, a new block coordinate descent method for nonsmooth compos-
 501 itive optimization under orthogonality constraints. **OBCD** operates on k rows of the solution matrix,
 502 offering lower computational complexity per iteration for $k \geq 2$. We also provide a novel optimality
 503 analysis, showing how **OBCD** exploits problem structure to escape bad local minima and find bet-
 504 ter stationary points than methods focused on critical points. Under the Kurdyka-Łojasiewicz (KL)
 505 inequality, we establish strong limit-point convergence. Additionally, we show how novel break-
 506 point search methods can be used to solve the subproblem when $k = 2$. Extensive experiments
 507 demonstrate that **OBCD** outperforms existing methods.

508
 509
 510
 511
 512
 513
 514
 515
 516
 517
 518
 519
 520
 521
 522
 523
 524
 525
 526
 527
 528
 529
 530
 531
 532
 533
 534
 535
 536
 537
 538
 539

540 LLM USAGE
541542 A large language model (LLM) was used to assist in refining the writing of this paper.
543544 REFERENCES
545546 Pierre Ablin and Gabriel Peyré. Fast and accurate optimization on the orthogonal manifold without
547 retraction. In *International Conference on Artificial Intelligence and Statistics*, pp. 5636–5657.
548 PMLR, 2022.549 Pierre Ablin, Simon Vary, Bin Gao, and Pierre-Antoine Absil. Infeasible deterministic, stochastic,
550 and variance-reduction algorithms for optimization under orthogonality constraints. *Journal of*
551 *Machine Learning Research*, 25(389):1–38, 2024.553 Traian E Abrudan, Jan Eriksson, and Visa Koivunen. Steepest descent algorithms for optimiza-
554 tion under unitary matrix constraint. *IEEE Transactions on Signal Processing*, 56(3):1134–1147,
555 2008.556 Pierre-Antoine Absil, Robert E. Mahony, and Rodolphe Sepulchre. *Optimization Algorithms on*
557 *Matrix Manifolds*. Princeton University Press, 2008.559 Hedy Attouch, Jérôme Bolte, Patrick Redont, and Antoine Soubeyran. Proximal alternating mini-
560 mization and projection methods for nonconvex problems: An approach based on the kurdyka-
561 lojasiewicz inequality. *Mathematics of Operations Research*, 35(2):438–457, 2010.562 Nitin Bansal, Xiaohan Chen, and Zhangyang Wang. Can we gain more from orthogonality regu-
563 larizations in training deep networks? *Advances in Neural Information Processing Systems*, 31,
564 2018.565 Amir Beck and Marc Teboulle. A fast iterative shrinkage-thresholding algorithm for linear inverse
566 problems. *SIAM journal on imaging sciences*, 2(1):183–202, 2009.568 Adel Bibi, Bernard Ghanem, Vladlen Koltun, and René Ranftl. Deep layers as stochastic solvers. In
569 *International Conference on Learning Representations (ICLR)*, 2019.571 Jérôme Bolte, Shoham Sabach, and Marc Teboulle. Proximal alternating linearized minimization
572 for nonconvex and nonsmooth problems. *Mathematical Programming*, 146(1-2):459–494, 2014.573 Arnaud Breloy, Sandeep Kumar, Ying Sun, and Daniel P Palomar. Majorization-minimization on the
574 stiefel manifold with application to robust sparse pca. *IEEE Transactions on Signal Processing*,
575 69:1507–1520, 2021.577 Shixiang Chen, Shiqian Ma, Anthony Man-Cho So, and Tong Zhang. Proximal gradient method
578 for nonsmooth optimization over the stiefel manifold. *SIAM Journal on Optimization*, 30(1):
579 210–239, 2020.580 Shixiang Chen, Shiqian Ma, Anthony Man-Cho So, and Tong Zhang. Nonsmooth optimization over
581 the stiefel manifold and beyond: Proximal gradient method and recent variants. *SIAM Review*, 66
582 (2):319–352, 2024.583 Weiqiang Chen, Hui Ji, and Yanfei You. An augmented lagrangian method for ℓ_1 -regularized opti-
584 mization problems with orthogonality constraints. *SIAM Journal on Scientific Computing*, 38(4):
585 B570–B592, 2016.587 Xiaojun Chen. Smoothing methods for nonsmooth, nonconvex minimization. *Mathematical pro-*
588 *gramming*, 134:71–99, 2012.589 Andy Yat-Ming Cheung, Jinxin Wang, Man-Chung Yue, and Anthony Man-Cho So. Random-
590 ized submanifold subgradient method for optimization over stiefel manifolds. *arXiv preprint*
591 *arXiv:2409.01770*, 2024.593 Minhyung Cho and Jaehyung Lee. Riemannian approach to batch normalization. *Advances in*
594 *Neural Information Processing Systems*, 30, 2017.

594 Michael Cogswell, Faruk Ahmed, Ross B. Girshick, Larry Zitnick, and Dhruv Batra. Reducing
 595 overfitting in deep networks by decorrelating representations. In Yoshua Bengio and Yann LeCun
 596 (eds.), *International Conference on Learning Representations (ICLR)*, 2016.

597

598 Alexandre d'Aspremont, Francis Bach, and Laurent El Ghaoui. Optimal solutions for sparse principal
 599 component analysis. *Journal of Machine Learning Research*, 9(7), 2008.

600 Alan Edelman, Tomás A. Arias, and Steven Thomas Smith. The geometry of algorithms with orthogonality
 601 constraints. *SIAM Journal on Matrix Analysis and Applications*, 20(2):303–353, 1998.

602

603 Thomas Frerix and Joan Bruna. Approximating orthogonal matrices with effective givens factorization.
 604 In *International Conference on Machine Learning (ICML)*, pp. 1993–2001, 2019.

605

606 Bin Gao, Xin Liu, Xiaojun Chen, and Ya-xiang Yuan. A new first-order algorithmic framework
 607 for optimization problems with orthogonality constraints. *SIAM Journal on Optimization*, 28(1):
 608 302–332, 2018.

609

610 Bin Gao, Xin Liu, and Ya-xiang Yuan. Parallelizable algorithms for optimization problems with
 611 orthogonality constraints. *SIAM Journal on Scientific Computing*, 41(3):A1949–A1983, 2019.

612

613 Gene H Golub and Charles F Van Loan. Matrix computations. 2013.

614

615 David H Gutman and Nam Ho-Nguyen. Coordinate descent without coordinates: Tangent subspace
 616 descent on riemannian manifolds. *Mathematics of Operations Research*, 48(1):127–159, 2023.

617

618 Bingsheng He and Xiaoming Yuan. On the $\mathcal{O}(1/n)$ convergence rate of the douglas-rachford alter-
 619 nating direction method. *SIAM Journal on Numerical Analysis*, 50(2):700–709, 2012.

620

621 Jiang Hu, Xin Liu, Zai-Wen Wen, and Ya-Xiang Yuan. A brief introduction to manifold optimiza-
 622 tion. *Journal of the Operations Research Society of China*, 8(2):199–248, 2020.

623

624 Feihu Huang and Shangqian Gao. Gradient descent ascent for minimax problems on riemannian
 625 manifolds. *IEEE Trans. Pattern Anal. Mach. Intell.*, 45(7):8466–8476, 2023.

626

627 Seong Jae Hwang, Maxwell D. Collins, Sathya N. Ravi, Vamsi K. Ithapu, Nagesh Adluru, Sterling C.
 628 Johnson, and Vikas Singh. A projection free method for generalized eigenvalue problem with a
 629 nonsmooth regularizer. In *IEEE International Conference on Computer Vision (ICCV)*, pp. 1841–
 630 1849, 2015.

631

632 Bo Jiang and Yu-Hong Dai. A framework of constraint preserving update schemes for optimization
 633 on stiefel manifold. *Mathematical Programming*, 153(2):535–575, 2015.

634

635 Bo Jiang, Ya-Feng Liu, and Zaiwen Wen. ℓ_p -norm regularization algorithms for optimization over
 636 permutation matrices. *SIAM Journal on Optimization*, 26(4):2284–2313, 2016.

637

638 Bo Jiang, Xiang Meng, Zaiwen Wen, and Xiaojun Chen. An exact penalty approach for optimization
 639 with nonnegative orthogonality constraints. *Mathematical Programming*, pp. 1–43, 2022.

640

641 Michel Journée, Yurii Nesterov, Peter Richtárik, and Rodolphe Sepulchre. Generalized power
 642 method for sparse principal component analysis. *Journal of Machine Learning Research*, 11
 643 (2), 2010.

644

645 Rongjie Lai and Stanley Osher. A splitting method for orthogonality constrained problems. *Journal
 646 of Scientific Computing*, 58(2):431–449, 2014.

647

648 Jiaxiang Li, Shiqian Ma, and Tejes Srivastava. A riemannian alternating direction method of multi-
 649 pliers. *Mathematics of Operations Research*, 2024a.

650

651 Xiao Li, Shixiang Chen, Zengde Deng, Qing Qu, Zhihui Zhu, and Anthony Man-Cho So. Weakly
 652 convex optimization over stiefel manifold using riemannian subgradient-type methods. *SIAM
 653 Journal on Optimization*, 31(3):1605–1634, 2021.

654

655 Yuchen Li, Laura Balzano, Deanna Needell, and Hanbaek Lyu. Convergence and complexity of
 656 block majorization-minimization for constrained block-riemannian optimization. *arXiv preprint
 657 arXiv:2312.10330*, 2023.

648 Yuchen Li, Laura Balzano, Deanna Needell, and Hanbaek Lyu. Convergence and complexity guar-
 649 antee for inexact first-order riemannian optimization algorithms. In *International Conference on*
 650 *Machine Learning (ICML)*, 2024b.

651

652 Huikang Liu, Weijie Wu, and Anthony Man-Cho So. Quadratic optimization with orthogonality
 653 constraints: Explicit lojasiewicz exponent and linear convergence of line-search methods. In
 654 *International Conference on Machine Learning (ICML)*, pp. 1158–1167, 2016.

655 Huikang Liu, Man-Chung Yue, and Anthony Man-Cho So. On the estimation performance and
 656 convergence rate of the generalized power method for phase synchronization. *SIAM Journal on*
 657 *Optimization*, 27(4):2426–2446, 2017.

658 Xin Liu, Xiao Wang, Zaiwen Wen, and Yaxiang Yuan. On the convergence of the self-consistent
 659 field iteration in kohn–sham density functional theory. *SIAM Journal on Matrix Analysis and*
 660 *Applications*, 35(2):546–558, 2014.

661

662 Zhihua Lu and Yi Zhang. An augmented lagrangian approach for sparse principal component anal-
 663 ysis. *Mathematical Programming*, 135(1-2):149–193, 2012.

664 Hanbaek Lyu and Yuchen Li. Block majorization-minimization with diminishing radius for con-
 665 strained nonsmooth nonconvex optimization. *SIAM Journal on Optimization*, 35(2):842–871,
 666 2025.

667

668 Julien Mairal. Optimization with first-order surrogate functions. In *International Conference on*
 669 *Machine Learning (ICML)*, volume 28, pp. 783–791, 2013.

670 Estelle Massart and Vinayak Abrol. Coordinate descent on the orthogonal group for recurrent neu-
 671 ral network training. In *Proceedings of the AAAI Conference on Artificial Intelligence (AAAI)*,
 672 volume 36, pp. 7744–7751, 2022.

673

674 Boris S. Mordukhovich. Variational analysis and generalized differentiation i: Basic theory. *Berlin*
 675 *Springer*, 330, 2006.

676

677 Yurii Nesterov. *Introductory lectures on convex optimization: A basic course*, volume 87. Springer
 678 Science & Business Media, 2003.

679

680 Feiping Nie, Jingjing Xue, Danyang Wu, Rong Wang, Hui Li, and Xuelong Li. Coordinate descent
 681 method for k-means. *IEEE Transactions on Pattern Analysis and Machine Intelligence*, 44(5):
 682 2371–2385, 2022.

683

684 Yitian Qian, Shaohua Pan, and Lianghai Xiao. Exact penalty methods for minimizing a smooth
 685 function over the nonnegative orthogonal set. *arXiv*, 11 2021.

686

687 Hugo Raguet, Jalal Fadili, and Gabriel Peyré. A generalized forward-backward splitting. *SIAM*
 688 *Journal on Imaging Sciences*, 6(3):1199–1226, 2013.

689

690 Meisam Razaviyayn, Mingyi Hong, and Zhi-Quan Luo. A unified convergence analysis of block
 691 successive minimization methods for nonsmooth optimization. *SIAM Journal on Optimization*,
 692 23(2):1126–1153, 2013.

693

694 R. Tyrrell Rockafellar and Roger J-B. Wets. Variational analysis. *Springer Science & Business*
 695 *Media*, 317, 2009.

696

697 Uri Shalit and Gal Chechik. Coordinate-descent for learning orthogonal matrices through givens
 698 rotations. In *International Conference on Machine Learning (ICML)*, pp. 548–556. PMLR, 2014.

699

700 Xiaobai Sun and Christian Bischof. A basis-kernel representation of orthogonal matrices. *SIAM*
 701 *Journal on Matrix Analysis and Applications*, 16(4):1184–1196, 1995.

702

703 Ying Sun, Prabhu Babu, and Daniel P Palomar. Majorization-minimization algorithms in signal
 704 processing, communications, and machine learning. *IEEE Transactions on Signal Processing*, 65
 705 (3):794–816, 2016.

706

707 Paul Tseng and Sangwoon Yun. A coordinate gradient descent method for nonsmooth separable
 708 minimization. *Mathematical Programming*, 117(1-2):387–423, 2009.

702 Simon Vary, Pierre Ablin, Bin Gao, and P.-A. Absil. Optimization without retraction on the random
 703 generalized stiefel manifold. In *International Conference on Machine Learning (ICML)*.
 704

705 Vincent Q Vu, Juhee Cho, Jing Lei, and Karl Rohe. Fantope projection and selection: A near-optimal
 706 convex relaxation of sparse pca. *Advances in Neural Information Processing Systems (NeurIPS)*,
 707 26, 2013.

708 Zaiwen Wen and Wotao Yin. A feasible method for optimization with orthogonality constraints.
 709 *Mathematical Programming*, 142(1-2):397, 2013.

710 WikiContributors. Quartic equation: https://en.wikipedia.org/wiki/Quartic_equation. pp. Last edited in March, 2023.

713 Nachuan Xiao, Xin Liu, and Ya-xiang Yuan. A class of smooth exact penalty function methods for
 714 optimization problems with orthogonality constraints. *Optimization Methods and Software*, 37
 715 (4):1205–1241, 2022.

716 Di Xie, Jiang Xiong, and Shiliang Pu. All you need is beyond a good init: Exploring better solution
 717 for training extremely deep convolutional neural networks with orthonormality and modulation.
 718 In *IEEE Conference on Computer Vision and Pattern Recognition*, pp. 6176–6185, 2017.

720 Yangyang Xu and Wotao Yin. A block coordinate descent method for regularized multiconvex
 721 optimization with applications to nonnegative tensor factorization and completion. *SIAM Journal*
 722 *on Imaging Sciences*, 6(3):1758–1789, 2013.

724 Ganzhao Yuan. Smoothing proximal gradient methods for nonsmooth sparsity constrained optimiza-
 725 tion: Optimality conditions and global convergence. In *International Conference on Machine*
 726 *Learning*, 2024.

727 Ron Zass and Amnon Shashua. Nonnegative sparse PCA. *Advances in Neural Information Process-
 728 ing Systems (NeurIPS)*, pp. 1561–1568, 2006.

729 Jinshan Zeng, Tim Tsz-Kit Lau, Shaobo Lin, and Yuan Yao. Global convergence of block coordinate
 730 descent in deep learning. In *International Conference on Machine Learning (ICML)*, pp. 7313–
 731 7323. PMLR, 2019.

733 Yuexiang Zhai, Zitong Yang, Zhenyu Liao, John Wright, and Yi Ma. Complete dictionary learning
 734 via l_4 -norm maximization over the orthogonal group. *Journal of Machine Learning Research*, 21
 735 (165):1–68, 2020.

736 Junyu Zhang, Shiqian Ma, and Shuzhong Zhang. Primal-dual optimization algorithms over rieman-
 737 nian manifolds: an iteration complexity analysis. *Mathematical Programming*, pp. 1–46, 2019.

739 Xin Zhang, Jinwei Zhu, Zaiwen Wen, and Aihui Zhou. Gradient type optimization methods for
 740 electronic structure calculations. *SIAM Journal on Scientific Computing*, 36(3):265–289, 2014.

741
 742
 743
 744
 745
 746
 747
 748
 749
 750
 751
 752
 753
 754
 755

756 Appendix

758 The appendix section is organized as follows.

759 Section A covers notations, technical preliminaries, and relevant lemmas.

760 Section B shows how to solve the subproblem when $k = 2$.

761 Section C offers further discussions on the proposed algorithm.

762 Section D contains proofs from Section 2.

763 Section E contains proofs from Section 3.

764 Section F contains proofs from Section 4.

765 Section G presents additional experiment details and results.

770 A NOTATIONS, TECHNICAL PRELIMINARIES, AND RELEVANT LEMMAS

771 A.1 NOTATIONS

772 Throughout this paper, $\mathcal{M} \triangleq \text{St}(n, r)$ denotes the Stiefel manifold, which is an embedded submanifold of the Euclidean space $\mathbb{R}^{n \times r}$. Boldfaced lowercase letters denote vectors and uppercase letters denote real-valued matrices. We adopt the Matlab colon notation to denote indices that describe submatrices. For given natural numbers n and k , we use $\{\mathcal{B}_1, \mathcal{B}_2, \dots, \mathcal{B}_{C_n^k}\}$ to denote all the possible combinations of the index vectors choosing k items from n without repetition, where C_n^k is the total number of such combinations and $\mathcal{B}_i \in \mathbb{N}^k$, $\forall i \in [C_n^k]$. For any one-dimensional function $p(t) : \mathbb{R} \mapsto \mathbb{R}$, we define: $p(\pm x \mp y) \triangleq \min\{p(x - y), p(-x + y)\}$. We use the following notations in this paper.

- 783 • $[n] : \{1, 2, \dots, n\}$
- 784 • $\|\mathbf{x}\|$: Euclidean norm: $\|\mathbf{x}\| = \|\mathbf{x}\|_2 = \sqrt{\langle \mathbf{x}, \mathbf{x} \rangle}$
- 785 • \mathbf{x}_i : the i -th element of vector \mathbf{x}
- 786 • $\mathbf{X}_{i,j}$ or \mathbf{X}_{ij} : the (i th, j th) element of matrix \mathbf{X}
- 787 • $\text{vec}(\mathbf{X})$: $\text{vec}(\mathbf{X}) \in \mathbb{R}^{nr \times 1}$, the vector formed by stacking the column vectors of \mathbf{X}
- 788 • $\text{mat}(\mathbf{x})$: $\text{mat}(\mathbf{x}) \in \mathbb{R}^{n \times r}$, Convert $\mathbf{x} \in \mathbb{R}^{nr \times 1}$ into a matrix with $\text{mat}(\text{vec}(\mathbf{X})) = \mathbf{X}$
- 789 • \mathbf{X}^\top : the transpose of the matrix \mathbf{X}
- 790 • $\text{sign}(t)$: the signum function, $\text{sign}(t) = 1$ if $t \geq 0$ and $\text{sign}(t) = -1$ otherwise
- 791 • $\det(\mathbf{D})$: Determinant of a square matrix $\mathbf{D} \in \mathbb{R}^{n \times n}$
- 792 • C_n^k : the number of possible combinations choosing k items from n without repetition
- 793 • $\mathbf{0}_{n,r}$: A zero matrix of size $n \times r$; the subscript is omitted sometimes
- 794 • \mathbf{I}_r : $\mathbf{I}_r \in \mathbb{R}^{r \times r}$, Identity matrix
- 795 • $\mathbf{X} \succeq \mathbf{0}$ (or $\succ \mathbf{0}$) : the Matrix \mathbf{X} is symmetric positive semidefinite (or definite)
- 796 • $\text{tr}(\mathbf{A})$: Sum of the elements on the main diagonal \mathbf{X} : $\text{tr}(\mathbf{A}) = \sum_i \mathbf{A}_{i,i}$
- 797 • $\langle \mathbf{X}, \mathbf{Y} \rangle$: Euclidean inner product, i.e., $\langle \mathbf{X}, \mathbf{Y} \rangle = \sum_{ij} \mathbf{X}_{ij} \mathbf{Y}_{ij}$
- 798 • $\mathbf{X} \otimes \mathbf{Y}$: Kronecker product of \mathbf{X} and \mathbf{Y}
- 799 • $\|\mathbf{X}\|_{\text{F}}$: Frobenius norm: $(\sum_{ij} \mathbf{X}_{ij}^2)^{1/2}$
- 800 • $\|\mathbf{X}\|_{\text{sp}}$: Operator/Spectral norm: the largest singular value of \mathbf{X}
- 801 • $\|\mathbf{X}\|_0$: the number of non-zero elements in the matrix \mathbf{X}
- 802 • $\|\mathbf{X}\|_1$: the absolute sum of the elements in the matrix \mathbf{X} with $\|\mathbf{X}\|_1 = \sum_{i,j} |\mathbf{X}_{i,j}|$
- 803 • $\|\max(|\mathbf{X}|, \tau)\|_1$: the capped- ℓ_1 norm of \mathbf{X} with $\|\max(|\mathbf{X}|, \tau)\|_1 = \sum_{i,j} \max(|\mathbf{X}_{i,j}|, \tau)$
- 804 • $\nabla f(\mathbf{X})$: Euclidean gradient of $f(\mathbf{X})$ at \mathbf{X}
- 805 • $\nabla_{\mathcal{M}} f(\mathbf{X})$: Riemannian gradient of $f(\mathbf{X})$ at \mathbf{X}

- $\partial F(\mathbf{X})$: limiting Euclidean subdifferential of $F(\mathbf{X})$ at \mathbf{X}
- $\partial_{\mathcal{M}} F(\mathbf{X})$: limiting Riemannian subdifferential of $F(\mathbf{X})$ at \mathbf{X}
- $\iota_{\Xi}(\mathbf{X})$: the indicator function of a set Ξ with $\iota_{\Xi}(\mathbf{X}) = 0$ if $\mathbf{X} \in \Xi$ and otherwise $+\infty$
- $\iota_{\geq 0}(\mathbf{X})$: indicator function of non-negativity constraint with $\iota_{\geq 0}(\mathbf{X}) = \begin{cases} 0, & \mathbf{X} \geq \mathbf{0}; \\ \infty, & \text{else.} \end{cases}$
- $\mathbb{P}_{\Xi}(\mathbf{Z})$: Orthogonal projection of \mathbf{Z} with $\mathbb{P}_{\Xi}(\mathbf{Z}) = \arg \min_{\mathbf{Z} \in \Xi} \|\mathbf{Z} - \mathbf{X}\|_F^2$
- $\mathbb{P}_{\mathcal{M}}(\mathbf{Y})$: Nearest orthogonal matrix of \mathbf{Y} with $\mathbb{P}_{\mathcal{M}}(\mathbf{Y}) = \arg \min_{\mathbf{X}^T \mathbf{X} = \mathbf{I}_r} \|\mathbf{X} - \mathbf{Y}\|_F^2$
- $\text{dist}(\Xi, \Xi')$: the distance between two sets with $\text{dist}(\Xi, \Xi') \triangleq \inf_{\mathbf{X} \in \Xi, \mathbf{X}' \in \Xi'} \|\mathbf{X} - \mathbf{X}'\|_F$
- $\mathbb{A} + \mathbb{B}, \mathbb{A} - \mathbb{B}$: standard Minkowski addition and subtraction between sets \mathbb{A} and \mathbb{B}
- $\mathbb{A} \oplus \mathbb{B}, \mathbb{A} \ominus \mathbb{B}$: element-wise addition and subtraction between sets \mathbb{A} and \mathbb{B}
- $\|\partial F(\mathbf{X})\|_F$: the distance from the origin to $\partial F(\mathbf{X})$ with $\|\partial F(\mathbf{X})\|_F = \inf_{\mathbf{Y} \in \partial F(\mathbf{X})} \|\mathbf{Y}\|_F$

A.2 TECHNICAL PRELIMINARIES

As the function $F(\cdot)$ can be non-convex and non-smooth, we introduce some tools in non-smooth analysis (Mordukhovich, 2006; Rockafellar & Wets., 2009). The domain of any extended real-valued function $F : \mathbb{R}^{n \times r} \rightarrow (-\infty, +\infty]$ is defined as $\text{dom}(F) \triangleq \{\mathbf{X} \in \mathbb{R}^{n \times r} : |F(\mathbf{X})| < +\infty\}$. The Fréchet subdifferential of F at $\mathbf{X} \in \text{dom}(F)$ is defined as

$$\hat{\partial}F(\mathbf{X}) \triangleq \{\boldsymbol{\xi} \in \mathbb{R}^{n \times r} : \lim_{\mathbf{Z} \rightarrow \mathbf{X}, \mathbf{Z} \neq \mathbf{X}} \inf_{\mathbf{Z} \neq \mathbf{X}} \frac{F(\mathbf{Z}) - F(\mathbf{X}) - \langle \boldsymbol{\xi}, \mathbf{Z} - \mathbf{X} \rangle}{\|\mathbf{Z} - \mathbf{X}\|_F} \geq 0\},$$

while the limiting subdifferential of $F(\mathbf{X})$ at $\mathbf{X} \in \text{dom}(F)$ is denoted as

$$\partial F(\mathbf{X}) \triangleq \{\boldsymbol{\xi} \in \mathbb{R}^n : \exists \mathbf{X}^t \rightarrow \mathbf{X}, F(\mathbf{X}^t) \rightarrow F(\mathbf{X}), \boldsymbol{\xi}^t \in \hat{\partial}F(\mathbf{X}^t) \rightarrow \boldsymbol{\xi}, \forall t\}.$$

We denote $\nabla F(\mathbf{X})$ as the gradient of $F(\cdot)$ at \mathbf{X} in the Euclidean space. We have the following relation between $\hat{\partial}F(\mathbf{X})$, $\partial F(\mathbf{X})$, and $\nabla F(\mathbf{X})$. (i) It holds that $\hat{\partial}F(\mathbf{X}) \subseteq \partial F(\mathbf{X})$. (ii) If the function $F(\cdot)$ is convex, $\partial F(\mathbf{X})$ and $\hat{\partial}F(\mathbf{X})$ essentially the classical subdifferential for convex functions, i.e.,

$$\partial F(\mathbf{X}) = \hat{\partial}F(\mathbf{X}) = \{\boldsymbol{\xi} \in \mathbb{R}^{n \times r} : F(\mathbf{Z}) \geq F(\mathbf{X}) + \langle \boldsymbol{\xi}, \mathbf{Z} - \mathbf{X} \rangle, \forall \mathbf{Z} \in \mathbb{R}^{n \times r}\}.$$

(iii) If the function $F(\cdot)$ is differentiable, then $\hat{\partial}F(\mathbf{X}) = \partial F(\mathbf{X}) = \{\nabla F(\mathbf{X})\}$.

We need some prerequisite knowledge in optimization with orthogonality constraints (Absil et al., 2008). The nearest orthogonality matrix to an arbitrary matrix $\mathbf{Y} \in \mathbb{R}^{n \times r}$ is given by $\mathbb{P}_{\mathcal{M}}(\mathbf{Y}) = \hat{\mathbf{U}}\hat{\mathbf{V}}^T$, where $\mathbf{Y} = \hat{\mathbf{U}}\text{Diag}(\mathbf{s})\hat{\mathbf{V}}^T$ is the singular value decomposition of \mathbf{Y} . We use $\mathcal{N}_{\mathcal{M}}(\mathbf{X})$ to denote the limiting normal cone to \mathcal{M} at \mathbf{X} , leading to

$$\mathcal{N}_{\mathcal{M}}(\mathbf{X}) = \partial \iota_{\mathcal{M}}(\mathbf{X}) = \{\mathbf{Z} \in \mathbb{R}^{n \times r} : \langle \mathbf{Z}, \mathbf{X} \rangle \geq \langle \mathbf{Z}, \mathbf{Y} \rangle, \forall \mathbf{Y} \in \mathcal{M}\}.$$

The tangent and norm space to \mathcal{M} at $\mathbf{X} \in \mathcal{M}$ are denoted as $T_{\mathbf{X}}\mathcal{M}$ and $N_{\mathbf{X}}\mathcal{M}$, respectively. For a given $\mathbf{X} \in \mathcal{M}$, we let $\mathcal{A}_{\mathbf{X}}(\mathbf{Y}) \triangleq \mathbf{X}^T \mathbf{Y} + \mathbf{Y}^T \mathbf{X}$ for $\mathbf{Y} \in \mathbb{R}^{n \times r}$, and we have $T_{\mathbf{X}}\mathcal{M} = \{\mathbf{Y} \in \mathbb{R}^{n \times r} | \mathcal{A}_{\mathbf{X}}(\mathbf{Y}) = \mathbf{0}\}$ and $N_{\mathbf{X}}\mathcal{M} = \{2\mathbf{X}\boldsymbol{\Lambda} | \boldsymbol{\Lambda} = \boldsymbol{\Lambda}^T, \boldsymbol{\Lambda} \in \mathbb{R}^{r \times r}\}$. For any non-convex and non-smooth function $F(\mathbf{X})$, we use $\partial_{\mathcal{M}} F(\mathbf{X})$ to denote the limiting Riemannian gradient of $F(\mathbf{X})$ at \mathbf{X} , and obtain $\partial_{\mathcal{M}} F(\mathbf{X}) = \mathbb{P}_{T_{\mathbf{X}}\mathcal{M}}(\partial F(\mathbf{X}))$. We denote $\partial F(\mathbf{X}) \ominus \mathbf{X}[\partial F(\mathbf{X})]^T \mathbf{X} \triangleq \{\mathbf{E} | \mathbf{E} = \mathbf{G} - \mathbf{X}\mathbf{G}^T \mathbf{X}, \mathbf{G} \in \partial F(\mathbf{X})\}$.

A.3 RELEVANT LEMMAS

We offer a set of useful lemmas, each of which stands independently of context and specific methodology.

Lemma A.1. *Let $k \geq 2$ and $\mathbf{W} \in \mathbb{R}^{n \times n}$. If $\mathbf{0}_{k,k} = \mathbf{U}_B^T \mathbf{W} \mathbf{U}_B$ for all $B \in \{\mathcal{B}_i\}_{i=1}^{C_n^k}$, then $\mathbf{W} = \mathbf{0}$. Here, the set $\{\mathcal{B}_1, \mathcal{B}_2, \dots, \mathcal{B}_{C_n^k}\}$ represents all possible combinations of the index vectors choosing k items from n without repetition.*

864 *Proof.* The proof is straightforward and relies on elementary reasoning.
 865

866 Notably, the conclusion of this lemma does not necessarily hold if $|\mathcal{B}| = k = 1$. This is because
 867 any matrix $\mathbf{W} \in \mathbb{R}^{n \times n}$ with $\mathbf{W}_{ii} = 0$ for all $i \in [n]$ satisfies the condition of this lemma but is not
 868 necessarily a zero matrix. \square

869 **Lemma A.2.** *For any matrices $\mathbf{A} \in \mathbb{R}^{k \times k}$ and $\mathbf{C} \in \mathbb{R}^{k \times k}$, we have:*

$$870 \quad \|\mathbf{A} - \mathbf{A}^\top\|_F \leq 2\|\mathbf{A} - \mathbf{C}\|_F + \|\mathbf{C} - \mathbf{C}^\top\|_F.$$

872 *Proof.* We derive: $\|\mathbf{A} - \mathbf{A}^\top\|_F = \|(\mathbf{A} - \mathbf{C}) + (\mathbf{C} - \mathbf{C}^\top) + (\mathbf{C}^\top - \mathbf{A}^\top)\|_F \stackrel{\textcircled{1}}{\leq} \|\mathbf{A} - \mathbf{C}\|_F + \|\mathbf{C} - \mathbf{C}^\top\|_F + \|\mathbf{C}^\top - \mathbf{A}^\top\|_F = 2\|\mathbf{A} - \mathbf{C}\|_F + \|\mathbf{C} - \mathbf{C}^\top\|_F$, where step ① uses the triangle inequality.

875 \square

876 **Lemma A.3.** *Let $\tau \in \mathbb{R}$, and $\mathbf{A} \in \mathbb{R}^{2 \times 2}$ be any skew-symmetric matrix with $\mathbf{A}^\top = -\mathbf{A}$. We have:*

$$878 \quad \det\left((\mathbf{I}_2 + \frac{\tau}{2}\mathbf{A})^{-1}(\mathbf{I}_k - \frac{\tau}{2}\mathbf{A})\right) = 1.$$

880 *Proof.* Since \mathbf{A} is a two-dimensional matrix, it can be expressed in the form: $\mathbf{A} = \begin{pmatrix} 0 & a \\ -a & 0 \end{pmatrix}$ for some
 881 $a \in \mathbb{R}$. Letting $b = \frac{\tau}{2}a$, we derive:

$$883 \quad \mathbf{Q} \triangleq (\mathbf{I}_2 + \frac{\tau}{2}\mathbf{A})^{-1}(\mathbf{I}_k - \frac{\tau}{2}\mathbf{A}) \stackrel{\textcircled{1}}{=} \begin{pmatrix} 1 & b \\ -b & 1 \end{pmatrix}^{-1} \stackrel{\textcircled{2}}{=} \frac{1}{1+b^2} \begin{pmatrix} 1 & -b \\ b & 1 \end{pmatrix} \begin{pmatrix} 1 & -b \\ b & 1 \end{pmatrix} = \frac{1}{1+b^2} \begin{pmatrix} 1-b^2 & -2b \\ 2b & 1-b^2 \end{pmatrix},$$

884 where step ① uses $\frac{\tau}{2}\mathbf{A} = \begin{pmatrix} 0 & b \\ -b & 0 \end{pmatrix}$; step ② uses the fact that $\begin{pmatrix} a & b \\ c & d \end{pmatrix}^{-1} = \frac{1}{ad-bc} \begin{pmatrix} d & -b \\ -c & a \end{pmatrix}^{-1}$ for all
 885 $a, b, c, d \in \mathbb{R}$. We further obtain: $\det(\mathbf{Q}) \stackrel{\textcircled{1}}{=} \frac{1-b^2}{1+b^2} \cdot \frac{1-b^2}{1+b^2} - \frac{2b}{1+b^2} \cdot \frac{-2b}{1+b^2} = \frac{(1-b^2)^2 + 4b^2}{(1+b^2)^2} = \frac{(1+b^2)^2}{(1+b^2)^2} = 1$,
 886 where step ① uses the fact that $\det\begin{pmatrix} a & b \\ c & d \end{pmatrix} = ad - bc$ for all $a, b, c, d \in \mathbb{R}$.
 887 \square

889 **Lemma A.4.** *For any $\mathbf{W} \in \mathbb{R}^{n \times n}$, we have*

$$892 \quad \sum_{i=1}^{C_n^k} \|\mathbf{W}(\mathcal{B}_i, \mathcal{B}_i)\|_F^2 = C_{n-2}^{k-2} \sum_i \sum_{j,j \neq i} \mathbf{W}_{ij}^2 + \frac{k}{n} C_n^k \sum_i \mathbf{W}_{ii}^2.$$

895 *Here, the set $\{\mathcal{B}_1, \mathcal{B}_2, \dots, \mathcal{B}_{C_n^k}\}$ represents all possible combinations of the index vectors choosing k
 896 items from n without repetition.*

897 *Proof.* For any matrix $\mathbf{W} \in \mathbb{R}^{n \times n}$, we define: $\mathbf{w} \triangleq \text{diag}(\mathbf{W}) \in \mathbb{R}^n$, and $\mathbf{W}' \triangleq \mathbf{W} - \text{Diag}(\mathbf{w})$.

898 We have: $\mathbf{W} = \text{Diag}(\mathbf{w}) + \mathbf{W}'$, this leads to the following decomposition:

$$900 \quad \sum_{i=1}^{C_n^k} \|\mathbf{U}_{\mathcal{B}_i}^\top \mathbf{W} \mathbf{U}_{\mathcal{B}_i}\|_F^2 = \sum_{i=1}^{C_n^k} \|\mathbf{U}_{\mathcal{B}_i}^\top (\text{Diag}(\mathbf{w}) + \mathbf{W}') \mathbf{U}_{\mathcal{B}_i}\|_F^2 \\ 902 \quad = \underbrace{\sum_{i=1}^{C_n^k} \|\mathbf{U}_{\mathcal{B}_i}^\top \text{Diag}(\mathbf{w}) \mathbf{U}_{\mathcal{B}_i}\|_F^2}_{\Gamma_1} + \underbrace{\sum_{i=1}^{C_n^k} \|\mathbf{U}_{\mathcal{B}_i}^\top \mathbf{W}' \mathbf{U}_{\mathcal{B}_i}\|_F^2}_{\Gamma_2}. \quad (12)$$

905 We first focus on the term Γ_1 . We have:

$$906 \quad \Gamma_1 = \sum_{i=1}^{C_n^k} \|\mathbf{U}_{\mathcal{B}_i}^\top \text{Diag}(\mathbf{w}) \mathbf{U}_{\mathcal{B}_i}\|_F^2 \stackrel{\textcircled{1}}{=} \sum_{i=1}^{C_n^k} \|\mathbf{w}_{\mathcal{B}_i}\|_2^2 \stackrel{\textcircled{2}}{=} C_n^k \cdot \frac{k}{n} \cdot \|\mathbf{w}\|_2^2 = C_n^k \cdot \frac{k}{n} \cdot \sum_i \mathbf{W}_{ii}^2, \quad (13)$$

908 where step ① uses the fact that $\|\mathbf{B}^\top \text{Diag}(\mathbf{w}) \mathbf{B}\|_F^2 = \|\text{Diag}(\mathbf{w})\|_{\mathbf{B}\mathbf{B}}^2 = \|\mathbf{w}_{\mathbf{B}}\|_2^2$ for any $\mathbf{B} \in \{\mathcal{B}_i\}_{i=1}^{C_n^k}$;
 909 step ② uses the observation that \mathbf{w}_i appears in the term $\sum_{i=1}^{C_n^k} \|\mathbf{w}_{\mathcal{B}_i}\|_2^2$ a total of $(C_n^k \cdot \frac{k}{n})$ times, which
 910 can be deduced using basic induction.

911 We now focus on the term Γ_2 . Noticing that $\mathbf{W}'_{ii} = 0$ for all $i \in [n]$, we have:

$$913 \quad \Gamma_2 = \sum_{i=1}^{C_n^k} \|\mathbf{U}_{\mathcal{B}_i}^\top \mathbf{W}' \mathbf{U}_{\mathcal{B}_i}\|_F^2 \stackrel{\textcircled{1}}{=} \sum_i \sum_{j \neq i} [C_{n-2}^{k-2} (\mathbf{W}'_{ij})^2] \stackrel{\textcircled{2}}{=} C_{n-2}^{k-2} \sum_i \sum_{j \neq i} (\mathbf{W}_{ij})^2, \quad (14)$$

915 where step ① uses the fact that the term $\sum_{i=1}^{C_n^k} \|\mathbf{U}_{\mathcal{B}_i}^\top \mathbf{W}' \mathbf{U}_{\mathcal{B}_i}\|_F^2$ comprises C_{n-2}^{k-2} distinct patterns,
 916 each including $\{i, j\}$ with $i \neq j$; step ② uses $\sum_{i,j \neq i} (\mathbf{W}_{ij})^2 = \sum_{i,j \neq i} (\mathbf{W}'_{ij})^2$.

917 In view of Equalities (12), (13), and (14), we complete the proof of this lemma. \square

918 **Lemma A.5.** Assume $\mathbf{Q}\mathbf{R} = \mathbf{X} \in \mathbb{R}^{n \times n}$, where $\mathbf{Q} \in \text{St}(n, n)$ and \mathbf{R} is a lower triangular matrix
 919 with $\mathbf{R}_{i,j} = 0$ for all $i < j$. If $\mathbf{X} \in \text{St}(n, n)$, then \mathbf{R} is a diagonal matrix with $\mathbf{R}_{i,i} \in \{-1, +1\}$ for
 920 all $i \in [n]$.
 921

922 *Proof.* We derive: $\mathbf{R}\mathbf{R}^\top \stackrel{\textcircled{1}}{=} (\mathbf{Q}\mathbf{X})(\mathbf{Q}\mathbf{X})^\top = \mathbf{Q}\mathbf{X}\mathbf{X}^\top\mathbf{Q}^\top \stackrel{\textcircled{2}}{=} \mathbf{I}$, where step ① uses $\mathbf{R} = \mathbf{Q}^\top\mathbf{X}$; step
 923 ② uses $\mathbf{X} \in \text{St}(n, n)$ and $\mathbf{Q} \in \text{St}(n, n)$. First, given $\|\mathbf{R}(1, :)\| = 1$ and $\mathbf{R}(1, 2:n) = 0$, we have
 924 $\mathbf{R}_{1,1} \in \{-1, +1\}$. Second, we have $\|\mathbf{R}(2, :)\| = 1$ and $\mathbf{R}(1, :)^T\mathbf{R}(:, 2) = 0$, leading to $\mathbf{R}_{1,2} = 0$
 925 and $\mathbf{R}_{2,2} \in \{-1, +1\}$. Finally, using similar recursive strategy, we conclude that \mathbf{R} is a diagonal
 926 matrix with $\mathbf{R}_{i,i} \in \{-1, +1\}$ for all $i \in [n]$. \square
 927

928 **Lemma A.6.** We define $\text{T}_{\mathbf{X}}\mathcal{M} \triangleq \{\mathbf{Y} \in \mathbb{R}^{n \times r} \mid \mathcal{A}_{\mathbf{X}}(\mathbf{Y}) = \mathbf{0}\}$ and $\mathcal{A}_{\mathbf{X}}(\mathbf{Y}) \triangleq \mathbf{X}^\top\mathbf{Y} + \mathbf{Y}^\top\mathbf{X}$. For
 929 any $\mathbf{G} \in \mathbb{R}^{n \times r}$ and $\mathbf{X} \in \text{St}(n, k)$, we have:

$$(\mathbf{G} - \frac{1}{2}\mathbf{X}\mathcal{A}_{\mathbf{X}}(\mathbf{G})) = \arg \min_{\mathbf{Y} \in \text{T}_{\mathbf{X}}\mathcal{M}} \|\mathbf{Y} - \mathbf{G}\|_F^2.$$

933 *Proof.* The conclusion of this lemma can be found in (Absil et al., 2008). For completeness, we
 934 present a short proof.
 935

936 Consider the convex problem: $\bar{\mathbf{Y}} = \arg \min_{\mathbf{Y}} \|\mathbf{Y} - \mathbf{G}\|_F^2$, s.t. $\mathbf{X}^\top\mathbf{Y} + \mathbf{Y}^\top\mathbf{X} = \mathbf{0}$. Introducing
 937 a multiplier $\Lambda \in \mathbb{R}^{r \times r}$ for the linear constraints leads to the following Lagrangian function:
 938 $\tilde{\mathcal{L}}(\mathbf{Y}; \Lambda) = \|\mathbf{Y} - \mathbf{G}\|_F^2 + \langle \mathbf{X}^\top\mathbf{Y} + \mathbf{Y}^\top\mathbf{X}, \Lambda \rangle$. We derive the subsequent first-order optimality
 939 condition: $2(\mathbf{Y} - \mathbf{G}) + \mathbf{X}(\Lambda + \Lambda^\top) = \mathbf{0}$, and $\mathbf{X}^\top\mathbf{Y} + \mathbf{Y}^\top\mathbf{X} = \mathbf{0}$. Given Λ is symmetric, we have $\mathbf{Y} = \mathbf{G} - \mathbf{X}\Lambda$. Incorporating this result into $\mathbf{X}^\top\mathbf{Y} + \mathbf{Y}^\top\mathbf{X} = \mathbf{0}$, we obtain:
 940 $\mathbf{X}^\top(\mathbf{G} - \mathbf{X}\Lambda) + (\mathbf{G} - \mathbf{X}\Lambda)^\top\mathbf{X} = \mathbf{0}$. Given $\mathbf{X} \in \text{St}(n, r)$, we have $\mathbf{X}^\top\mathbf{G} - \Lambda + \mathbf{G}^\top\mathbf{X} - \Lambda^\top = \mathbf{0}$,
 941 leading to: $\Lambda = \frac{1}{2}(\mathbf{X}^\top\mathbf{G} + \mathbf{G}^\top\mathbf{X})$. Therefore, the optimal solution $\bar{\mathbf{Y}}$ can be computed as
 942 $\bar{\mathbf{Y}} = \mathbf{G} - \mathbf{X}\Lambda = \mathbf{G} - \frac{1}{2}\mathbf{X}(\mathbf{X}^\top\mathbf{G} + \mathbf{G}^\top\mathbf{X})$.
 943 \square

945 **Lemma A.7.** Consider the following problem: $\min_{\mathbf{X}} F_\iota(\mathbf{X}) \triangleq F(\mathbf{X}) + \iota_{\mathcal{M}}(\mathbf{X})$, where $F(\mathbf{X})$ is
 946 defined in Equation (1). For any $\mathbf{X} \in \text{St}(n, r)$, it holds that
 947

$$\text{dist}(\mathbf{0}, \partial F_\iota(\mathbf{X})) \leq \text{dist}(\mathbf{0}, \partial_{\mathcal{M}} F(\mathbf{X})).$$

950 *Proof.* We let $\mathbf{G} \in \partial F(\mathbf{X})$ and define $\mathcal{A}_{\mathbf{X}}(\mathbf{G}) \triangleq \mathbf{X}^\top\mathbf{G} + \mathbf{G}^\top\mathbf{X}$.
 951

952 Recall that the following first-order optimality conditions are equivalent for all $\mathbf{X} \in \text{St}(n, r)$:
 953 $(\mathbf{0} \in \partial F_\iota(\mathbf{X})) \Leftrightarrow (\mathbf{0} \in \mathbb{P}_{\text{T}_{\mathbf{X}}\mathcal{M}}(\partial F(\mathbf{X})))$. Therefore, we derive:

$$\begin{aligned} \text{dist}(\mathbf{0}, \partial F_\iota(\mathbf{X})) &= \inf_{\mathbf{Y} \in \partial F_\iota(\mathbf{X})} \|\mathbf{Y}\|_F = \inf_{\mathbf{Y} \in \mathbb{P}_{\text{T}_{\mathbf{X}}\mathcal{M}}(\partial F(\mathbf{X}))} \|\mathbf{Y}\|_F \\ &\stackrel{\textcircled{1}}{=} \|\mathbb{P}_{\text{T}_{\mathbf{X}}\mathcal{M}}(\mathbf{G})\|_F \\ &\stackrel{\textcircled{2}}{=} \|\mathbf{G} - \frac{1}{2}\mathbf{X}\mathcal{A}_{\mathbf{X}}(\mathbf{G})\|_F \\ &\stackrel{\textcircled{3}}{=} \|\mathbf{G} - \frac{1}{2}\mathbf{X}(\mathbf{X}^\top\mathbf{G} + \mathbf{G}^\top\mathbf{X})\|_F \\ &\stackrel{\textcircled{4}}{=} \|(\mathbf{I} - \frac{1}{2}\mathbf{X}\mathbf{X}^\top)(\mathbf{G} - \mathbf{X}\mathbf{G}^\top\mathbf{X})\|_F \\ &\stackrel{\textcircled{5}}{\leq} \|\mathbf{G} - \mathbf{X}\mathbf{G}^\top\mathbf{X}\|_F, \end{aligned}$$

944 where step ① uses $\mathbf{G} \in \partial F(\mathbf{X})$; step ② uses Lemma A.6; step ③ uses the definition of $\mathcal{A}_{\mathbf{X}}(\mathbf{G})$;
 945 step ④ uses the identity that $\mathbf{G} - \frac{1}{2}\mathbf{X}(\mathbf{X}^\top\mathbf{G} + \mathbf{G}^\top\mathbf{X}) = (\mathbf{I} - \frac{1}{2}\mathbf{X}\mathbf{X}^\top)(\mathbf{G} - \mathbf{X}\mathbf{G}^\top\mathbf{X})$; step ⑤ uses
 946 the norm inequality and fact that the matrix $\mathbf{I} - \frac{1}{2}\mathbf{X}\mathbf{X}^\top$ only contains eigenvalues that are $\frac{1}{2}$ or 1.
 947 \square

948 **Lemma A.8.** Assume $\cos(\theta) \neq 0$. Any pair of trigonometric functions $(\cos(\theta), \sin(\theta))$ can be
 949 represented as follows:

$$\text{a)} \cos(\theta) = \frac{1}{\sqrt{1+\tan^2(\theta)}}, \text{ and } \sin(\theta) = \frac{\tan(\theta)}{\sqrt{1+\tan^2(\theta)}}.$$

972 **b)** $\cos(\theta) = \frac{-1}{\sqrt{1+\tan^2(\theta)}}$, and $\sin(\theta) = \frac{-\tan(\theta)}{\sqrt{1+\tan^2(\theta)}}$.

973

975 *Proof.* For all values of θ where $\cos(\theta) \neq 0$, the trigonometric functions $\{\sin(\theta), \cos(\theta), \tan(\theta)\}$
 976 are well-defined. Utilizing the identity $\sin^2(\theta) + \cos^2(\theta) = 1$ and $\tan(\theta) \cos(\theta) = \sin(\theta)$, we
 977 derive: $(\tan(\theta) \cdot \cos(\theta))^2 + \cos^2(\theta) = 1$. Consequently, we find: $\cos(\theta) = \frac{\pm 1}{\sqrt{\tan^2(\theta)+1}}$. Finally, we
 978 can express $\sin(\theta)$ as $\sin(\theta) = \tan(\theta) \cdot \cos(\theta) = \frac{\tan(\theta)}{\sqrt{\tan^2(\theta)+1}}$.

979

980

981

982 **Lemma A.9.** Assume $(E_{t+1})^2 \leq E_t(p_t - p_{t+1})$ and $p_t \geq p_{t+1}$, where $\{E_t, p_t\}_{t=0}^\infty$ are two non-
 983 negative sequences. For all $i \geq 1$, we have: $\sum_{t=i}^\infty E_{t+1} \leq E_i + 2p_i$.

984

985

986 *Proof.* We define $w_t \triangleq p_t - p_{t+1}$. We let $1 \leq i < T$.

987 First, for any $i \geq 1$, we have:

988

$$\sum_{t=i}^T w_t = \sum_{t=i}^T (p_t - p_{t+1}) = p_i - p_{T+1} \stackrel{\textcircled{1}}{\leq} p_i, \quad (15)$$

991

992

993

where step ① uses $p_i \geq 0$ for all i .

Second, we obtain:

994

995

996

997

998

999

$$\begin{aligned} E_{t+1} &\stackrel{\textcircled{1}}{\leq} \sqrt{E_t w_t} \\ &\stackrel{\textcircled{2}}{\leq} \sqrt{\frac{\alpha}{2}(E_t)^2 + (w_t)^2 / (2\alpha)}, \forall \alpha > 0 \\ &\stackrel{\textcircled{3}}{\leq} \sqrt{\frac{\alpha}{2}} \cdot E_t + w_t \sqrt{1/(2\alpha)}, \forall \alpha > 0. \end{aligned} \quad (16)$$

1000

1001

1002

1003

Here, step ① uses $(E_{t+1})^2 \leq E_t(p_t - p_{t+1})$ and $w_t \triangleq p_t - p_{t+1}$; step ② uses the fact that $ab \leq \frac{\alpha}{2}a^2 + \frac{1}{2\alpha}b^2$ for all $\alpha > 0$; step ③ uses the fact that $\sqrt{a+b} \leq \sqrt{a} + \sqrt{b}$ for all $a, b \geq 0$.

Assume $1 - \sqrt{\frac{\alpha}{2}} > 0$. Telescoping Inequality (16) over t from i to T , we have:

1004

1005

1006

1007

1008

1009

1010

1011

1012

1013

$$\begin{aligned} &\sum_{t=i}^T w_t \sqrt{1/(2\alpha)} \\ &\geq \{\sum_{t=i}^T E_{t+1}\} - \sqrt{\frac{\alpha}{2}} \{\sum_{t=i}^T E_t\} \\ &= \{E_{T+1} + \sum_{t=i}^{T-1} E_{t+1}\} - \sqrt{\frac{\alpha}{2}} \{E_i + \sum_{t=i}^{T-1} E_{t+1}\} \\ &= E_{T+1} - \sqrt{\frac{\alpha}{2}} E_i + (1 - \sqrt{\frac{\alpha}{2}}) \sum_{t=i}^{T-1} E_{t+1} \\ &\stackrel{\textcircled{1}}{\geq} -\sqrt{\frac{\alpha}{2}} E_i + (1 - \sqrt{\frac{\alpha}{2}}) \sum_{t=i}^{T-1} E_{t+1}, \end{aligned}$$

where step ① uses $E_{T+1} \geq 0$ and $1 - \sqrt{\frac{\alpha}{2}} > 0$. This leads to:

1014

1015

1016

1017

1018

1019

$$\begin{aligned} \sum_{t=i}^{T-1} E_{t+1} &\leq (1 - \sqrt{\frac{\alpha}{2}})^{-1} \cdot \{\sqrt{\frac{\alpha}{2}} E_i + \sqrt{\frac{1}{2\alpha}} \sum_{t=i}^T w_t\} \\ &\stackrel{\textcircled{1}}{=} E_i + 2 \sum_{t=i}^T w_t \\ &\stackrel{\textcircled{2}}{\leq} E_i + 2p_i, \end{aligned}$$

1020

1021

1022

1023

1024

1025

step ① uses the fact that $(1 - \sqrt{\frac{\alpha}{2}})^{-1} \cdot \sqrt{\frac{\alpha}{2}} = 1$ and $(1 - \sqrt{\frac{\alpha}{2}})^{-1} \cdot \sqrt{\frac{1}{2\alpha}} = 2$ when $\alpha = \frac{1}{2}$; step ② uses Inequalities (15). Letting $T \rightarrow \infty$, we conclude this lemma.

□

Lemma A.10. Assume that $[D_t]^{\tau+1} \leq a(D_{t-1} - D_t)$, where $\tau, a > 0$, and $\{D_t\}_{t=0}^\infty$ is a nonnegative sequence. We have: $D_T \leq \mathcal{O}(T^{-1/\tau})$.

1026 *Proof.* We let $\kappa > 1$ be any constant. We define $h(s) = s^{-\tau-1}$, where $\tau > 0$.
 1027

1028 We consider two cases for $r^t \triangleq h(D_t)/h(D_{t-1})$.
 1029

1030 **Case (1).** $r^t \leq \kappa$. We define $\check{h}(s) \triangleq -\frac{1}{\tau} \cdot s^{-\tau}$. We derive:
 1031

$$\begin{aligned} 1 &\stackrel{\textcircled{1}}{\leq} a(D_{t-1} - D_t) \cdot h(D_t) \\ &\stackrel{\textcircled{2}}{\leq} a(D_{t-1} - D_t) \cdot \kappa h(D_{t-1}) \\ &\stackrel{\textcircled{3}}{\leq} a\kappa \int_{D_t}^{D_{t-1}} h(s) ds \\ &\stackrel{\textcircled{4}}{=} a\kappa \cdot (\check{h}(D_{t-1}) - \check{h}(D_t)) \\ &\stackrel{\textcircled{5}}{=} a\kappa \cdot \frac{1}{\tau} \cdot ([D_t]^{-\tau} - [D_{t-1}]^{-\tau}), \end{aligned}$$

1040 where step ① uses $[D_t]^{\tau+1} \leq a(D_{t-1} - D_t)$; step ② uses $h(D_t) \leq \kappa h(D_{t-1})$; step ③ uses the fact
 1041 that $h(s)$ is a nonnegative and increasing function that $(a-b)h(a) \leq \int_b^a h(s) ds$ for all $a, b \in [0, \infty)$;
 1042 step ④ uses the fact that $\nabla \check{h}(s) = h(s)$; step ⑤ uses the definition of $\check{h}(\cdot)$. This leads to:
 1043

$$[D_t]^{-\tau} - [D_{t-1}]^{-\tau} \geq \frac{\tau}{\kappa\alpha}. \quad (17)$$

1045 **Case (2).** $r^t > \kappa$. We have:
 1046

$$\begin{aligned} h(D_t) > \kappa h(D_{t-1}) &\stackrel{\textcircled{1}}{\Rightarrow} [D_t]^{-(\tau+1)} > \kappa \cdot [D_{t-1}]^{-(\tau+1)} \\ &\stackrel{\textcircled{2}}{\Rightarrow} ([D_t]^{-(\tau+1)})^{\frac{\tau}{\tau+1}} > \kappa^{\frac{\tau}{\tau+1}} \cdot ([D_{t-1}]^{-(\tau+1)})^{\frac{\tau}{\tau+1}} \\ &\Rightarrow [D_t]^{-\tau} > \kappa^{\frac{\tau}{\tau+1}} \cdot [D_{t-1}]^{-\tau}, \end{aligned} \quad (18)$$

1052 where step ① uses the definition of $h(\cdot)$; step ② uses the fact that if $a > b > 0$, then $a^{\frac{\tau}{\tau+1}} > b^{\frac{\tau}{\tau+1}}$ for any
 1053 exponent $\frac{\tau}{\tau+1} \in (0, 1)$. For any $t \geq 1$, we derive:
 1054

$$\begin{aligned} [D_t]^{-\tau} - [D_{t-1}]^{-\tau} &\stackrel{\textcircled{1}}{\geq} (\kappa^{\frac{\tau}{\tau+1}} - 1) \cdot [D_{t-1}]^{-\tau} \\ &\stackrel{\textcircled{2}}{\geq} (\kappa^{\frac{\tau}{\tau+1}} - 1) \cdot [D_0]^{-\tau}, \end{aligned} \quad (19)$$

1058 where step ① uses Inequality (18); step ② uses $\tau > 0$ and $D_{t-1} \leq D_0$ for all $t \geq 1$.
 1059

1060 In view of Inequalities (17) and (19), we have:
 1061

$$[D_t]^{-\tau} - [D_{t-1}]^{-\tau} \geq \underbrace{\min\left(\frac{\tau}{\kappa\alpha}, (\kappa^{\frac{\tau}{\tau+1}} - 1) \cdot [D_0]^{-\tau}\right)}_{\triangleq \bar{c}}. \quad (20)$$

1064 Telescoping Inequality (20) over t from 1 to T , we have:
 1065

$$[D_T]^{-\tau} - [D_0]^{-\tau} \geq T\bar{c}.$$

1066 This leads to:
 1067

$$D_T = ([D_T]^{-\tau})^{-1/\tau} \leq \mathcal{O}(T^{-1/\tau}).$$

1071 \square
 1072

1073 B SOLVING THE SUBPROBLEM WHEN $k = 2$

1075 This section presents a novel Breakpoint Searching Method (**BSM**) to find the *global optimal solution* of Problem (3) when $k = 2$.
 1076

1078 Initially, Problem (3) boils down to the following one-dimensional subproblem:
 1079

$$\min_{\theta} \frac{1}{2} \|\mathbf{V}\|_{\mathbf{Q}}^2 + \langle \mathbf{V}, \mathbf{P} \rangle + h(\mathbf{VZ}), \text{ s.t. } \mathbf{V} \in \{\mathbf{V}_{\theta}^{\text{rot}}, \mathbf{V}_{\theta}^{\text{ref}}\},$$

1080 which can be further rewritten as:
 1081

$$1082 \bar{\theta} \in \arg \min_{\theta} \frac{1}{2} \text{vec}(\mathbf{V})^T \mathbf{Q} \text{vec}(\mathbf{V}) + \langle \mathbf{V}, \mathbf{P} \rangle + h(\mathbf{VZ}), \text{ s.t. } \mathbf{V} \triangleq \begin{pmatrix} \pm \cos(\theta) & \sin(\theta) \\ \mp \sin(\theta) & \cos(\theta) \end{pmatrix},$$

1083 where $\mathbf{Q} \in \mathbb{R}^{4 \times 4}$, $\mathbf{P} \in \mathbb{R}^{2 \times 2}$, and $\mathbf{Z} \in \mathbb{R}^{2 \times r}$. Given $h(\cdot)$ is coordinate-wise separable, we have the
 1084 following equivalent optimization problem:
 1085

$$1086 \min_{\theta} h(\cos(\theta)\mathbf{x} + \sin(\theta)\mathbf{y}) + a \cos(\theta) + b \sin(\theta) \\ 1087 + c \cos^2(\theta) + d \cos(\theta) \sin(\theta) + e \sin^2(\theta), \quad (21)$$

1089 where $a = \mathbf{P}_{22} \pm \mathbf{P}_{11}$, $b = \mathbf{P}_{12} \mp \mathbf{P}_{21}$, $c = 0.5(\mathbf{Q}_{11} + \mathbf{Q}_{44}) \pm \mathbf{Q}_{14}$, $d = -\mathbf{Q}_{12} \pm \mathbf{Q}_{13} \mp \mathbf{Q}_{24} + \mathbf{Q}_{34}$,
 1090 $e = 0.5(\mathbf{Q}_{22} + \mathbf{Q}_{33}) \mp \mathbf{Q}_{23}$, $\mathbf{r} = \pm \mathbf{Z}(1, :)$, $\mathbf{s} = \mathbf{Z}(2, :)$, $\mathbf{p} = \mathbf{Z}(2, :)$, $\mathbf{u} = \mp \mathbf{Z}(1, :)$, $\mathbf{x} \triangleq [\mathbf{r}; \mathbf{p}] \in$
 1091 $\mathbb{R}^{2r \times 1}$, and $\mathbf{y} \triangleq [\mathbf{s}; \mathbf{u}] \in \mathbb{R}^{2r \times 1}$.
 1092

1093 Our key strategy is to perform a variable substitution to convert Problem (21) into an equivalent
 1094 problem that depends on the variable $\tan(\theta) \triangleq t$. The substitution is based on the trigonometric
 1095 identities that $\cos(\theta) = \pm 1/\sqrt{1 + \tan^2(\theta)}$ and $\sin(\theta) = \pm \tan(\theta)/\sqrt{1 + \tan^2(\theta)}$.
 1096

1097 The following lemma provides a characterization of the global optimal solution for Problem (21).
 1098

1099 **Lemma B.1.** *We define $\check{F}(\tilde{c}, \tilde{s}) \triangleq a\tilde{c} + b\tilde{s} + c\tilde{c}^2 + d\tilde{c}\tilde{s} + e\tilde{s}^2 + h(\tilde{c}\mathbf{x} + \tilde{s}\mathbf{y})$, and $w \triangleq c - e$. The
 1100 optimal solution $\bar{\theta}$ to (21) can be computed as:*

$$1100 [\cos(\bar{\theta}), \sin(\bar{\theta})] \in \arg \min_{[c, s]} \check{F}(c, s), \text{ s.t. } [c, s] \in \{[c_1, s_1], [c_2, s_2], [0, 1], [0, -1]\}, \\ 1101$$

1102 where $c_1 \triangleq \frac{1}{\sqrt{1+(\bar{t}_+)^2}}$, $s_1 = \frac{\bar{t}_+}{\sqrt{1+(\bar{t}_+)^2}}$, $c_2 \triangleq \frac{-1}{\sqrt{1+(\bar{t}_-)^2}}$, and $s_2 \triangleq \frac{-\bar{t}_-}{\sqrt{1+(\bar{t}_-)^2}}$. Furthermore, \bar{t}_+ and
 1103 \bar{t}_- are respectively defined as:
 1104

$$1105 \bar{t}_+ \in \arg \min_t p(t) \triangleq \frac{a+bt}{\sqrt{1+t^2}} + \frac{w+dt}{1+t^2} + h\left(\frac{\mathbf{x}+t\mathbf{y}}{\sqrt{1+t^2}}\right), \quad (22)$$

$$1106 \bar{t}_- \in \arg \min_t \tilde{p}(t) \triangleq \frac{-a-bt}{\sqrt{1+t^2}} + \frac{w+dt}{1+t^2} + h\left(\frac{-\mathbf{x}-t\mathbf{y}}{\sqrt{1+t^2}}\right). \quad (23)$$

1107 *Proof.* We define $w \triangleq c - e$, and $\check{F}(\tilde{c}, \tilde{s}) \triangleq a\tilde{c} + b\tilde{s} + c\tilde{c}^2 + d\tilde{c}\tilde{s} + e\tilde{s}^2 + h(\tilde{c}\mathbf{x} + \tilde{s}\mathbf{y})$.
 1108

1109 With the identity $\sin^2(\theta) = 1 - \cos^2(\theta)$, Problem (21) can be equivalently written as:
 1110

$$1111 \bar{\theta} \in \arg \min_{\theta} h(\cos(\theta)\mathbf{x} + \sin(\theta)\mathbf{y}) + a \cos(\theta) + b \sin(\theta) \\ 1112 + w \cos^2(\theta) + d \cos(\theta) \sin(\theta) + e. \quad (24)$$

1113 We first consider the case $\cos(\theta) \neq 0$. By Lemma A.8, there are two possible parameterizations for
 1114 $(\cos(\theta), \sin(\theta))$ in Problem (24).
 1115

1116 **Case a).** $\cos(\theta) = \frac{1}{\sqrt{1+\tan^2(\theta)}}$ and $\sin(\theta) = \frac{\tan(\theta)}{\sqrt{1+\tan^2(\theta)}}$. Then Problem (21) becomes:
 1117

$$1118 \bar{\theta}_+ \in \arg \min_{\theta} \frac{a+\tan(\theta)b}{\sqrt{1+\tan^2(\theta)}} + \frac{w+\tan(\theta)d}{1+\tan^2(\theta)} + h\left(\frac{\mathbf{x}+\tan(\theta)\mathbf{y}}{\sqrt{1+\tan^2(\theta)}}\right).$$

1119 Setting $t = \tan(\theta)$, we have the equivalent problem:
 1120

$$1121 \bar{t}_+ \in \arg \min_t \frac{a+bt}{\sqrt{1+t^2}} + \frac{w+dt}{1+t^2} + h\left(\frac{\mathbf{x}+t\mathbf{y}}{\sqrt{1+t^2}}\right).$$

1122 Hence the corresponding optimal trigonometric pair is
 1123

$$1124 \cos(\bar{\theta}_+) = \frac{1}{\sqrt{1+(\bar{t}_+)^2}}, \sin(\bar{\theta}_+) = \frac{\bar{t}_+}{\sqrt{1+(\bar{t}_+)^2}}. \quad (25)$$

1125 **Case b).** $\cos(\theta) = \frac{-1}{\sqrt{1+\tan^2(\theta)}}$ and $\sin(\theta) = \frac{-\tan(\theta)}{\sqrt{1+\tan^2(\theta)}}$. In this case, Problem (21) reduces to
 1126

$$1127 \bar{\theta}_- \in \arg \min_{\theta} \frac{-a-\tan(\theta)b}{\sqrt{1+\tan^2(\theta)}} + \frac{w+\tan(\theta)d}{1+\tan^2(\theta)} + h\left(\frac{-\mathbf{x}-\tan(\theta)\mathbf{y}}{\sqrt{1+\tan^2(\theta)}}\right).$$

1134 Again letting $t = \tan \theta$, we obtain
 1135

$$\bar{t}_- \in \arg \min_t \frac{-a-bt}{\sqrt{1+t^2}} + \frac{w+dt}{1+t^2} + h\left(\frac{-\mathbf{x}-\mathbf{y}t}{\sqrt{1+t^2}}\right).$$

1138 Thus, the corresponding optimal trigonometric pair is
 1139

$$\cos(\bar{\theta}_-) = \frac{-1}{\sqrt{1+(\bar{t}_-)^2}}, \sin(\bar{\theta}_-) = \frac{-\bar{t}_-}{\sqrt{1+(\bar{t}_-)^2}} \quad (26)$$

1142 Combining (25) and (26), when $\cos(\theta) \neq 0$ the optimal solution $\bar{\theta}$ to (24) satisfies $[\cos(\bar{\theta}), \sin(\bar{\theta})] \in$
 1143 $\arg \min_{c,s} \check{F}(c,s)$, s.t. $[c,s] \in \{[\cos(\bar{\theta}_+), \sin(\bar{\theta}_+)], [\cos(\bar{\theta}_-), \sin(\bar{\theta}_-)]\}$. Including the case
 1144 $\cos(\theta) = 0$, that is, $[c,s] \in \{[0,1], [0,-1]\}$, the final selection rule for the optimal pair is
 1145

$$[\cos(\bar{\theta}), \sin(\bar{\theta})] \in \arg \min_{c,s} \check{F}(c,s),$$

$$\text{s.t. } [c,s] \in \{[\cos(\bar{\theta}_+), \sin(\bar{\theta}_+)], [\cos(\bar{\theta}_-), \sin(\bar{\theta}_-)], [0,1], [0,-1]\}.$$

1150 Note that $\{\cos(\bar{\theta}), \sin(\bar{\theta})\}$ uniquely determines $\bar{\theta}$, and the objective in Problem (21) depends only
 1151 on $\{\cos(\theta), \sin(\theta)\}$ for some θ . Thus, it is not necessary to explicitly recover the angles $\bar{\theta}_+$ and $\bar{\theta}_-$;
 1152 it suffices to work with their cosine–sine representations.

1153 \square
 1154

1155 We describe our **BSM** to solve Problem (22); our approach can be naturally extended to tackle
 1156 Problem (23). **BSM** first identifies all the possible breakpoints / critical points Θ , and then picks the
 1157 solution that leads to the lowest value as the optimal solution \bar{t} , i.e., $\bar{t} \in \arg \min_t p(t)$, s.t. $t \in \Theta$.

1158 We assume $\mathbf{y}_i \neq 0$. If this is not true and there exists $\mathbf{y}_i = 0$ for some i , then $\{\mathbf{x}_i, \mathbf{y}_i\}$ can be
 1159 removed since it does not affect the minimizer of the problem.

1160 **► Finding the Breakpoint Set for $h(\mathbf{x}) \triangleq \lambda \|\mathbf{x}\|_0$**

1161 Since the function $h(\mathbf{x}) \triangleq \lambda \|\mathbf{x}\|_0$ is scale-invariant and symmetric with $\|\pm t\mathbf{x}\|_0 = \|\mathbf{x}\|_0$ for all
 1162 $t > 0$, Problem (22) reduces to the following problem:
 1163

$$\min_t p(t) \triangleq \frac{a+bt}{\sqrt{1+t^2}} + \frac{w+dt}{1+t^2} + \lambda \|\mathbf{x} + t\mathbf{y}\|_0. \quad (27)$$

1164 Given the limiting subdifferential of the ℓ_0 norm function can be computed as $\partial \|\mathbf{t}\|_0 \in$
 1165 $\{\begin{array}{ll} \mathbb{R}, & t=0; \\ \{0\}, & \text{else.} \end{array}\}$ (see Appendix C.5), we consider the following two cases. (i) We assume
 1166 $(\mathbf{x} + t\mathbf{y})_i = 0$ for some i . Then the solution \bar{t} can be determined using $\bar{t} = \frac{\mathbf{x}_i}{\mathbf{y}_i}$. There are
 1167 $2r$ breakpoints $\{\frac{\mathbf{x}_1}{\mathbf{y}_1}, \frac{\mathbf{x}_2}{\mathbf{y}_2}, \dots, \frac{\mathbf{x}_{2r}}{\mathbf{y}_{2r}}\}$ for this case. (ii) We now assume $(\mathbf{x} + t\mathbf{y})_i \neq 0$ for all i .
 1168 Then $\lambda \|\mathbf{x} + t\mathbf{y}\|_0 = 2r\lambda$ becomes a constant. Setting the subgradient of $p(t)$ to zero yields:
 1169 $0 = \nabla p(t) = [b(1+t^2) - (a+bt)t] \cdot \sqrt{1+t^2} \cdot t^\circ + [d(1+t^2) - (w+dt)(2t)] \cdot t^\circ$, where
 1170 $t^\circ = (1+t^2)^{-2}$. Since $t^\circ > 0$, we obtain: $d(1+t^2) - (w+dt)2t = -(b-at) \cdot \sqrt{1+t^2}$.
 1171 Squaring both sides, we obtain the following quartic equation: $c_4 t^4 + c_3 t^3 + c_2 t^2 + c_1 t + c_0 = 0$
 1172 for some suitable c_4, c_3, c_2, c_1 and c_0 . Solving this equation analytically using Lodovico Ferrari's
 1173 method (WikiContributors), we obtain all its real roots $\{\bar{t}_1, \bar{t}_2, \dots, \bar{t}_j\}$ with $1 \leq j \leq 4$. There are
 1174 at most 4 breakpoints for this case. Therefore, Problem (27) contains at most $2r + 4$ breakpoints
 1175 $\Theta = \{\frac{\mathbf{x}_1}{\mathbf{y}_1}, \frac{\mathbf{x}_2}{\mathbf{y}_2}, \dots, \frac{\mathbf{x}_{2r}}{\mathbf{y}_{2r}}, \bar{t}_1, \bar{t}_2, \dots, \bar{t}_j\}$.
 1176

1177 **► Finding the Breakpoint Set for $h(\mathbf{x}) \triangleq \lambda \|\mathbf{x}\|_1$**

1178 Since the function $h(\mathbf{x}) \triangleq \lambda \|\mathbf{x}\|_1$ is symmetric, Problem (22) reduces to the following problem:
 1179

$$\bar{t} \in \arg \min_t p(t) \triangleq \frac{a+bt}{\sqrt{1+t^2}} + \frac{w+dt}{1+t^2} + \frac{\lambda \|\mathbf{x} + t\mathbf{y}\|_1}{\sqrt{1+t^2}}. \quad (28)$$

1180 Setting the subgradient of $p(\cdot)$ to zero yields: $0 \in \partial p(t) = t^\circ [d(1+t^2) - (w+dt)2t + (b-at) \cdot$
 1181 $\sqrt{1+t^2}] + t^\circ \lambda \cdot \sqrt{1+t^2} \cdot [\langle \text{sign}(\mathbf{x} + t\mathbf{y}), \mathbf{y} \rangle (1+t^2) - \|\mathbf{x} + t\mathbf{y}\|_1 t]$, where $t^\circ = (1+t^2)^{-2}$. We
 1182 consider the following two cases. (i) We assume $(\mathbf{x} + t\mathbf{y})_i = 0$ for some i . Then the solution \bar{t}
 1183 can be determined using $\bar{t} = \frac{\mathbf{x}_i}{\mathbf{y}_i}$. There are $2r$ breakpoints $\{\frac{\mathbf{x}_1}{\mathbf{y}_1}, \frac{\mathbf{x}_2}{\mathbf{y}_2}, \dots, \frac{\mathbf{x}_{2r}}{\mathbf{y}_{2r}}\}$ for this case. (ii) We

now assume $(\mathbf{x} + t\mathbf{y})_i \neq 0$ for all i . We define $\mathbf{z} \triangleq \{+\frac{\mathbf{x}_1}{\mathbf{y}_1}, -\frac{\mathbf{x}_1}{\mathbf{y}_1}, +\frac{\mathbf{x}_2}{\mathbf{y}_2}, -\frac{\mathbf{x}_2}{\mathbf{y}_2}, \dots, +\frac{\mathbf{x}_{2r}}{\mathbf{y}_{2r}}, -\frac{\mathbf{x}_{2r}}{\mathbf{y}_{2r}}\} \in \mathbb{R}^{4r \times 1}$, and sort \mathbf{z} in non-descending order. Given $\bar{t} \neq \mathbf{z}_i$ for all i in this case, the domain $p(t)$ can be divided into $(4r + 1)$ non-overlapping intervals: $(-\infty, \mathbf{z}_1), (\mathbf{z}_1, \mathbf{z}_2), \dots, (\mathbf{z}_{4r}, +\infty)$. In each interval, $\text{sign}(\mathbf{x} + t\mathbf{y}) \triangleq \mathbf{o}$ can be determined. Combining with the fact that $t^\circ > 0$ and $\|\mathbf{x} + t\mathbf{y}\|_1 = \langle \mathbf{o}, \mathbf{x} + t\mathbf{y} \rangle$, the first-order optimality condition reduces to: $0 = [d(1 + t^2) - (w + dt)2t + (b - at) \cdot \sqrt{1 + t^2}] + \lambda \cdot \sqrt{1 + t^2} \cdot [\langle \mathbf{o}, \mathbf{y} \rangle(1 + t^2) - \langle \mathbf{o}, \mathbf{x} + t\mathbf{y} \rangle t]$, which can be simplified as: $(at - b) \cdot \sqrt{1 + t^2} - \lambda \cdot \sqrt{1 + t^2} \cdot [\langle \mathbf{o}, \mathbf{y} - t\mathbf{x} \rangle] = [d(1 + t^2) - (w + dt)2t]$. We square both sides and then solve the quartic equation. We obtain all its real roots $\{t_1, t_2, \dots, t_j\}$ with $1 \leq j \leq 4$. Therefore, Problem (28) contains at most $2r + (4r + 1) \times 4$ breakpoints.

► Finding the Breakpoint Set for $h(\mathbf{x}) \triangleq I_{\geq 0}(\mathbf{x})$

Since the function $h(\mathbf{x}) \triangleq I_{\geq 0}(\mathbf{x})$ is scale-invariant with $h(t\mathbf{x}) = h(\mathbf{x})$ for all $t \geq 0$, Problem (22) reduces to the following problem:

$$\bar{t} \in \arg \min_t p(t) \triangleq \frac{a+bt}{\sqrt{1+t^2}} + \frac{w+dt}{1+t^2}, \text{ s.t. } \mathbf{x} + t\mathbf{y} \geq \mathbf{0}. \quad (29)$$

We define $I \triangleq \{i | \mathbf{y}_i > 0\}$ and $J \triangleq \{i | \mathbf{y}_i < 0\}$. It is not difficult to verify that $\{x + t\mathbf{y} \geq 0\} \Leftrightarrow \{-\frac{\mathbf{x}_I}{\mathbf{y}_I} \leq t, t \leq -\frac{\mathbf{x}_J}{\mathbf{y}_J}\} \Leftrightarrow \{lb \triangleq \max(-\frac{\mathbf{x}_I}{\mathbf{y}_I}) \leq t \leq \min(-\frac{\mathbf{x}_J}{\mathbf{y}_J}) \triangleq ub\}$. When $lb > ub$, we can directly conclude that the problem has no solution for this case. Now we assume $ub \geq lb$ and define $P(t) \triangleq \min(ub, \max(t, lb))$. We omit the bound constraint and set the gradient of $p(t)$ to zero, which yields: $0 = \nabla p(t) = [b(1 + t^2) - (a + bt)t] \cdot \sqrt{1 + t^2} \cdot t^\circ + [d(1 + t^2) - (w + dt)(2t)] \cdot t^\circ$, where $t^\circ = (1 + t^2)^{-\frac{1}{2}}$. We obtain all its real roots $\{\bar{t}_1, \bar{t}_2, \dots, \bar{t}_j\}$ with $1 \leq j \leq 4$ after squaring both sides and solving the quartic equation. Combining with the bound constraints, we conclude that Problem (29) contains at most $(4 + 2)$ breakpoints $\{P(\bar{t}_1), P(\bar{t}_2), \dots, P(\bar{t}_j), lb, ub\}$ with $1 \leq j \leq 4$.

C ADDITIONAL DISCUSSIONS

This section encompasses various discussions, covering topics such as: (i) simple examples for the optimality hierarchy, (ii) computation of the matrix \mathbf{Q} , (iii) complexity comparison between **OBCD** and full gradient methods, (iv) generalization to multiple row updates, and (v) the subdifferential of the cardinality function.

C.1 SIMPLE EXAMPLES FOR THE OPTIMALITY HIERARCHY

To demonstrate the strong optimality of BS_2 -points and the advantages of the proposed method, we examine the following simple examples of 2×2 optimization problems mentioned in the paper:

$$\min_{\mathbf{V} \in \text{St}(2,2)} F(\mathbf{V}) \triangleq \|\mathbf{V} - \mathbf{A}\|_F^2, \text{ with } \mathbf{A} = \begin{pmatrix} 1 & 0 \\ -1 & -1 \end{pmatrix}. \quad (30)$$

$$\min_{\mathbf{V} \in \text{St}(2,2)} F(\mathbf{V}) \triangleq \|\mathbf{V} - \mathbf{B}\|_F^2 + 5\|\mathbf{V}\|_1, \text{ with } \mathbf{B} = \begin{pmatrix} 1 & 0 \\ 1 & 2 \end{pmatrix}. \quad (31)$$

Figure 2 shows the geometric visualizations of Problems (30) and (31) using the relation $\min_\theta \min(F(\mathbf{V}_\theta^{\text{rot}}), F(\mathbf{V}_\theta^{\text{ref}})) = \min_{\mathbf{V} \in \text{St}(2,2)} F(\mathbf{V})$. The two objective functions exhibit periodicity with a period of 2π . Within the interval $[0, 2\pi]$, each of them contains one unique BS_2 -point, while the two respective examples contain 4 and 8 critical points. Therefore, the optimality condition of BS_2 -points might be much stronger than that of critical points.

BS₂-points vs. Critical Point: Algorithm Instance Study. We briefly review methods that seek critical points of Problem (30) and demonstrate that they may lead to suboptimal solutions for Problem (30). As a representative example, we consider the well-known feasible method based on the Cayley transform (Wen & Yin, 2013). According to Equation (7) in (Wen & Yin, 2013), the update rule is:

$$\mathbf{X}^{t+1} \Leftarrow \mathbf{Q} \mathbf{X}^t, \quad \mathbf{Q} \triangleq [(\mathbf{I}_2 + \frac{\tau}{2} \tilde{\mathbf{A}})^{-1} (\mathbf{I}_2 - \frac{\tau}{2} \tilde{\mathbf{A}})], \quad (32)$$

where $\tau \in \mathbb{R}$, and $\tilde{\mathbf{A}} \in \mathbb{R}^{2 \times 2}$ is a suitable skew-symmetric matrix. Lemma A.3 shows that the matrix \mathbf{Q} is always a rotation matrix. Consequently, if \mathbf{X}^0 is initialized as a rotation matrix with $\det(\mathbf{Q}) = 1$, all iterates \mathbf{X}^{t+1} remain rotation matrices, which in general do not coincide with the optimal solution.

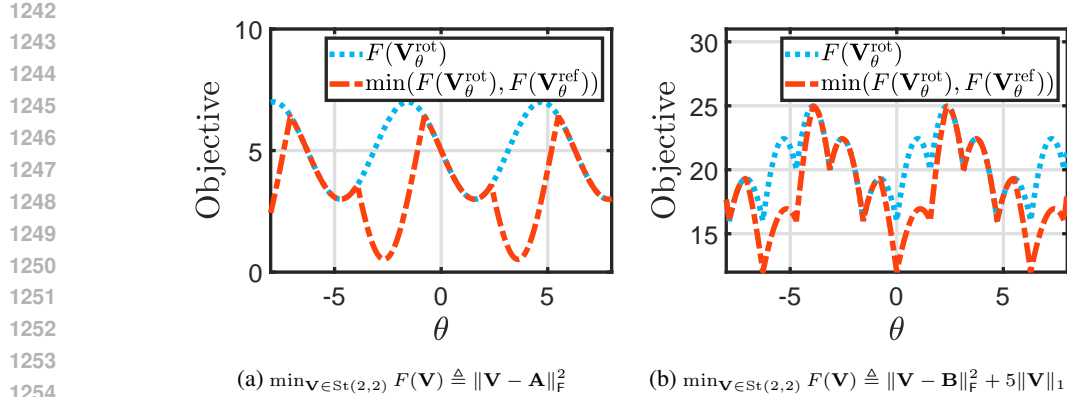


Figure 2: Geometric Visualizations of Two Examples of 2×2 Optimization Problems with Orthogonality Constraints with $\mathbf{A} = \begin{pmatrix} 1 & 0 \\ -1 & -1 \end{pmatrix}$ and $\mathbf{B} = \begin{pmatrix} 1 & 0 \\ 1 & 2 \end{pmatrix}$.

C.2 COMPUTING THE MATRIX \mathbf{Q}

Computing the matrix $\mathbf{Q} \in \mathbb{R}^{k^2 \times k^2}$ as in (8) can be a challenging task because it involves the matrix $\mathbf{H} \in \mathbb{R}^{nr \times nr}$. However, in practice, \mathbf{H} often has some special structure that enables fast matrix computation. For example, \mathbf{H} might take a diagonal matrix that is equal to $L\mathbf{I}_{nr}$ for some $L \geq 0$ or has a Kronecker structure where $\mathbf{H} = \mathbf{H}_1 \otimes \mathbf{H}_2$ for some $\mathbf{H}_1 \in \mathbb{R}^{r \times r}$ and $\mathbf{H}_2 \in \mathbb{R}^{n \times n}$. The lemmas provided below demonstrate how to compute the matrix \mathbf{Q} .

Lemma C.1. *Assume (8) is used to find \mathbf{Q} . (a) If $\mathbf{H} = \mathbf{H}_1 \otimes \mathbf{H}_2$, we have: $\mathbf{Q} = \mathbf{Q}_1 \otimes \mathbf{Q}_2$, where $\mathbf{Q}_1 = \mathbf{Z}\mathbf{H}_1\mathbf{Z}^T \in \mathbb{R}^{k \times k}$ and $\mathbf{Q}_2 = \mathbf{U}_B^T\mathbf{H}_2\mathbf{U}_B \in \mathbb{R}^{k \times k}$. (b) If $\mathbf{H} = L\mathbf{I}_{nr}$, we have $\mathbf{Q} = (L\mathbf{Z}\mathbf{Z}^T) \otimes \mathbf{I}_k$.*

Proof. Recall that for any matrices $\bar{\mathbf{A}}, \bar{\mathbf{B}}, \bar{\mathbf{C}}, \bar{\mathbf{D}}$ of suitable dimensions, we have the following equality: $(\bar{\mathbf{A}} \otimes \bar{\mathbf{B}})(\bar{\mathbf{C}} \otimes \bar{\mathbf{D}}) = (\bar{\mathbf{A}}\bar{\mathbf{C}}) \otimes (\bar{\mathbf{B}}\bar{\mathbf{D}})$.

(a) If $\mathbf{H} = \mathbf{H}_1 \otimes \mathbf{H}_2$, we derive: $\mathbf{Q} \triangleq (\mathbf{Z}^T \otimes \mathbf{U}_B)^T \mathbf{H} (\mathbf{Z}^T \otimes \mathbf{U}_B) = (\mathbf{Z}^T \otimes \mathbf{U}_B)^T (\mathbf{H}_1 \otimes \mathbf{H}_2) (\mathbf{Z}^T \otimes \mathbf{U}_B) = (\mathbf{Z}^T \otimes \mathbf{U}_B)^T [(\mathbf{H}_1 \mathbf{Z}^T) \otimes (\mathbf{H}_2 \mathbf{U}_B)] = (\mathbf{Z}\mathbf{H}_1\mathbf{Z}^T) \otimes (\mathbf{U}_B^T\mathbf{H}_2\mathbf{U}_B) = \mathbf{Q}_1 \otimes \mathbf{Q}_2$.

(b) If $\mathbf{H} = L\mathbf{I}_{nr}$, we have: $\mathbf{Q} \triangleq (\mathbf{Z}^T \otimes \mathbf{U}_B)^T \mathbf{H} (\mathbf{Z}^T \otimes \mathbf{U}_B) = L(\mathbf{Z}^T \otimes \mathbf{U}_B)^T (\mathbf{Z}^T \otimes \mathbf{U}_B) = L(\mathbf{Z}\mathbf{Z}^T) \otimes \mathbf{I}_k$.

□

Lemma C.2. *Assume (9) is used to find \mathbf{Q} . (a) If $\mathbf{H} = \mathbf{H}_1 \otimes \mathbf{H}_2$, we have $\mathbf{Q} = \|\mathbf{Q}_1\|_{\text{sp}} \cdot \|\mathbf{Q}_2\|_{\text{sp}} \cdot \mathbf{I}$, where \mathbf{Q}_1 and \mathbf{Q}_2 are defined in Lemma C.1. (b) If $\mathbf{H} = L\mathbf{I}_{nr}$, we have $\mathbf{Q} = L\|\mathbf{Z}\|_{\text{sp}}^2 \cdot \mathbf{I}$.*

Proof. (a) Using the results Lemma C.1(a), we have: $(\mathbf{Z}^T \otimes \mathbf{U}_B)^T \mathbf{H} (\mathbf{Z}^T \otimes \mathbf{U}_B) = \mathbf{Q}_1 \otimes \mathbf{Q}_2 \preceq \|\mathbf{Q}_1\|_{\text{sp}} \cdot \|\mathbf{Q}_2\|_{\text{sp}} \cdot \mathbf{I}$.

(b) Using the results in Claim (b) of Lemma C.1, we have: $(\mathbf{Z}^T \otimes \mathbf{U}_B)^T \mathbf{H} (\mathbf{Z}^T \otimes \mathbf{U}_B) = L\mathbf{Z}\mathbf{Z}^T \otimes \mathbf{I}_k \preceq L\|\mathbf{Z}\|_{\text{sp}}^2 \cdot \mathbf{I}$.

□

C.3 COMPLEXITY COMPARISON BETWEEN **OB****CD** AND FULL GRADIENT METHODS

We present a computational complexity comparison with full gradient methods using the linear eigenvalue problem: $\min_{\mathbf{X}} F(\mathbf{X}) \triangleq \frac{1}{2} \langle \mathbf{X}, \mathbf{C}\mathbf{X} \rangle$, s.t. $\mathbf{X}^T \mathbf{X} = \mathbf{I}_r$, where $\mathbf{C} \in \mathbb{R}^{n \times n}$ is given.

We first examine full gradient methods such as the Riemannian gradient method (Jiang & Dai, 2015; Liu et al., 2016). The computation of the Riemannian gradient $\nabla_{\mathcal{M}} F(\mathbf{X}) = \mathbf{C}\mathbf{X} - \mathbf{X}[\mathbf{C}\mathbf{X}]^T \mathbf{X}$ requires $\mathcal{O}(n^2r)$ time, while the retraction step using SVD, QR, or polar decomposition demands

1296 $\mathcal{O}(nr^2)$. Consequently, the overall complexity for Riemannian gradient method is $N_1 \times \mathcal{O}(n^2r)$,
 1297 where N_1 is the number of iterations required for convergence.
 1298

1299 We now consider the proposed **OBCD** method where the matrix \mathbf{Q} is chosen to be a diagonal matrix
 1300 as in Equality (9). (i) We adopt an incremental update strategy for computing the Euclidean gradient
 1301 $\nabla F(\mathbf{X}) = \mathbf{C}\mathbf{X}$, maintaining the relationship $\mathbf{Y}^t = \mathbf{C}\mathbf{X}^t$ for all t . The initialization $\mathbf{Y}^0 = \mathbf{C}\mathbf{X}^0$
 1302 occurs only once. When \mathbf{X}^t is updated via a k -row change, resulting in $\mathbf{X}^{t+1} = \mathbf{X}^t + \mathbf{U}_B(\mathbf{V} -$
 1303 $\mathbf{I})\mathbf{U}_B^\top\mathbf{X}^t$, we efficiently reconstruct $\mathbf{C}\mathbf{X}^{t+1}$ by updating $\mathbf{Y}^{t+1} = \mathbf{Y}^t + \mathbf{C}\mathbf{U}_B(\mathbf{V} - \mathbf{I})\mathbf{U}_B^\top\mathbf{X}^t$ in
 1304 $\mathcal{O}(nr)$ time. (ii) Computing the matrix \mathbf{P} as shown in (3) involves matrix multiplication between
 1305 matrices $[\nabla f(\mathbf{X}^t)]_{B:} \in \mathbb{R}^{k \times r}$ and $[[\mathbf{X}^t]_{B:}]^\top \in \mathbb{R}^{r \times k}$, which can be done in $\mathcal{O}(rk^2)$. (iii) Solving
 1306 the subproblem using small-size SVD takes $\mathcal{O}(k^3)$ time. Thus, the total complexity for **OBCD** is
 1307 $N_2 \times \mathcal{O}(nr + rk^2 + k^3)$, with N_2 denoting the number of **OBCD** iterations.
 1308
 1309

1310 C.4 GENERALIZATION TO MULTIPLE ROW UPDATES

1311 The proposed **OBCD** algorithm can be generalized to multiple row updates scheme.
 1312

1313 Assume that n is an even number, and $k = 2$. As mentioned in Lemma 2.3, when (9) is used to find
 1314 \mathbf{Q} , the subproblem $\tilde{\mathbf{V}}^t \in \arg \min_{\mathbf{V} \in \text{St}(k,k)} \mathcal{K}(\mathbf{V}; \mathbf{X}^t, \mathbf{B})$ in Algorithm 1 reduces to:
 1315

$$1317 \min_{\mathbf{V} \in \text{St}(2,2)} \langle \mathbf{V}, (\nabla f(\mathbf{X}^t)[\mathbf{X}^t]^\top)_{BB} \rangle + h(\mathbf{V}\mathbf{U}_B\mathbf{X}^t). \quad (33)$$

1320 One can independently solve $(n/2)$ subproblems, each formulated as follows:
 1321

1322 $\min_{\mathbf{V} \in \text{St}(2,2)} \langle \mathbf{V}, (\nabla f(\mathbf{X}^t)[\mathbf{X}^t]^\top)_{BB} \rangle + h(\mathbf{V}\mathbf{U}_B\mathbf{X}^t)$ with $B = [1, 2]$.
 1323

1324 $\min_{\mathbf{V} \in \text{St}(2,2)} \langle \mathbf{V}, (\nabla f(\mathbf{X}^t)[\mathbf{X}^t]^\top)_{BB} \rangle + h(\mathbf{V}\mathbf{U}_B\mathbf{X}^t)$ with $B = [3, 4]$.
 1325

1326 \dots

1327 $\min_{\mathbf{V} \in \text{St}(2,2)} \langle \mathbf{V}, (\nabla f(\mathbf{X}^t)[\mathbf{X}^t]^\top)_{BB} \rangle + h(\mathbf{V}\mathbf{U}_B\mathbf{X}^t)$ with $B = [n-1, n]$.
 1328

1329 This approach, known as the Jacobi update in the literature, allows for the parallel update of n rows
 1330 of the matrix \mathbf{X} .
 1331

1332 Notably, one can consider $k \triangleq |\mathbf{B}| > 2$ when $h(\cdot) = 0$, and the associated subproblems can be
 1333 solved using SVD.
 1334

1335 C.5 LIMITING SUBDIFFERENTIAL OF THE CARDINALITY FUNCTION

1336 We demonstrate how to calculate the limiting subdifferential of the cardinality function $h(\mathbf{X}) =$
 1337 $\|\mathbf{X}\|_0$. Given that $h(\mathbf{X}) = \|\mathbf{X}\|_0$ is coordinate-wise separable, we focus only on the scalar function
 1338 $h(x) = |x|_0$, where $|x|_0 = \begin{cases} 0, & x = 0; \\ 1, & \text{else.} \end{cases}$.
 1339

1340 The Fréchet subdifferential of the function $h(x) = |x|_0$ at $x \in \text{dom}(h)$ is defined as $\hat{\partial}h(x) \triangleq$
 1341 $\{\xi \in \mathbb{R} : \lim_{z \rightarrow x} \inf_{z \neq x} \frac{h(z) - h(x) - \langle \xi, z - x \rangle}{|z - x|} \geq 0\}$, while the limiting subdifferential of $h(x)$ at $x \in$
 1342 $\text{dom}(h)$ is denoted as $\partial h(x) \triangleq \{\xi \in \mathbb{R} : \exists x^t \rightarrow x, h(x^t) \rightarrow h(x), \xi^t \in \hat{\partial}h(x^t) \rightarrow \xi, \forall t\}$. We con-
 1343 sider the following two cases. (i) $x \neq 0$. We have: $\hat{\partial}h(x) = \{\xi \in \mathbb{R} : \lim_{z \rightarrow x} \inf_{z \neq x} \frac{-\langle \xi, z - x \rangle}{|z - x|} \geq$
 1344 $0\} = \{0\}$. (ii) $x = 0$. We have: $\hat{\partial}h(x) = \{\xi \in \mathbb{R} : \lim_{z \rightarrow x} \inf_{z \neq x} \frac{|z|_0 - \langle \xi, z - x \rangle}{|z - x|} \geq 0\} = \{\xi \in \mathbb{R} :$
 1345 $\lim_{z \rightarrow x} \inf_{z \neq x} \frac{1 - \langle \xi, z \rangle}{|z|} \geq 0\} = \mathbb{R}$.
 1346

1347 We therefore conclude that $[\partial\|\mathbf{X}\|_0]_{i,j} \in \begin{cases} \mathbb{R}, & \mathbf{X}_{i,j} = 0; \\ \{0\}, & \text{else.} \end{cases}$ for all $i \in [n]$ and $j \in [r]$.
 1348

1350 **D PROOF FOR SECTION 2**1351 **D.1 PROOF FOR LEMMA 2.1**1352 *Proof.* **Part (a).** For any $\mathbf{V} \in \mathbb{R}^{k \times k}$ and $\mathbf{B} \in \{\mathcal{B}_i\}_{i=1}^{C_n^k}$, we have:

$$\begin{aligned}
& [\mathbf{X}^+]^\top \mathbf{X}^+ - \mathbf{X}^\top \mathbf{X} \\
& \stackrel{\textcircled{1}}{=} [\mathbf{X} + \mathbf{U}_B(\mathbf{V} - \mathbf{I}_k)\mathbf{U}_B^\top \mathbf{X}]^\top [\mathbf{X} + \mathbf{U}_B(\mathbf{V} - \mathbf{I}_k)\mathbf{U}_B^\top \mathbf{X}] - \mathbf{X}^\top \mathbf{X} \\
& = \mathbf{X}^\top \mathbf{U}_B(\mathbf{V} - \mathbf{I}_k)\mathbf{U}_B^\top \mathbf{X} + [\mathbf{U}_B(\mathbf{V} - \mathbf{I}_k)\mathbf{U}_B^\top \mathbf{X}]^\top \mathbf{X} + [\mathbf{U}_B(\mathbf{V} - \mathbf{I}_k)\mathbf{U}_B^\top \mathbf{X}]^\top [\mathbf{U}_B(\mathbf{V} - \mathbf{I}_k)\mathbf{U}_B^\top \mathbf{X}] \\
& = \mathbf{X}^\top \mathbf{U}_B [(\mathbf{V} - \mathbf{I}_k + \mathbf{V}^\top - \mathbf{I}_k) + (\mathbf{V} - \mathbf{I}_k)^\top \mathbf{U}_B^\top \mathbf{U}_B(\mathbf{V} - \mathbf{I}_k)] \mathbf{U}_B^\top \mathbf{X} \\
& \stackrel{\textcircled{2}}{=} \mathbf{X}^\top \mathbf{U}_B [(\mathbf{V} - \mathbf{I}_k + \mathbf{V}^\top - \mathbf{I}_k) + (\mathbf{V} - \mathbf{I}_k)^\top (\mathbf{V} - \mathbf{I}_k)] \mathbf{U}_B^\top \mathbf{X} \\
& = \mathbf{X}^\top \mathbf{U}_B(\mathbf{V} - \mathbf{I}_k + \mathbf{V}^\top - \mathbf{I}_k + \mathbf{V}^\top \mathbf{V} - \mathbf{V}^\top - \mathbf{V} + \mathbf{I}_k) \mathbf{U}_B^\top \mathbf{X} \\
& = \mathbf{X}^\top \mathbf{U}_B(-\mathbf{I}_k + \mathbf{V}^\top \mathbf{V}) \mathbf{U}_B^\top \mathbf{X} \\
& \stackrel{\textcircled{3}}{=} \mathbf{X}^\top \mathbf{U}_B \cdot \mathbf{0} \cdot \mathbf{U}_B^\top \mathbf{X} \\
& = \mathbf{0},
\end{aligned}$$

1368 where step ① uses $\mathbf{X}^+ = \mathbf{X} + \mathbf{U}_B(\mathbf{V} - \mathbf{I}_k)\mathbf{U}_B^\top \mathbf{X}$; step ② uses $\mathbf{U}_B^\top \mathbf{U}_B = \mathbf{I}_k$; step ③ uses $\mathbf{V}^\top \mathbf{V} = \mathbf{I}_k$.1369 **Part (b).** Obvious. □1373 **D.2 PROOF OF LEMMA 2.2**1374 *Proof.* We define $\mathbf{X}^+ \triangleq \mathbf{X} + \mathbf{U}_B(\mathbf{V} - \mathbf{I}_k)\mathbf{U}_B^\top \mathbf{X}$, $\underline{\mathbf{Q}} \triangleq (\mathbf{Z}^\top \otimes \mathbf{U}_B)^\top \mathbf{H}(\mathbf{Z}^\top \otimes \mathbf{U}_B)$, and $\mathbf{Z} \triangleq \mathbf{U}_B^\top \mathbf{X}$.1375 **Part (a).** We derive the following results:

$$\begin{aligned}
\|\mathbf{X}^+ - \mathbf{X}\|_{\mathbf{H}}^2 & \stackrel{\textcircled{1}}{=} \|\mathbf{U}_B(\mathbf{V} - \mathbf{I}_k)\mathbf{Z}\|_{\mathbf{H}}^2 \\
& \stackrel{\textcircled{2}}{=} \text{vec}(\mathbf{U}_B(\mathbf{V} - \mathbf{I}_k)\mathbf{Z})^\top \mathbf{H} \text{vec}(\mathbf{U}_B(\mathbf{V} - \mathbf{I}_k)\mathbf{Z}) \\
& \stackrel{\textcircled{3}}{=} \text{vec}(\mathbf{V} - \mathbf{I}_k)^\top (\mathbf{Z}^\top \otimes \mathbf{U}_B)^\top \mathbf{H}(\mathbf{Z}^\top \otimes \mathbf{U}_B) \text{vec}(\mathbf{V} - \mathbf{I}_k) \\
& \stackrel{\textcircled{4}}{=} \|\mathbf{V} - \mathbf{I}_k\|_{(\mathbf{Z}^\top \otimes \mathbf{U}_B)^\top \mathbf{H}(\mathbf{Z}^\top \otimes \mathbf{U}_B)}^2 \\
& \stackrel{\textcircled{5}}{=} \|\mathbf{V} - \mathbf{I}_k\|_{\underline{\mathbf{Q}}}^2,
\end{aligned}$$

1386 where step ① uses $\mathbf{X}^+ \triangleq \mathbf{X} + \mathbf{U}_B(\mathbf{V} - \mathbf{I}_k)\mathbf{Z}$; step ② uses $\|\mathbf{X}\|_{\mathbf{H}}^2 = \text{vec}(\mathbf{X})^\top \mathbf{H} \text{vec}(\mathbf{X})$; step ③
1387 uses $(\mathbf{Z}^\top \otimes \mathbf{R}) \text{vec}(\mathbf{U}) = \text{vec}(\mathbf{R} \mathbf{U} \mathbf{Z})$ for all \mathbf{R} , \mathbf{Z} , and \mathbf{U} of suitable dimensions; step ④ uses
1388 $\|\mathbf{X}\|_{\mathbf{H}}^2 = \text{vec}(\mathbf{X})^\top \mathbf{H} \text{vec}(\mathbf{X})$ again; step ⑤ uses the definition of $\underline{\mathbf{Q}}$.1389 **Part (b).** We derive the following equalities:

$$\begin{aligned}
\|\mathbf{X}^+ - \mathbf{X}\|_{\mathbf{F}}^2 & \stackrel{\textcircled{1}}{=} \|\mathbf{U}_B(\mathbf{V} - \mathbf{I}_k)\mathbf{Z}\|_{\mathbf{F}}^2 \\
& \stackrel{\textcircled{2}}{=} \|(\mathbf{V} - \mathbf{I}_k)\mathbf{Z}\|_{\mathbf{F}}^2 \\
& = \langle (\mathbf{V} - \mathbf{I}_k)^\top (\mathbf{V} - \mathbf{I}_k), \mathbf{Z} \mathbf{Z}^\top \rangle \\
& \stackrel{\textcircled{3}}{=} 2\langle \mathbf{I}_k - \mathbf{V}, \mathbf{Z} \mathbf{Z}^\top \rangle + \langle \mathbf{V} - \mathbf{V}^\top, \mathbf{Z} \mathbf{Z}^\top \rangle. \\
& \stackrel{\textcircled{4}}{=} 2\langle \mathbf{I}_k - \mathbf{V}, \mathbf{Z} \mathbf{Z}^\top \rangle + 0.
\end{aligned}$$

1398 where step ① uses $\mathbf{X}^+ \triangleq \mathbf{X} + \mathbf{U}_B(\mathbf{V} - \mathbf{I}_k)\mathbf{Z}$; step ② uses the fact that $\|\mathbf{U}_B \mathbf{V}\|_{\mathbf{F}}^2 = \|\mathbf{V}\|_{\mathbf{F}}^2$ for any
1399 $\mathbf{V} \in \mathbb{R}^{k \times k}$; step ③ uses

1400
$$(\mathbf{V} - \mathbf{I}_k)^\top (\mathbf{V} - \mathbf{I}_k) = \mathbf{I}_k - \mathbf{V}^\top - \mathbf{V} + \mathbf{I}_k = 2(\mathbf{I}_k - \mathbf{V}) + (\mathbf{V} - \mathbf{V}^\top);$$

1402 step ④ uses the fact that $\langle \mathbf{V}, \mathbf{Z} \mathbf{Z}^\top \rangle = \langle \mathbf{V}^\top, (\mathbf{Z} \mathbf{Z}^\top)^\top \rangle = \langle \mathbf{V}^\top, \mathbf{Z} \mathbf{Z}^\top \rangle$ which holds true as the matrix
1403 $\mathbf{Z} \mathbf{Z}^\top$ is symmetric.

1404 **Part (c).** We have:

$$\begin{aligned}
 \|\mathbf{X}^+ - \mathbf{X}\|_F^2 &= \|\mathbf{U}_B(\mathbf{V} - \mathbf{I}_k)\mathbf{U}_B^\top \mathbf{X}\|_F^2 \\
 &\stackrel{\textcircled{1}}{\leq} \|\mathbf{U}_B\|_{\text{sp}}^2 \cdot \|(\mathbf{V} - \mathbf{I}_k)\mathbf{U}_B^\top \mathbf{X}\|_F^2 \\
 &\stackrel{\textcircled{2}}{\leq} \|\mathbf{U}_B\|_{\text{sp}}^2 \cdot \|\mathbf{V} - \mathbf{I}_k\|_F^2 \cdot \|\mathbf{U}_B^\top\|_{\text{sp}}^2 \cdot \|\mathbf{X}\|_{\text{sp}}^2 \\
 &\stackrel{\textcircled{3}}{=} \|\mathbf{V} - \mathbf{I}_k\|_F^2 \\
 &\stackrel{\textcircled{4}}{=} 2\langle \mathbf{I}_k - \mathbf{V}, \mathbf{I}_k \rangle,
 \end{aligned}$$

1414 where step $\textcircled{1}$ and step $\textcircled{2}$ uses the norm inequality that $\|\mathbf{A}\mathbf{X}\|_F \leq \|\mathbf{A}\|_F \cdot \|\mathbf{X}\|_{\text{sp}}$ for any \mathbf{A} and
1415 \mathbf{X} ; step $\textcircled{3}$ uses $\|\mathbf{U}_B\|_{\text{sp}} = \|\mathbf{U}_B^\top\|_{\text{sp}} = \|\mathbf{X}\|_{\text{sp}} = 1$ for any $\mathbf{X} \in \text{St}(n, r)$; step $\textcircled{4}$ uses the following
1416 equalities for any $\mathbf{V} \in \text{St}(k, k)$:

$$\|\mathbf{V} - \mathbf{I}_k\|_F^2 = \|\mathbf{V}\|_F^2 + \|\mathbf{I}_k\|_F^2 - 2\langle \mathbf{I}_k, \mathbf{V} \rangle = \|\mathbf{I}_k\|_F^2 + \|\mathbf{I}_k\|_F^2 - 2\langle \mathbf{I}_k, \mathbf{V} \rangle = 2\langle \mathbf{I}_k, \mathbf{I}_k - \mathbf{V} \rangle.$$

□

D.3 PROOF OF LEMMA 2.3

1422 *Proof.* We define $\mathcal{K}(\mathbf{V}; \mathbf{X}^t, B) \triangleq \frac{1}{2}\|\mathbf{V} - \mathbf{I}_k\|_{Q+\alpha\mathbf{I}}^2 + h(\mathbf{V}\mathbf{Z}) + \langle \mathbf{V}, [\nabla f(\mathbf{X}^t)(\mathbf{X}^t)^\top]_{BB} \rangle + \ddot{c}$, where
1423 $\mathbf{Z} \triangleq \mathbf{U}_B^\top \mathbf{X}^t$, and $\ddot{c} = h(\mathbf{U}_B^\top \mathbf{X}^t) + f(\mathbf{X}^t) - \langle \mathbf{I}_k, [\nabla f(\mathbf{X}^t)(\mathbf{X}^t)^\top]_{BB} \rangle$ is a constant.

1425 **Part (a).** Using the definition of $\mathcal{K}(\mathbf{V}; \mathbf{X}^t, B)$, we have the following equalities for all $\mathbf{V} \in \text{St}(k, k)$:

$$\begin{aligned}
 &\mathcal{K}(\mathbf{V}; \mathbf{X}^t, B) \\
 &\triangleq \ddot{c} + \frac{1}{2}\|\mathbf{V} - \mathbf{I}_k\|_{Q+\alpha\mathbf{I}_k}^2 + \langle \mathbf{V}, [\nabla f(\mathbf{X}^t)(\mathbf{X}^t)^\top]_{BB} \rangle + h(\mathbf{V}\mathbf{Z}) \\
 &= \ddot{c} + \frac{1}{2}\|\mathbf{V} - \mathbf{I}_k\|_Q^2 + \frac{\alpha}{2}\|\mathbf{V} - \mathbf{I}_k\|_F^2 + \langle \mathbf{V}, [\nabla f(\mathbf{X}^t)(\mathbf{X}^t)^\top]_{BB} \rangle + h(\mathbf{V}\mathbf{Z}) \\
 &\stackrel{\textcircled{1}}{=} \ddot{c} + \frac{1}{2}\|\mathbf{V}\|_Q^2 - \langle \mathbf{V}, \text{mat}(\mathbf{Q}\text{vec}(\mathbf{I}_k)) \rangle + \frac{1}{2}\|\mathbf{I}_k\|_Q^2 + \alpha\langle \mathbf{I}_k, \mathbf{I}_k - \mathbf{V} \rangle + \langle \mathbf{V}, [\nabla f(\mathbf{X}^t)(\mathbf{X}^t)^\top]_{BB} \rangle + h(\mathbf{V}\mathbf{Z}) \\
 &\stackrel{\textcircled{2}}{=} \ddot{c} + \frac{1}{2}\|\mathbf{V}\|_Q^2 + \langle \mathbf{V}, \underbrace{[\nabla f(\mathbf{X}^t)(\mathbf{X}^t)^\top]_{BB} - \text{mat}(\mathbf{Q}\text{vec}(\mathbf{I}_k)) - \alpha\mathbf{I}_k}_{\triangleq \mathbf{P}} \rangle + h(\mathbf{V}\mathbf{Z}) + \frac{1}{2}\|\mathbf{I}_k\|_Q^2,
 \end{aligned}$$

1435 where step $\textcircled{1}$ uses Lemma 2.2(c) that: $\frac{1}{2}\|\mathbf{V} - \mathbf{I}_k\|_F^2 = \langle \mathbf{I}_k, \mathbf{I}_k - \mathbf{V} \rangle$; step $\textcircled{2}$ uses the definition of \mathbf{P} .

1436 **Part (b).** We consider the case that \mathbf{Q} is chosen to be a diagonal matrix that $\mathbf{Q} = \varsigma\mathbf{I}_k$, where ς is defined in Equation (9). Using $\mathbf{V} \in \text{St}(k, k)$, the term $\frac{1}{2}\|\mathbf{V}\|_Q^2$ simplifies to a constant with
1437 $\frac{1}{2}\|\mathbf{V}\|_Q^2 = \frac{1}{2}\varsigma k$. We can deduce from (3):

$$\bar{\mathbf{V}}^t \in \arg \min_{\mathbf{V} \in \text{St}(k, k)} \mathcal{P}(\mathbf{V}) \triangleq \langle \mathbf{V}, \mathbf{P} \rangle + h(\mathbf{X}). \quad (34)$$

1442 In particular, when $h(\mathbf{X}) = 0$, Problem (34) becomes the nearest orthogonality matrix problem and
1443 can be solved analytically, yielding a closed-form solution that:

$$\bar{\mathbf{V}}^t \in \arg \min_{\mathbf{V} \in \text{St}(k, k)} \frac{1}{2}\|\mathbf{V} - (-\mathbf{P})\|_F^2 = \mathbb{P}_{\mathcal{M}}(-\mathbf{P}) = -\mathbb{P}_{\mathcal{M}}(\mathbf{P}) = -\tilde{\mathbf{U}}\tilde{\mathbf{V}}^\top.$$

1446 Here, $\mathbf{P} = \tilde{\mathbf{U}}\text{Diag}(\mathbf{s})\tilde{\mathbf{V}}^\top$ is the singular value decomposition of \mathbf{P} with $\tilde{\mathbf{U}}, \tilde{\mathbf{V}} \in \text{St}(k, k)$, $\mathbf{s} \in \mathbb{R}^k$,
1447 and $\mathbf{s} \geq \mathbf{0}$.

1449 Notably, the multiplier for the orthogonality constraint $\mathbf{V}^\top \mathbf{V} = \mathbf{I}_k$ can be computed as: $\mathbf{\Lambda} = -\mathbf{P}^\top \bar{\mathbf{V}}^t \stackrel{\textcircled{1}}{=} -[\tilde{\mathbf{U}}\text{Diag}(\mathbf{s})\tilde{\mathbf{V}}^\top]^\top \cdot [-\tilde{\mathbf{U}}\tilde{\mathbf{V}}^\top] = \tilde{\mathbf{V}}\text{Diag}(\mathbf{s})\tilde{\mathbf{U}}^\top \tilde{\mathbf{U}}\tilde{\mathbf{V}}^\top \stackrel{\textcircled{2}}{=} \tilde{\mathbf{V}}\text{Diag}(\mathbf{s})\tilde{\mathbf{V}}^\top \stackrel{\textcircled{3}}{\succeq} \mathbf{0}$, where step
1450 $\textcircled{1}$ uses $\mathbf{P} = \tilde{\mathbf{U}}\text{Diag}(\mathbf{s})\tilde{\mathbf{V}}^\top$ and $\bar{\mathbf{V}}^t = -\tilde{\mathbf{U}}\tilde{\mathbf{V}}^\top$; step $\textcircled{2}$ uses $\tilde{\mathbf{U}}^\top \tilde{\mathbf{U}} = \mathbf{I}_k$; step $\textcircled{3}$ uses $\mathbf{s} \geq \mathbf{0}$.

□

D.4 PROOF OF LEMMA 2.5

1454 *Proof.* Any 2×2 matrix takes the form $\mathbf{V} = \begin{pmatrix} a & b \\ c & d \end{pmatrix}$. The orthogonality constraint implies that
1455 $\mathbf{V} \in \text{St}(2, 2)$ meets the following three equations: $1 = a^2 + b^2$, $1 = c^2 + d^2$, $0 = ac + bd$.

Without loss of generality, we let $c = \sin(\theta)$ and $d = \cos(\theta)$ with $\theta \in \mathbb{R}$. Then we obtain either **(i)** $a = \cos(\theta), b = -\sin(\theta)$ or **(ii)** $a = -\cos(\theta), b = \sin(\theta)$. Therefore, we have the following Givens rotation matrix $\mathbf{V}_\theta^{\text{rot}}$ and Jacobi reflection matrix $\mathbf{V}_\theta^{\text{ref}}$:

$$\mathbf{V}_\theta^{\text{rot}} \triangleq \begin{bmatrix} \cos(\theta) & -\sin(\theta) \\ \sin(\theta) & \cos(\theta) \end{bmatrix}, \quad \mathbf{V}_\theta^{\text{ref}} \triangleq \begin{bmatrix} -\cos(\theta) & \sin(\theta) \\ \sin(\theta) & \cos(\theta) \end{bmatrix}.$$

Note that for any $a, b, c, d \in \mathbb{R}$, we have: $\det\begin{bmatrix} a & b \\ c & d \end{bmatrix} = ad - bc$. Therefore, we obtain: $\det(\mathbf{V}_\theta^{\text{rot}}) = \cos^2(\theta) + \sin^2(\theta) = 1$ and $\det(\mathbf{V}_\theta^{\text{ref}}) = -\cos^2(\theta) - \sin^2(\theta) = -1$ for any $\theta \in \mathbb{R}$.

□

E PROOF FOR SECTION 3

```

1471 function [Q,R] = JacobiGivensQR(X)
1472 n = size(X,1); Q = eye(n); R = X;
1473 for j=1:n
1474     for i=n:-1:(j+1)
1475         B = [i-1:i]; V = Givens(R(i-1,j),R(i,j));
1476         R(B,:) = V'*R(B,:); Q(:,B) = Q(:,B)*V;
1477         if (i==j+1 & R(j,j)<0)
1478             V = [-1 0; 0 -1]; % or V = [-1 0; 0 1];
1479             R(B,:) = V'*R(B,:); Q(:,B) = Q(:,B)*V;
1480         end
1481     end
1482     if(R(n,n)<0)
1483         V = [1 0; 0 -1]; R(B,:) = V'*R(B,:); Q(:,B) = Q(:,B)*V;
1484     end
1485
1486 function V = Givens(a,b)
1487 % Find a Givens rotation that V' * [a;b] = [r;0]
1488 if (b==0)
1489     c = 1; s = 0;
1490 else
1491     if (abs(b) > abs(a))
1492         tau = -a/b; s = 1/sqrt(1+tau^2); c = s*tau;
1493     else
1494         tau = -b/a; c = 1/sqrt(1+tau^2); s = c*tau;
1495     end
1496 V = [c s;-s c];
1497
1498
1499
1500
1501
1502
1503
1504
1505
1506
1507
1508
1509
1510
1511
```

Listing 1: Matlab implementation for our **Jacobi-Givens-QR** algorithm.

E.1 PROOF OF THEOREM 3.1

Proof. Part (a). First, recall the classical **Givens-QR** algorithm, which is detailed in Section 5.2.5 of (Golub & Van Loan, 2013)). This algorithm can decompose any matrix $\mathbf{X} \in \mathbb{R}^{n \times n}$ (not necessarily orthogonal) into the form $\mathbf{X} = \mathbf{QR}$, where \mathbf{Q} is an orthogonal matrix ($\mathbf{Q} \in \text{St}(n, n)$) and \mathbf{R} is a lower triangular matrix with $\mathbf{R}_{ij} = 0$ for all $i < j$, achieved through $C_n^2 = \frac{n(n-1)}{2}$ Givens rotation steps.

Combining the result from Lemma A.5, we can conclude that classical **Givens-QR** algorithm can decompose any orthogonal matrix into the form $\mathbf{X} = \mathbf{QR}$, where $\mathbf{Q} \in \text{St}(n, n)$ and \mathbf{R} is diagonal matrix with $\mathbf{R}_{i,i} \in \{-1, +1\}$ for all $i \in [n]$.

We introduce a modification to the **Givens-QR** algorithm, resulting in our **Jacobi-Givens-QR** algorithm as presented in Listing 1. This algorithm can decompose any matrix $\mathbf{X} \in \text{St}(n, n)$ into the form $\mathbf{X} = \mathbf{QR}$, where $\mathbf{Q} = \mathbf{X}$ and $\mathbf{R} = \mathbf{I}_n$, using a sequence of C_n^k Givens rotation or Jacobi reflection steps.

1512 Please take note of the following four important points in Listing 1.

1513 **a)** When we remove Lines 7-10 and Lines 13-15 from Listing 1, it essentially reverts to the clas-
 1514 sical **Givens-QR** algorithm. **Givens-QR** operates by selecting an appropriate Givens rotation
 1515 matrix $\mathbf{V} = \begin{bmatrix} \cos(\theta) & \sin(\theta) \\ -\sin(\theta) & \cos(\theta) \end{bmatrix}$ with a suitable rotation angle θ to zero-out the matrix element
 1516 \mathbf{R}_{ij} systematically from left to right ($j = 1 \rightarrow n$) and bottom to top ($i = n \rightarrow (j+1)$) within
 1517 every pair of neighboring columns.

1518 **b)** Lines 7-10 and Lines 13-15 can be viewed as correction steps to ensure that the entries $\mathbf{R}_{j,j} =$
 1519 1 for all $j = n$.

1520 **c)** Line 7-10 is executed for $(n-2)$ times. In Line 7-10, when **Jacobi-Givens-QR** detects a
 1521 negative entry $\mathbf{R}_{i-1,i-1}$ with $i = j+1$, it applies a rotation matrix $\mathbf{V} \triangleq \begin{pmatrix} -1 & 0 \\ 0 & -1 \end{pmatrix}$ to the two
 1522 rows $\mathbf{B} = [i-1, i]$ to ensure that³ $\mathbf{R}_{i-1,i-1} = 1$.

1523 **d)** Line 13-15 is executed only once when $\det(\mathbf{X}) = -1$. In such cases, we have $\mathbf{R}_{\text{BB}} = \begin{pmatrix} 1 & 0 \\ 0 & -1 \end{pmatrix}$
 1524 and $\det(\mathbf{R}_{\text{BB}}) = -1$, where $\mathbf{B} = [n-1, n]$ is the two indices for the final rotation or reflection
 1525 step. To ensure that the resulting \mathbf{R}_{BB} is an identity matrix, **Jacobi-Givens-QR** employs a
 1526 reflection matrix $\mathbf{V} = \begin{pmatrix} 1 & 0 \\ 0 & -1 \end{pmatrix}$, leading to $\mathbf{V}^T \mathbf{R}_{\text{BB}} = \mathbf{I}_2$.

1527 Therefore, we establish the conclusion that any orthogonal matrix $\mathbf{X} \in \text{St}(n, n)$ can be expressed
 1528 as $\mathbf{D} = \mathcal{W}_{C_n^k} \dots \mathcal{W}_2 \mathcal{W}_1$, where $\mathcal{W}_i = \mathbf{U}_{\mathcal{B}_i} \mathcal{V}_i \mathbf{U}_{\mathcal{B}_i}^T + \mathbf{U}_{\mathcal{B}_i^c} \mathcal{V}_i \mathbf{U}_{\mathcal{B}_i^c}^T$, and $\mathcal{V}_i \in \text{St}(2, 2)$ is a suitable matrix
 1529 associated with \mathcal{B}_i . Furthermore, if $\forall i, \mathcal{V}_i = \mathbf{I}_2$, we have $\forall i, \mathcal{W}_i = \mathbf{I}_n$, leading to $\mathbf{D} = \mathbf{I}_n$. This
 1530 concludes the proof of the first part of this theorem.

1531 **Part (b).** For any given $\mathbf{X} \in \text{St}(n, r)$ and $\mathbf{X}^0 \in \text{St}(n, r)$, we let:

$$\bar{\mathbf{D}} = \mathbb{P}_{\text{St}(n, n)}(\mathbf{X}[\mathbf{X}^0]^T), \quad (35)$$

1532 where $\mathbb{P}_{\text{St}(n, n)}(\mathbf{Y})$ denotes the nearest orthogonality matrix to the given matrix \mathbf{Y} .

1533 Assume that the matrix $\mathbf{X}[\mathbf{X}^0]^T$ has the following singular value decomposition:

$$\mathbf{X}[\mathbf{X}^0]^T = \mathbf{U} \text{Diag}(\mathbf{z}) \mathbf{V}^T, \quad \mathbf{z} \in \{0, 1\}^n, \quad \mathbf{U} \in \text{St}(n, n), \quad \mathbf{V} \in \text{St}(n, n).$$

1534 Therefore, we have the following equalities:

$$\text{Diag}(\mathbf{z}) = \mathbf{U}^T \mathbf{X}[\mathbf{X}^0]^T \mathbf{V}. \quad (36)$$

$$\bar{\mathbf{D}} = \mathbf{U} \mathbf{V}^T \in \text{St}(n, n). \quad (37)$$

1535 Furthermore, we derive the following results:

$$\begin{aligned} \mathbf{z} &\in \{0, 1\}^n \\ \Rightarrow \text{Diag}(\mathbf{z})^T &= \text{Diag}(\mathbf{z}) \text{Diag}(\mathbf{z})^T \\ \Rightarrow \mathbf{U}[\text{Diag}(\mathbf{z})^T - \text{Diag}(\mathbf{z}) \text{Diag}(\mathbf{z})^T] \mathbf{U}^T \mathbf{X} &= \mathbf{0} \\ \stackrel{\textcircled{1}}{\Rightarrow} \mathbf{U}[\mathbf{V}^T \mathbf{X}^0 \mathbf{X}^T \mathbf{U} - \mathbf{U}^T \mathbf{X}(\mathbf{X}^0)^T \mathbf{V} \mathbf{V}^T \mathbf{X}^0 \mathbf{X}^T \mathbf{U}] \mathbf{U}^T \mathbf{X} &= \mathbf{0} \\ \Rightarrow \mathbf{U} \mathbf{V}^T \mathbf{X}^0 \mathbf{X}^T \mathbf{U} \mathbf{U}^T \mathbf{X} - \mathbf{U} \mathbf{U}^T \mathbf{X}(\mathbf{X}^0)^T \mathbf{V} \mathbf{V}^T \mathbf{X}^0 \mathbf{X}^T \mathbf{U} \mathbf{U}^T \mathbf{X} &= \mathbf{0} \\ \stackrel{\textcircled{2}}{\Rightarrow} \mathbf{U} \mathbf{V}^T \mathbf{X}^0 - \mathbf{X} &= \mathbf{0} \\ \stackrel{\textcircled{3}}{\Rightarrow} \bar{\mathbf{D}} \cdot \mathbf{X}^0 - \mathbf{X} &= \mathbf{0}, \end{aligned}$$

1536 where step $\textcircled{1}$ uses (36); step $\textcircled{2}$ uses $\mathbf{U} \mathbf{U}^T = \mathbf{I}_n$, $\mathbf{V} \mathbf{V}^T = \mathbf{I}_n$, $\mathbf{X}^T \mathbf{X} = \mathbf{I}_r$, and $[\mathbf{X}^0]^T \mathbf{X}^0 = \mathbf{I}_r$; step
 1537 $\textcircled{3}$ uses (37). We conclude that, for any given $\mathbf{X} \in \text{St}(n, r)$ and $\mathbf{X}^0 \in \text{St}(n, r)$, we can always find
 1538 a matrix $\bar{\mathbf{D}} \in \text{St}(n, n)$ such that $\bar{\mathbf{D}} \mathbf{X}^0 = \mathbf{X}$.

1539 Since the matrix $\bar{\mathbf{D}} \in \text{St}(n, n)$ can be represented as $\bar{\mathbf{D}} = \mathcal{W}_{C_n^k} \dots \mathcal{W}_2 \mathcal{W}_1$, where $\mathcal{W}_i =$
 1540 $\mathbf{U}_{\mathcal{B}_i} \mathcal{V}_i \mathbf{U}_{\mathcal{B}_i}^T + \mathbf{U}_{\mathcal{B}_i^c} \mathcal{V}_i \mathbf{U}_{\mathcal{B}_i^c}^T$ for some suitable $\mathcal{V}_i \in \text{St}(2, 2)$ (as established in the first part of this
 1541 theorem), we can conclude that any matrix $\mathbf{X} \in \text{St}(n, r)$ can be expressed as $\mathbf{X} = \bar{\mathbf{D}} \mathbf{X}^0 =$
 1542 $\mathcal{W}_{C_n^k} \dots \mathcal{W}_2 \mathcal{W}_1 \mathbf{X}^0$.

1543 \square

1544 ³ Alternatively, one can use the reflection matrix $\mathbf{V} \triangleq \begin{pmatrix} -1 & 0 \\ 0 & 1 \end{pmatrix}$ instead of the rotation matrix $\mathbf{V} \triangleq \begin{pmatrix} -1 & 0 \\ 0 & -1 \end{pmatrix}$
 1545 to ensure that $\mathbf{R}_{i-1,i-1} = 1$.

1566 E.2 PROOF OF COROLLARY 3.2
15671568 *Proof.* We denote e_i as the i -th canonical basis vector in \mathbb{R}^n .1569 We denote the set $\{\mathcal{B}_1, \mathcal{B}_2, \dots, \mathcal{B}_{C_n^k}\}$ as all possible combinations of the index vectors choosing k
1570 items from n without repetition.1571
1572 **Part (a).** Fix any $k \geq 2$. By Theorem 3.1(a) for the case $k = 2$, for every $\mathbf{D} \in \text{St}(n, n)$ there exist
1573 index pairs (p_i, q_i) and matrices $\mathcal{V}_i^{(2)} \in \text{St}(2, 2)$ such that

1574
1575
$$\mathbf{D} = \mathcal{W}_{C_n^2}^{(2)} \cdots \mathcal{W}_2^{(2)} \mathcal{W}_1^{(2)},$$

1576 where

1577
1578
$$\mathcal{W}_i^{(2)} = \mathbf{I}_n + \mathbf{U}_{\mathcal{B}_i}^{(2)} (\mathcal{V}_j^{(2)} - \mathbf{I}_2) [\mathbf{U}_{\mathcal{B}_i}^{(2)}]^\top, \quad \mathbf{U}_{\mathcal{B}_i}^{(2)} = [e_{p_i}, e_{q_i}] \in \mathbb{R}^{n \times 2}.$$

1579 We let

1580
1581
$$\mathcal{V}_i \triangleq \begin{pmatrix} \mathcal{V}_i^{(2)} & \mathbf{0} \\ \mathbf{0} & \mathbf{I}_{k-2} \end{pmatrix} \in \text{St}(k, k), \quad \mathcal{W}_i \triangleq \mathbf{I}_n + \mathbf{U}_{\mathcal{B}_i} (\mathcal{V}_i - \mathbf{I}_k) \mathbf{U}_{\mathcal{B}_i}^\top.$$

1582 By construction, \mathcal{W}_j acts as $\mathcal{V}_j^{(2)}$ on the two coordinates p_j, q_j and as the identity on all other
1583 coordinates, hence $\mathcal{W}_j = \mathcal{W}_j^{(2)}$ as linear operators on \mathbb{R}^n . Therefore

1584
1585
$$\mathbf{D} = \mathcal{W}_{C_n^2}^{(2)} \cdots \mathcal{W}_1^{(2)} = \mathcal{W}_{C_n^2} \cdots \mathcal{W}_1,$$

1586 which proves the first part of this corollary for any $k \geq 2$.1587 **Part (b).** A similar argument to that used in the proof of Theorem 3.1(b) yields the second part of
1588 this corollary.1589
1590 \square 1591 E.3 PROOF FOR THEOREM 3.7
15921593 *Proof.* We use $\bar{\mathbf{X}}$, $\ddot{\mathbf{X}}$, and $\check{\mathbf{X}}$ to denote a *global optimal point*, a BS_k -*point*, and a *critical point* of
1594 Problem (1), respectively.1595 Setting the Riemannian subgradient of $\mathcal{K}(\mathbf{V}; \ddot{\mathbf{X}}, \mathbf{B})$ w.r.t. \mathbf{V} to zero, we have $\mathbf{0} \in \partial_{\mathcal{M}} \mathcal{K}(\mathbf{V}; \ddot{\mathbf{X}}, \mathbf{B}) =$
1596 $\ddot{\mathbf{G}}(\mathbf{V}) \ominus \mathbf{V}[\ddot{\mathbf{G}}(\mathbf{V})]^\top \mathbf{V}$, where $\ddot{\mathbf{G}}(\mathbf{V}) = \alpha(\mathbf{V} - \mathbf{I}_k) + \mathbf{U}_B^\top [\text{mat}(\mathbf{H}\text{vec}(\mathbf{X}^+ - \ddot{\mathbf{X}})) + \nabla f(\ddot{\mathbf{X}}) +$
1597 $\partial h(\mathbf{X}^+)] \ddot{\mathbf{X}}^\top \mathbf{U}_B$ and $\mathbf{X}^+ = \ddot{\mathbf{X}} + \mathbf{U}_B(\mathbf{V} - \mathbf{I}_k) \mathbf{U}_B^\top \ddot{\mathbf{X}}$. Letting $\mathbf{V} = \mathbf{I}_k$, we have the following
1598 **necessary but not sufficient** condition for any BS_k -*point*:

1599
1600
$$\forall B \in \{\mathcal{B}_i\}_{i=1}^{C_n^k}, \quad \mathbf{0} = \mathbf{U}_B^\top (\mathbf{G} \ddot{\mathbf{X}}^\top - \ddot{\mathbf{X}} \mathbf{G}^\top) \mathbf{U}_B, \text{ with } \mathbf{G} \in \nabla f(\ddot{\mathbf{X}}) + \partial h(\ddot{\mathbf{X}}). \quad (38)$$

1601 **Part (a).** We now show that $\{\text{critical points } \check{\mathbf{X}}\} \supseteq \{\text{BS}_k\text{-points } \ddot{\mathbf{X}}\}$ for all $k \geq 2$. We let $\mathbf{G} \in$
1602 $\nabla f(\ddot{\mathbf{X}}) + \partial h(\ddot{\mathbf{X}})$. Using Lemma A.1, we have:

1603
1604
$$\begin{aligned} \mathbf{0}_{n,n} = \mathbf{G} \ddot{\mathbf{X}}^\top - \ddot{\mathbf{X}} \mathbf{G}^\top &\Rightarrow (\mathbf{0}_{n,n} \cdot \ddot{\mathbf{X}}) = (\mathbf{G} \ddot{\mathbf{X}}^\top - \ddot{\mathbf{X}} \mathbf{G}^\top) \ddot{\mathbf{X}} \\ &\stackrel{\textcircled{1}}{\Rightarrow} \mathbf{0}_{n,r} = \mathbf{G} - \ddot{\mathbf{X}} \mathbf{G}^\top \ddot{\mathbf{X}}, \\ &\Rightarrow \ddot{\mathbf{X}}^\top \cdot \mathbf{0}_{n,r} = \ddot{\mathbf{X}}^\top (\mathbf{G} - \ddot{\mathbf{X}} \mathbf{G}^\top \ddot{\mathbf{X}}) \\ &\stackrel{\textcircled{2}}{\Rightarrow} \mathbf{0}_{r,r} = \ddot{\mathbf{X}}^\top \mathbf{G} - \mathbf{G}^\top \ddot{\mathbf{X}} \\ &\Rightarrow \mathbf{0}_{n,n} = \ddot{\mathbf{X}}^\top (\ddot{\mathbf{X}} \mathbf{G} - \mathbf{G}^\top \ddot{\mathbf{X}}) \ddot{\mathbf{X}}^\top \\ &\stackrel{\textcircled{3}}{\Rightarrow} \mathbf{0}_{n,n} = \underbrace{\ddot{\mathbf{X}}^\top \mathbf{G}^\top \ddot{\mathbf{X}}}_{\triangleq \mathbf{G}^\top} - \underbrace{\ddot{\mathbf{X}} \mathbf{G}^\top \ddot{\mathbf{X}}^\top}_{\triangleq \mathbf{G}}, \end{aligned} \quad (39)$$

1605 where steps ① and ② use $\ddot{\mathbf{X}}^\top \ddot{\mathbf{X}} = \mathbf{I}_r$; step ③ uses Equality (39) that $\mathbf{G} = \ddot{\mathbf{X}} \mathbf{G}^\top \ddot{\mathbf{X}}$. We conclude
1606 that the necessary condition in Equation (38) is equivalent to the optimality condition of critical
1607 points.

1620 **Part (b).** We now show that $\{\text{BS}_k\text{-points } \ddot{\mathbf{X}}\} \supseteq \{\text{global optimal points } \bar{\mathbf{X}}\}$ for all $k \in \{2, 3, \dots, n\}$. We define $\mathcal{X}_B^*(\mathbf{V}) \triangleq \bar{\mathbf{X}} + \mathbf{U}_B(\mathbf{V} - \mathbf{I}_k)\mathbf{U}_B^\top \bar{\mathbf{X}}$, and $\mathcal{K}(\mathbf{V}; \mathbf{X}, B) \triangleq f(\mathbf{X}) + \langle \mathbf{V} - \mathbf{I}_k, [\nabla f(\mathbf{X})(\mathbf{X})^\top]_{BB} \rangle + \frac{1}{2}\|\mathbf{V} - \mathbf{I}_k\|_{\mathbf{Q} + \alpha \mathbf{I}_k}^2 + h(\mathbf{U}_{B^c}^\top \mathbf{X}) + h(\mathbf{V} \mathbf{U}_B^\top \mathbf{X})$. We let $\mathbf{V}_{(i)} \in \text{St}(k, k)$ and $\mathcal{B}_i \in \{\mathcal{B}_i\}_{i=1}^{C_n^k}$. We derive:

$$\begin{aligned}
 & \mathcal{K}(\mathbf{I}_2; \bar{\mathbf{X}}, \mathcal{B}_i), \forall \mathcal{B}_i \\
 & \stackrel{\textcircled{1}}{=} F(\bar{\mathbf{X}}) = h(\bar{\mathbf{X}}) + f(\bar{\mathbf{X}}) \\
 & \stackrel{\textcircled{2}}{\leq} h(\mathbf{X}) + f(\mathbf{X}), \forall \mathbf{X} \in \text{St}(n, r) \\
 & \stackrel{\textcircled{3}}{\leq} h(\bar{\mathbf{X}} + \mathbf{U}_{\mathcal{B}_i}(\mathbf{V}_{(i)} - \mathbf{I}_k)\mathbf{U}_{\mathcal{B}_i}^\top \bar{\mathbf{X}}) + f(\bar{\mathbf{X}} + \mathbf{U}_{\mathcal{B}_i}(\mathbf{V}_{(i)} - \mathbf{I}_k)\mathbf{U}_{\mathcal{B}_i}^\top \bar{\mathbf{X}}), \forall \mathbf{V}_{(i)}, \forall \mathcal{B}_i \\
 & \stackrel{\textcircled{4}}{=} h(\mathcal{X}_{\mathcal{B}_i}^*(\mathbf{V}_{(i)})) + f(\mathcal{X}_{\mathcal{B}_i}^*(\mathbf{V}_{(i)})), \forall \mathbf{V}_{(i)}, \forall \mathcal{B}_i \\
 & \stackrel{\textcircled{5}}{=} \mathcal{K}(\mathbf{V}_{(i)}; \bar{\mathbf{X}}, \mathcal{B}_i), \forall \mathbf{V}_{(i)}, \forall \mathcal{B}_i \\
 & \leq \min_{\mathbf{V} \in \text{St}(k, k)} \mathcal{K}(\mathbf{V}; \bar{\mathbf{X}}, \mathcal{B}_i), \forall \mathcal{B}_i,
 \end{aligned} \tag{40}$$

1636 where step ① uses the definition of $\mathcal{K}(\mathbf{V}; \mathbf{X}, B) \triangleq f(\mathbf{X}) + \langle \mathbf{V} - \mathbf{I}_k, [\nabla f(\mathbf{X})(\mathbf{X})^\top]_{BB} \rangle + \frac{1}{2}\|\mathbf{V} - \mathbf{I}_k\|_{\mathbf{Q} + \alpha \mathbf{I}_k}^2 + h(\mathbf{U}_{B^c}^\top \mathbf{X}) + h(\mathbf{V} \mathbf{U}_B^\top \mathbf{X})$; step ② uses the definition of $\bar{\mathbf{X}}$; step ③ uses the basis representation of orthogonal matrices for all $k \geq 2$, as shown in Corollary 3.2; step ④ uses the definition of $\mathcal{X}_B^*(\mathbf{V})$; step ⑤ uses the same strategy as in deriving Inequality (10). This leads to:

$$\mathbf{I}_k \in \arg \min_{\mathbf{V} \in \text{St}(k, k)} \mathcal{K}(\mathbf{V}; \bar{\mathbf{X}}, \mathcal{B}_i), \forall \mathcal{B}_i.$$

1642 The inclusion above implies that $\{\text{BS}_k\text{-points } \ddot{\mathbf{X}}\} \supseteq \{\text{global optimal points } \bar{\mathbf{X}}\}$.

1644 **Part (c).** We now show that $\{\text{BS}_k\text{-points } \ddot{\mathbf{X}}\} \supseteq \{\text{BS}_{k+1}\text{-points } \ddot{\mathbf{X}}\}$. It is evident that the subproblem 1645 of finding $\text{BS}_k\text{-points}$ is encompassed within that of finding $\text{BS}_{k+1}\text{-points}$ stationary point. Thus, 1646 we conclude that the optimality of the latter is stronger.

1647 **Part (d).** The inclusion $\{\text{critical points } \ddot{\mathbf{X}}\} \subseteq \{\text{BS}_k\text{-points } \ddot{\mathbf{X}}\}$ may not always hold true. This 1648 can be illustrated through simple examples of 2×2 optimization problems under orthogonality 1649 constraints (see Appendix Section C.1 for more details). Lastly, it is also evident that the inclusions 1650 $\{\text{BS}_2\text{-points } \ddot{\mathbf{X}}\} \subseteq \{\text{global optimal points } \bar{\mathbf{X}}\}$ and $\{\text{BS}_k\text{-points } \ddot{\mathbf{X}}\} \subseteq \{\text{BS}_{k+1}\text{-points } \ddot{\mathbf{X}}\}$ may 1651 not always hold true.

1652 \square

F PROOF FOR SECTION 4

F.1 PROOF FOR THEOREM 4.2

1658 *Proof.* We define $\mathcal{K}(\mathbf{V}; \mathbf{X}^t, B) \triangleq \frac{1}{2}\|\mathbf{V} - \mathbf{I}_k\|_{\mathbf{Q} + \alpha \mathbf{I}_k}^2 + h(\mathbf{V} \mathbf{Z}) + \langle \mathbf{V}, [\nabla f(\mathbf{X}^t)(\mathbf{X}^t)^\top]_{BB} \rangle + \tilde{c}$, where 1659 $\mathbf{Z} \triangleq \mathbf{U}_B^\top \mathbf{X}^t$ and $\tilde{c} = h(\mathbf{U}_{B^c}^\top \mathbf{X}^t) + f(\mathbf{X}^t) - \langle \mathbf{I}_k, [\nabla f(\mathbf{X}^t)(\mathbf{X}^t)^\top]_{BB} \rangle$ is a constant.

1661 We define $\tilde{c} \triangleq \frac{2}{\alpha} \cdot (F(\mathbf{X}^0) - F(\mathbf{X}^\infty))$.

1663 **Part (a).** First, we have the following equalities:

$$\begin{aligned}
 h(\mathbf{X}^{t+1}) - h(\mathbf{X}^t) & \stackrel{\textcircled{1}}{=} h(\mathbf{U}_B \bar{\mathbf{V}}^t \mathbf{U}_B^\top \mathbf{X}^t + \mathbf{U}_{B^c} \mathbf{U}_{B^c}^\top \mathbf{X}^t) - h(\mathbf{U}_B \mathbf{U}_B^\top \mathbf{X}^t + \mathbf{U}_{B^c} \mathbf{U}_{B^c}^\top \mathbf{X}^t) \\
 & \stackrel{\textcircled{2}}{=} h(\mathbf{U}_B \bar{\mathbf{V}}^t \mathbf{U}_B^\top \mathbf{X}^t) + h(\mathbf{U}_{B^c} \mathbf{U}_{B^c}^\top \mathbf{X}^t) - h(\mathbf{U}_B \mathbf{U}_B^\top \mathbf{X}^t) - h(\mathbf{U}_{B^c} \mathbf{U}_{B^c}^\top \mathbf{X}^t) \\
 & \stackrel{\textcircled{3}}{=} h(\bar{\mathbf{V}}^t \mathbf{U}_B^\top \mathbf{X}^t) - h(\mathbf{U}_B^\top \mathbf{X}^t),
 \end{aligned} \tag{41}$$

1669 where step ① uses $\mathbf{X}^{t+1} = \mathbf{U}_B \mathbf{V} \mathbf{U}_B^\top \mathbf{X}^t + \mathbf{U}_{B^c} \mathbf{U}_{B^c}^\top \mathbf{X}^t$ as in (4) and $\mathbf{I}_k = \mathbf{U}_B \mathbf{U}_B^\top + \mathbf{U}_{B^c} \mathbf{U}_{B^c}^\top$; step ② 1670 and step ③ use the coordinate-wise separable structure of $h(\cdot)$.

1671 Second, since $\bar{\mathbf{V}}^t \in \arg \min_{\mathbf{V} \in \text{St}(k, k)} \mathcal{K}(\mathbf{V}; \mathbf{X}^t, B)$, it follows that $\mathcal{K}(\bar{\mathbf{V}}^t; \mathbf{X}^t, B) \leq \mathcal{K}(\mathbf{I}_k; \mathbf{X}^t, B)$. 1672 This further leads to:

$$h(\bar{\mathbf{V}}^t \mathbf{U}_B^\top \mathbf{X}^t) + \frac{1}{2}\|\bar{\mathbf{V}}^t - \mathbf{I}_k\|_{\mathbf{Q} + \alpha \mathbf{I}_k}^2 + \langle \bar{\mathbf{V}}^t - \mathbf{I}_k, [\nabla f(\mathbf{X}^t)(\mathbf{X}^t)^\top]_{BB} \rangle \leq h(\mathbf{U}_B^\top \mathbf{X}^t). \tag{42}$$

1674 Third, we denote $\mathbf{X}^{t+1} = \mathcal{X}_{\mathbb{B}}^t(\bar{\mathbf{V}}^t)$ and derive:
1675

$$\begin{aligned} 1676 \quad f(\mathbf{X}^{t+1}) - f(\mathbf{X}^t) &\stackrel{\textcircled{1}}{\leq} \langle \mathcal{X}_{\mathbb{B}}^t(\bar{\mathbf{V}}^t) - \mathbf{X}^t, \nabla f(\mathbf{X}^t) \rangle + \frac{1}{2} \|\mathcal{X}_{\mathbb{B}}^t(\bar{\mathbf{V}}^t) - \mathbf{X}^t\|_{\mathbf{H}}^2 \\ 1677 &\stackrel{\textcircled{2}}{=} \langle \mathbf{U}_{\mathbb{B}}(\bar{\mathbf{V}}^t - \mathbf{I}_k) \mathbf{U}_{\mathbb{B}}^T \mathbf{X}^t, \nabla f(\mathbf{X}^t) \rangle + \frac{1}{2} \|\bar{\mathbf{V}}^t - \mathbf{I}_k\|_{\underline{\mathbf{Q}}}^2 \\ 1678 &\stackrel{\textcircled{3}}{\leq} \langle \bar{\mathbf{V}}^t - \mathbf{I}_k, [\nabla f(\mathbf{X}^t)(\mathbf{X}^t)^T]_{\mathbb{B}\mathbb{B}} \rangle + \frac{1}{2} \|\bar{\mathbf{V}}^t - \mathbf{I}_k\|_{\underline{\mathbf{Q}}}^2, \end{aligned} \quad (43)$$

1681 where step ① uses Inequality (2); step ② uses Lemma 2.2(a); step ③ uses $\underline{\mathbf{Q}} \succcurlyeq \underline{\mathbf{Q}}$.

1682 Adding (41), (42), and (43) together, we obtain the following sufficient decrease condition:
1683

$$1684 \quad F(\mathbf{X}^{t+1}) - F(\mathbf{X}^t) \leq -\frac{\alpha}{2} \|\bar{\mathbf{V}}^t - \mathbf{I}_k\|_{\mathbb{F}}^2 \stackrel{\textcircled{1}}{\leq} -\frac{\alpha}{2} \|\mathbf{X}^{t+1} - \mathbf{X}^t\|_{\mathbb{F}}^2, \quad (44)$$

1686 where step ① uses Lemma 2.2(c).

1687 **Part (b).** We assume that \mathbb{B}^t is selected from $\{\mathcal{B}_i\}_{i=1}^{C_n^k}$ randomly and uniformly.

1688 Taking the expectation for Inequality (44), we obtain a lower bound on the expected progress made
1689 by each iteration:
1690

$$1691 \quad \mathbb{E}_{\xi^t}[F(\mathbf{X}^{t+1})] - F(\mathbf{X}^t) \leq -\mathbb{E}_{\xi^t}[\frac{\alpha}{2} \|\bar{\mathbf{V}}^t - \mathbf{I}_k\|_{\mathbb{F}}^2].$$

1692 Telescoping the inequality above over $t = 0, 1, \dots, T$, we have:
1693

$$\mathbb{E}_{\xi^T}[\frac{\alpha}{2} \sum_{t=0}^T \|\bar{\mathbf{V}}^t - \mathbf{I}_k\|_{\mathbb{F}}^2] \leq \mathbb{E}_{\xi^T}[F(\mathbf{X}^0) - F(\mathbf{X}^{T+1})] \leq \mathbb{E}_{\xi^T}[F(\mathbf{X}^0) - F(\mathbf{X}^\infty)],$$

1694 where \mathbf{X}^∞ denotes the limit point of Algorithm 1. As a result, there exists an index \bar{t} with $0 \leq \bar{t} \leq T$
1695 such that
1696

$$1697 \quad \mathbb{E}_{\xi^T}[\|\bar{\mathbf{V}}^{\bar{t}} - \mathbf{I}_k\|_{\mathbb{F}}^2] \leq \frac{2}{\alpha(T+1)} [F(\mathbf{X}^0) - F(\mathbf{X}^\infty)] = \frac{\tilde{c}}{T+1}. \quad (45)$$

1698 Furthermore, for any t , $\bar{\mathbf{V}}^t$ is the optimal solution of the following minimization problem at \mathbf{X}^t :
1699 $\bar{\mathbf{V}}^t \in \arg \min_{\mathbf{V}} \mathcal{K}(\mathbf{V}; \mathbf{X}^t, \mathbb{B}^t)$. Since $\bar{\mathbf{V}}^t$ is a random output matrix that depends on the observed
1700 realization of the random variable \mathbb{B}^t , we directly obtain the following equality:
1701

$$1702 \quad \frac{1}{C_n^k} \sum_{i=1}^{C_n^k} \text{dist}(\mathbf{I}_k, \arg \min_{\mathbf{V}} \mathcal{K}(\mathbf{V}; \mathbf{X}^t, \mathcal{B}_i))^2 = \mathbb{E}_{\xi^t}[\|\bar{\mathbf{V}}^t - \mathbf{I}_k\|_{\mathbb{F}}^2]. \quad (46)$$

1703 Combining (45) and (46), we conclude that there exists an index \bar{t} with $\bar{t} \in [0, T]$ such that the
1704 associated solution $\mathbf{X}^{\bar{t}}$ qualifies as an ϵ -BS_k-point of Problem (1), provided that T is sufficiently
1705 large such that $\frac{\tilde{c}}{T+1} \leq \epsilon$.
1706

□

1709 F.2 PROOF OF LEMMA 4.4

1710 *Proof.* We define $\mathbb{A} \ominus \mathbb{B}$ as the element-wise subtraction between sets \mathbb{A} and \mathbb{B} .

1711 We let $\mathbb{H}^{t+1} \in \partial h(\mathbf{X}^{t+1})$, and define:

$$1713 \quad \Omega_0 \triangleq \mathbf{U}_{\mathbb{B}^t}^T [\nabla f(\mathbf{X}^{t+1}) + \mathbb{H}^{t+1}] [\mathbf{X}^{t+1}]^T \mathbf{U}_{\mathbb{B}^t} \in \mathbb{R}^{k \times k}, \quad (47)$$

$$1714 \quad \Omega_1 \triangleq \mathbf{U}_{\mathbb{B}^t}^T [\nabla f(\mathbf{X}^{t+1}) + \mathbb{H}^{t+1}] [\mathbf{X}^t]^T \mathbf{U}_{\mathbb{B}^t} \in \mathbb{R}^{k \times k}, \quad (48)$$

$$1716 \quad \Omega_2 \triangleq \mathbf{U}_{\mathbb{B}^t}^T [\nabla f(\mathbf{X}^t) - \nabla f(\mathbf{X}^{t+1})] [\mathbf{X}^t]^T \mathbf{U}_{\mathbb{B}^t} \in \mathbb{R}^{k \times k}. \quad (49)$$

1718 **Part (a).** First, using the optimality of $\bar{\mathbf{V}}^t$ for the subproblem, we have:
1719

$$\mathbf{0}_{k,k} = \tilde{\mathbf{G}} - \bar{\mathbf{V}}^t \tilde{\mathbf{G}}^T \bar{\mathbf{V}}^t$$

$$1720 \quad \text{where } \tilde{\mathbf{G}} = \underbrace{(\mathbf{Q} + \alpha \mathbf{I}_k) \text{vec}(\bar{\mathbf{V}}^t - \mathbf{I}_k)}_{\triangleq \Upsilon_1} + \underbrace{\mathbf{U}_{\mathbb{B}^t}^T [\nabla f(\mathbf{X}^t) + \mathbb{H}^{t+1}] (\mathbf{X}^t)^T \mathbf{U}_{\mathbb{B}^t}}_{\triangleq \Upsilon_2}.$$

1723 Using the relation that $\tilde{\mathbf{G}} = \Upsilon_1 + \Upsilon_2$, we obtain the following results from the above equality:
1724

$$\begin{aligned} 1725 \quad \mathbf{0}_{k,k} &= (\Upsilon_1 + \Upsilon_2) - \bar{\mathbf{V}}^t (\Upsilon_1 + \Upsilon_2)^T \bar{\mathbf{V}}^t \\ 1726 &\stackrel{\textcircled{1}}{=} \mathbf{0}_{k,k} = \Upsilon_1 + \Omega_1 + \Omega_2 - \bar{\mathbf{V}}^t (\Upsilon_1 + \Omega_1 + \Omega_2)^T \bar{\mathbf{V}}^t \\ 1727 &\Rightarrow \Omega_1 = \bar{\mathbf{V}}^t (\Upsilon_1 + \Omega_1 + \Omega_2)^T \bar{\mathbf{V}}^t - \Upsilon_1 - \Omega_2, \end{aligned} \quad (50)$$

1728 where step ① uses $\Upsilon_2 = \Omega_1 + \Omega_2$.
1729

1730 Second, since both \mathbf{B}^t and \mathbf{B}^{t+1} are randomly and dependently selected from $\{\mathcal{B}_i\}_{i=1}^{C_n^k}$ with replace-
1731 $\tilde{\mathbf{A}} \in \mathbb{R}^{n \times n}$, we have:
1732

$$1733 \mathbb{E}_{\mathbf{B}^{t+1}}[\|\mathbf{U}_{\mathbf{B}^{t+1}}^\top \tilde{\mathbf{A}} \mathbf{U}_{\mathbf{B}^{t+1}}\|_F^2] = \frac{1}{C_n^k} \sum_{i=1}^{C_n^k} \|\mathbf{U}_{\mathbf{B}_i}^\top \tilde{\mathbf{A}} \mathbf{U}_{\mathbf{B}_i}\|_F^2 = \mathbb{E}_{\mathbf{B}^t}[\|\mathbf{U}_{\mathbf{B}^t}^\top \tilde{\mathbf{A}} \mathbf{U}_{\mathbf{B}^t}\|_F^2].$$

1735 Using the definition $\xi^t \triangleq (\mathbf{B}^1, \mathbf{B}^2, \dots, \mathbf{B}^t)$, we have:
1736

$$1737 \mathbb{E}_{\xi^{t+1}}[\|\mathbf{U}_{\mathbf{B}^{t+1}}^\top \tilde{\mathbf{A}} \mathbf{U}_{\mathbf{B}^{t+1}}\|_F^2] = \mathbb{E}_{\xi^t}[\|\mathbf{U}_{\mathbf{B}^t}^\top \tilde{\mathbf{A}} \mathbf{U}_{\mathbf{B}^t}\|_F^2]. \quad (51)$$

1739 Third, we derive the following results:
1740

$$\begin{aligned} 1741 \mathbb{E}_{\xi^{t+1}}[\text{dist}(\mathbf{0}, \partial_{\mathcal{M}} \mathcal{K}(\mathbf{I}_k; \mathbf{X}^{t+1}, \mathbf{B}^{t+1}))] &= \mathbb{E}_{\xi^{t+1}}[\|\partial_{\mathcal{M}} \mathcal{K}(\mathbf{I}_k; \mathbf{X}^{t+1}, \mathbf{B}^{t+1})\|_F] \\ 1742 &\stackrel{\textcircled{1}}{=} \mathbb{E}_{\xi^{t+1}}[\|\mathbf{U}_{\mathbf{B}^{t+1}}^\top \{\partial F(\mathbf{X}^{t+1})[\mathbf{X}^{t+1}]^\top \ominus \mathbf{X}^{t+1}[\partial F(\mathbf{X}^{t+1})]^\top\} \mathbf{U}_{\mathbf{B}^{t+1}}\|_F] \\ 1743 &\stackrel{\textcircled{2}}{=} \mathbb{E}_{\xi^t}[\|\mathbf{U}_{\mathbf{B}^t}^\top \{\partial F(\mathbf{X}^{t+1})[\mathbf{X}^{t+1}]^\top \ominus \mathbf{X}^{t+1}[\partial F(\mathbf{X}^{t+1})]^\top\} \mathbf{U}_{\mathbf{B}^t}\|_F] \\ 1744 &\stackrel{\textcircled{3}}{\leq} \mathbb{E}_{\xi^t}[\|\Omega_0 - \Omega_0^\top\|_F] \\ 1745 &\stackrel{\textcircled{4}}{\leq} 2\mathbb{E}_{\xi^t}[\|\Omega_0 - \Omega_1\|_F] + \mathbb{E}_{\xi^t}[\|\Omega_1 - \Omega_1^\top\|_F] \\ 1746 &\stackrel{\textcircled{5}}{=} 2\mathbb{E}_{\xi^t}[\|\Omega_0 - \Omega_1\|_F] + \mathbb{E}_{\xi^t}[\|\bar{\mathbf{V}}^t(\Upsilon_1 + \Omega_1 + \Omega_2)^\top \bar{\mathbf{V}}^t - \Upsilon_1 - \Omega_2 - \Omega_1^\top\|_F] \\ 1747 &\stackrel{\textcircled{6}}{=} 2\mathbb{E}_{\xi^t}[\|\Omega_0 - \Omega_1\|_F] + \mathbb{E}_{\xi^t}[\|\bar{\mathbf{V}}^t \Upsilon_1^\top \bar{\mathbf{V}}^t - \Upsilon_1\|_F] + \mathbb{E}_{\xi^t}[\|\bar{\mathbf{V}}^t \Omega_1^\top \bar{\mathbf{V}}^t - \Omega_1^\top\|_F] \\ 1748 &\quad + \mathbb{E}_{\xi^t}[\|\bar{\mathbf{V}}^t \Omega_2^\top \bar{\mathbf{V}}^t - \Omega_2\|_F] \end{aligned} \quad (52)$$

1749 where step ① uses the definition of $\partial_{\mathcal{M}} \mathcal{K}(\mathbf{V}; \mathbf{X}^{t+1}, \mathbf{B}^{t+1})$ at the point $\mathbf{V} = \mathbf{I}_k$; step ② uses Equality
1750 (51) with $\tilde{\mathbf{A}} = \partial F(\mathbf{X}^{t+1})[\mathbf{X}^{t+1}]^\top \ominus \mathbf{X}^{t+1}[\partial F(\mathbf{X}^{t+1})]^\top$; step ③ uses the definition of Ω_0 in Equation
1751 (47); step ④ uses Lemma A.2; step ⑤ uses Equality (50); step ⑥ uses the triangle inequality.
1752

1753 We now establish individual bounds for each term in Inequality (52). For the first term $2\mathbb{E}_{\xi^t}[\|\Omega_0 - \Omega_1\|_F]$ in (52), we have:
1754

$$\begin{aligned} 1755 &2\mathbb{E}_{\xi^t}[\|\Omega_0 - \Omega_1\|_F] \\ 1756 &\leq 2\mathbb{E}_{\xi^t}[\|\mathbf{U}_{\mathbf{B}^t}^\top [\nabla f(\mathbf{X}^{t+1}) + \mathbb{H}^{t+1}] [\mathbf{X}^{t+1} - \mathbf{X}^t]^\top \mathbf{U}_{\mathbf{B}^t}\|_F] \\ 1757 &\stackrel{\textcircled{1}}{=} 2\mathbb{E}_{\xi^t}[\|\mathbf{U}_{\mathbf{B}^t}^\top [\nabla f(\mathbf{X}^{t+1}) + \mathbb{H}^{t+1}] [\mathbf{U}_{\mathbf{B}}(\bar{\mathbf{V}}^t - \mathbf{I}_k) \mathbf{U}_{\mathbf{B}^t} \mathbf{X}^t]^\top \mathbf{U}_{\mathbf{B}^t}\|_F] \\ 1758 &\stackrel{\textcircled{2}}{\leq} 2C_F \mathbb{E}_{\xi^t}[\|\bar{\mathbf{V}}^t - \mathbf{I}_k\|_F], \end{aligned} \quad (53)$$

1759 where step ① uses $\mathbf{X}^{t+1} = \mathbf{X}^t + \mathbf{U}_{\mathbf{B}}(\bar{\mathbf{V}}^t - \mathbf{I}_k) \mathbf{U}_{\mathbf{B}^t}^\top \mathbf{X}^t$; step ② uses the inequality $\|\mathbf{XY}\|_F \leq \|\mathbf{X}\|_F \|\mathbf{Y}\|_{\text{sp}}$ for all \mathbf{X} and \mathbf{Y} repeatedly, and the fact that $\|\mathbf{G}\|_F \leq C_F$ for all $\mathbf{X} \in \text{St}(n, r)$ and all $\mathbf{G} \in \partial F(\mathbf{X})$.
1760

1761 For the second term $\mathbb{E}_{\xi^t}[\|\bar{\mathbf{V}}^t \Upsilon_1^\top \bar{\mathbf{V}}^t - \Upsilon_1\|_F]$ in (52), we have::
1762

$$\begin{aligned} 1763 &\mathbb{E}_{\xi^t}[\|\bar{\mathbf{V}}^t \Upsilon_1^\top \bar{\mathbf{V}}^t - \Upsilon_1\|_F] \\ 1764 &\stackrel{\textcircled{1}}{\leq} \mathbb{E}_{\xi^t}[\|\bar{\mathbf{V}}^t \Upsilon_1^\top \bar{\mathbf{V}}^t\|_F] + \mathbb{E}_{\xi^t}[\|\Upsilon_1\|_F] \\ 1765 &\stackrel{\textcircled{2}}{\leq} 2\mathbb{E}_{\xi^t}[\|\Upsilon_1\|_F] \\ 1766 &\stackrel{\textcircled{3}}{=} 2\mathbb{E}_{\xi^t}[\|\text{mat}((\mathbf{Q} + \alpha \mathbf{I}_k) \text{vec}(\bar{\mathbf{V}}^t - \mathbf{I}_k))\|_F] \\ 1767 &\leq 2\|\mathbf{Q} + \alpha \mathbf{I}_k\|_{\text{sp}} \cdot \mathbb{E}_{\xi^t}[\|\bar{\mathbf{V}}^t - \mathbf{I}_k\|_F] \\ 1768 &\stackrel{\textcircled{4}}{\leq} 2(L_f + \alpha) \cdot \mathbb{E}_{\xi^t}[\|\bar{\mathbf{V}}^t - \mathbf{I}_k\|_F] \end{aligned} \quad (54)$$

1769 where step ① uses the triangle inequality; step ② uses the inequality $\|\mathbf{XY}\|_F \leq \|\mathbf{X}\|_F \|\mathbf{Y}\|_{\text{sp}}$ for all
1770 \mathbf{X} and \mathbf{Y} ; step ③ uses the definition of Ω_1 in (48); step ④ uses the fact that $\|\mathbf{Q}\|_{\text{sp}} \leq L_f$.
1771

1782 For the third term $\mathbb{E}_{\xi^t}[\|\bar{\mathbf{V}}^t \Omega_1^\top \bar{\mathbf{V}}^t - \Omega_1^\top\|_F]$ in (52), we have:
1783

$$\begin{aligned}
 1784 \quad & \mathbb{E}_{\xi^t}[\|\bar{\mathbf{V}}^t \Omega_1^\top \bar{\mathbf{V}}^t - \Omega_1^\top\|_F] \\
 1785 \quad & \stackrel{\textcircled{1}}{=} \mathbb{E}_{\xi^t}[\|\bar{\mathbf{V}}^t \Omega_1^\top (\bar{\mathbf{V}}^t - \mathbf{I}_k) + (\bar{\mathbf{V}}^t - \mathbf{I}_k) \Omega_1^\top\|_F] \\
 1786 \quad & \stackrel{\textcircled{2}}{\leq} 2\mathbb{E}_{\xi^t}[\|\Omega_1\|_{\text{sp}} \cdot \|(\bar{\mathbf{V}}^t - \mathbf{I}_k)\|_F] \\
 1787 \quad & \stackrel{\textcircled{3}}{\leq} 2\mathbb{E}_{\xi^t}[\|\nabla f(\mathbf{X}^{t+1}) + \mathbb{H}^{t+1}\|_{\text{sp}} \cdot \|(\bar{\mathbf{V}}^t - \mathbf{I}_k)\|_F] \\
 1788 \quad & \stackrel{\textcircled{4}}{\leq} 2C_F \mathbb{E}_{\xi^t}[\|(\bar{\mathbf{V}}^t - \mathbf{I}_k)\|_F]
 \end{aligned} \tag{55}$$

1793 where step ① uses the fact that $-\bar{\mathbf{V}}^t \Omega_1^\top \mathbf{I}_k + \bar{\mathbf{V}}^t \Omega_1^\top = \mathbf{0}$; step ② uses the norm inequality; step ③
1794 uses the fact that $\|\Omega_1\|_{\text{sp}} = \|\mathbf{U}_{\mathbb{B}^t}^\top [\nabla f(\mathbf{X}^{t+1}) + \mathbb{H}^{t+1}] [\mathbf{X}^t]^\top \mathbf{U}_{\mathbb{B}^t}\|_{\text{sp}} \leq \|\nabla f(\mathbf{X}^{t+1}) + \mathbb{H}^{t+1}\|_{\text{sp}} \leq$
1795 $\|\nabla f(\mathbf{X}^{t+1}) + \mathbb{H}^{t+1}\|_F$ which can be derived using the norm inequality.

1796 For the fourth term $\mathbb{E}_{\xi^t}[\|\bar{\mathbf{V}}^t \Omega_2^\top \bar{\mathbf{V}}^t - \Omega_2\|_F]$ in (52), we have:
1797

$$\begin{aligned}
 1798 \quad & \mathbb{E}_{\xi^t}[\|\bar{\mathbf{V}}^t \Omega_2^\top \bar{\mathbf{V}}^t - \Omega_2\|_F] \\
 1799 \quad & \stackrel{\textcircled{1}}{\leq} \mathbb{E}_{\xi^t}[\|\bar{\mathbf{V}}^t \Omega_2^\top \bar{\mathbf{V}}^t\|_F] + \mathbb{E}[\|\Omega_2\|_F] \\
 1800 \quad & \stackrel{\textcircled{2}}{\leq} 2\mathbb{E}_{\xi^t}[\|\Omega_2\|_F] \\
 1801 \quad & \stackrel{\textcircled{3}}{=} 2\mathbb{E}_{\xi^t}[\|\mathbf{U}_{\mathbb{B}^t}^\top [\nabla f(\mathbf{X}^t) - \nabla f(\mathbf{X}^{t+1})] [\mathbf{X}^t]^\top \mathbf{U}_{\mathbb{B}^t}\|_F] \\
 1802 \quad & \stackrel{\textcircled{4}}{\leq} 2\mathbb{E}_{\xi^t}[\|\nabla f(\mathbf{X}^t) - \nabla f(\mathbf{X}^{t+1})\|_F] \\
 1803 \quad & \stackrel{\textcircled{5}}{\leq} 2L_f \mathbb{E}_{\xi^t}[\|\mathbf{X}^t - \mathbf{X}^{t+1}\|_F] \\
 1804 \quad & \stackrel{\textcircled{6}}{\leq} 2L_f \mathbb{E}_{\xi^t}[\|\bar{\mathbf{V}}^t - \mathbf{I}_k\|_F],
 \end{aligned} \tag{56}$$

1811 where step ① uses the triangle inequality; step ② uses the norm inequality; step ③ uses the definition
1812 of $\Omega_2 = \mathbf{U}_{\mathbb{B}^t}^\top [\nabla f(\mathbf{X}^t) - \nabla f(\mathbf{X}^{t+1})] [\mathbf{X}^t]^\top \mathbf{U}_{\mathbb{B}^t}$ in (49); step ④ uses the norm inequality; step ⑤ uses
1813 the fact that $\nabla f(\mathbf{X})$ is L_f -Lipschitz continuous; step ⑥ uses Lemma 2.2(c).

1814 In view of (53), (54), (55), (56), and (52), we have:
1815

$$\mathbb{E}_{\xi^{t+1}}[\|\partial_{\mathcal{M}} \mathcal{K}(\mathbf{I}_k; \mathbf{X}^{t+1}, \mathbb{B}^{t+1})\|_F] \leq \underbrace{(c_1 + c_2 + c_3 + c_4)}_{\triangleq \phi} \cdot \mathbb{E}_{\xi^t}[\|\bar{\mathbf{V}}^t - \mathbf{I}_k\|_F],$$

1820 where $c_1 = 2C_F$, $c_2 = 2(L_f + \alpha)$, $c_3 = 2C_F$, and $c_4 = 2L_f$.
1821

1822 **Part (b).** we show that $\mathbb{E}_{\xi^t}[\text{dist}(\mathbf{0}, \partial_{\mathcal{M}} F(\mathbf{X}^t))] \leq \gamma \cdot \mathbb{E}_{\xi^t}[\text{dist}(\mathbf{0}, \partial_{\mathcal{M}} \mathcal{K}(\mathbf{I}_k; \mathbf{X}^t, \mathbb{B}^t))]$, where $\gamma \triangleq$
1823 $(C_n^k / C_{n-2}^{k-2})^{1/2}$. For all $\mathbf{D}^t \triangleq \partial F(\mathbf{X}^t) [\mathbf{X}^t]^\top \ominus \mathbf{X}^t [\partial F(\mathbf{X}^t)]^\top$, we obtain:
1824

$$\begin{aligned}
 1825 \quad & \|\mathbf{D}^t\|_F^2 = \sum_i \sum_{j \neq i} (\mathbf{D}_{ij}^t)^2 + \sum_i \sum_{j=i} (\mathbf{D}_{ij}^t)^2 \\
 1826 \quad & \stackrel{\textcircled{1}}{=} \sum_i \sum_{j \neq i} (\mathbf{D}_{ij}^t)^2 \\
 1827 \quad & \stackrel{\textcircled{2}}{=} \frac{1}{C_{n-2}^{k-2}} \sum_{i=1}^{C_n^k} \|\mathbf{U}_{\mathcal{B}_i}^\top \mathbf{D}^t \mathbf{U}_{\mathcal{B}_i}\|_F^2 \\
 1828 \quad & \stackrel{\textcircled{3}}{=} \frac{1}{C_{n-2}^{k-2}} \cdot C_n^k \mathbb{E}_{\mathbb{B}^t}[\|\mathbf{U}_{\mathbb{B}^t}^\top \mathbf{D}^t \mathbf{U}_{\mathbb{B}^t}\|_F^2] \\
 1829 \quad & \stackrel{\textcircled{4}}{=} \gamma^2 \mathbb{E}_{\mathbb{B}^t}[\|\mathbf{U}_{\mathbb{B}^t}^\top \mathbf{D}^t \mathbf{U}_{\mathbb{B}^t}\|_F^2],
 \end{aligned} \tag{57}$$

1834 where step ① uses the fact that $\mathbf{D}_{ii}^t = 0$ for all $i \in [n]$; step ② uses Claim (a) of this lemma with
1835 $\mathbf{D}_{ii}^t = 0$ for all $i \in [n]$; step ③ uses $\mathbb{E}_{\mathbb{B}^t}[\|\mathbf{U}_{\mathbb{B}^t}^\top \mathbf{W} \mathbf{U}_{\mathbb{B}^t}\|_F^2] = \frac{1}{C_n^k} \sum_{i=1}^{C_n^k} \|\mathbf{U}_{\mathcal{B}_i}^\top \mathbf{W} \mathbf{U}_{\mathcal{B}_i}\|_F^2$ as \mathbb{B}^t are

chosen from $\{\mathcal{B}_i\}_{i=1}^{C_n^k}$ randomly and uniformly; ④ uses the definition of γ . We further derive:

$$\begin{aligned}
 \mathbb{E}_{\xi^t} \|\partial_{\mathcal{M}} F(\mathbf{X}^t)\|_{\mathbb{F}} &\stackrel{\textcircled{1}}{=} \|\partial F(\mathbf{X}^t) \ominus \mathbf{X}^t [\partial F(\mathbf{X}^t)]^{\mathbb{T}} \mathbf{X}^t\|_{\mathbb{F}} \\
 &\stackrel{\textcircled{2}}{=} \|\partial F(\mathbf{X}^t) [\mathbf{X}^t]^{\mathbb{T}} \mathbf{X}^t \ominus \mathbf{X}^t [\partial F(\mathbf{X}^t)]^{\mathbb{T}} \mathbf{X}^t\|_{\mathbb{F}} \\
 &\stackrel{\textcircled{3}}{\leq} \|\partial F(\mathbf{X}^t) [\mathbf{X}^t]^{\mathbb{T}} \ominus \mathbf{X}^t [\partial F(\mathbf{X}^t)]^{\mathbb{T}}\|_{\mathbb{F}} \\
 &\stackrel{\textcircled{4}}{=} \gamma \mathbb{E}_{\mathbb{B}^t} [\|\mathbf{U}_{\mathbb{B}^t}^{\mathbb{T}} \{\partial F(\mathbf{X}^t) [\mathbf{X}^t]^{\mathbb{T}} \ominus \mathbf{X}^t [\partial F(\mathbf{X}^t)]^{\mathbb{T}}\} \mathbf{U}_{\mathbb{B}^t}\|_{\mathbb{F}}] \\
 &\stackrel{\textcircled{5}}{=} \gamma \|\partial_{\mathcal{M}} \mathcal{K}(\mathbf{I}_k; \mathbf{X}^t, \mathbb{B}^t)\|_{\mathbb{F}}
 \end{aligned} \tag{58}$$

where step ① uses the definition of $\partial_{\mathcal{M}} F(\mathbf{X}^t)$; step ② uses $[\mathbf{X}^t]^{\mathbb{T}} \mathbf{X}^t = \mathbf{I}_k$; step ③ uses the inequality that $\|\mathbf{A}\mathbf{X}\|_{\mathbb{F}}^2 \leq \|\mathbf{A}\|_{\mathbb{F}}^2$ for all $\mathbf{X} \in \text{St}(n, r)$; step ④ uses Equality (57); step ⑤ uses the definition of $\partial_{\mathcal{M}} \mathcal{K}(\mathbf{I}_k; \mathbf{X}^t, \mathbb{B}^t)$. \square

F.3 PROOF OF THEOREM 4.6

Proof. We derive the following results:

$$\begin{aligned}
 \mathbb{E}_{\xi^T} [\text{dist}^2(\mathbf{0}, \partial_{\mathcal{M}} F(\mathbf{X}^{T+1}))] &\stackrel{\textcircled{1}}{=} \gamma^2 \cdot \mathbb{E}_{\xi^{T+1}} [\text{dist}^2(\mathbf{0}, \partial_{\mathcal{M}} \mathcal{K}(\mathbf{I}_k; \mathbf{X}^{T+1}, \mathbb{B}^{T+1}))] \\
 &\stackrel{\textcircled{2}}{\leq} \gamma^2 \cdot \phi^2 \cdot \mathbb{E}_{\xi^T} [\|\bar{\mathbf{V}}^T - \mathbf{I}_k\|_{\mathbb{F}}^2] \\
 &\stackrel{\textcircled{3}}{\leq} \gamma^2 \cdot \phi^2 \cdot \frac{\tilde{c}}{T+1},
 \end{aligned}$$

where step ① uses Lemma 4.4(b); step ② uses Lemma 4.4(a); step ③ uses Inequality (45).

Therefore, we conclude that there exists an index \bar{t} with $\bar{t} \in [0, T]$ such that the associated solution $\mathbf{X}^{\bar{t}}$ qualifies as an ϵ -critical point of Problem (1) satisfying $\mathbb{E}_{\xi^{\bar{t}}} [\text{dist}^2(\mathbf{0}, \partial_{\mathcal{M}} F(\mathbf{X}^{\bar{t}+1}))] \leq \epsilon$, provided that T is sufficiently large to ensure $\gamma^2 \cdot \phi^2 \cdot \frac{\tilde{c}}{T+1} \leq \epsilon$. \square

F.4 PROOF OF THEOREM 4.10

Proof. By Theorem 4.2(a) and Theorem 4.6, the composite function $F_{\iota}(\mathbf{X}) \triangleq F(\mathbf{X}) + \iota_{\mathcal{M}}(\mathbf{X})$ is monotonically non-increasing, i.e., $F_{\iota}(\mathbf{X}^{t+1}) \leq F_{\iota}(\mathbf{X}^t)$. Moreover, the sequence $\{\mathbf{X}^t\}_{t=1}^{\infty}$ has a limit point \mathbf{X}^{∞} .

Since $F_{\iota}(\mathbf{X}) \triangleq F(\mathbf{X}) + \iota_{\mathcal{M}}(\mathbf{X})$ is a KL function by assumption, Proposition 4.9 implies that there exists an index $t_{\star} \in \mathbb{N}$ such that, for all $t \geq t_{\star}$,

$$\frac{1}{\varphi'(F_{\iota}(\mathbf{X}^t) - F_{\iota}(\mathbf{X}^{\infty}))} \leq \text{dist}(0, \partial F_{\iota}(\mathbf{X}^t)). \tag{59}$$

Since $\varphi(\cdot)$ is a concave desingularization function, we have: $\varphi(b) + (a - b)\varphi'(a) \leq \varphi(a)$. Applying the inequality above with $a = F(\mathbf{X}^t) - F(\mathbf{X}^{\infty})$ and $b = F(\mathbf{X}^{t+1}) - F(\mathbf{X}^{\infty})$, we have:

$$\begin{aligned}
 &(F(\mathbf{X}^t) - F(\mathbf{X}^{t+1}))\varphi'(F(\mathbf{X}^t) - F(\mathbf{X}^{\infty})) \\
 &\leq \underbrace{\varphi(F(\mathbf{X}^t) - F(\mathbf{X}^{\infty})) - \varphi(F(\mathbf{X}^{t+1}) - F(\mathbf{X}^{\infty}))}_{\triangleq \varphi_t}.
 \end{aligned} \tag{60}$$

1890 **Part (a).** We derive the following inequalities:
1891

$$\begin{aligned}
 1892 \quad (E_{t+1})^2 &\triangleq \mathbb{E}_{\xi^t}[\|\bar{\mathbf{V}}^t - \mathbf{I}_k\|_{\mathbb{F}}^2] \stackrel{\textcircled{1}}{\leq} \frac{2}{\alpha} \cdot \mathbb{E}_{\xi^t}[F(\mathbf{X}^t) - F(\mathbf{X}^{t+1})] \\
 1893 &\stackrel{\textcircled{2}}{\leq} \frac{2}{\alpha} \cdot \mathbb{E}_{\xi^t}[(\varphi_t - \varphi_{t+1}) \cdot \frac{1}{\varphi'(F(\mathbf{X}^t) - F(\mathbf{X}^\infty))}] \\
 1894 &\stackrel{\textcircled{3}}{\leq} \frac{2}{\alpha} \cdot \mathbb{E}_{\xi^t}[(\varphi_t - \varphi_{t+1}) \cdot \text{dist}(0, \partial F_\nu(\mathbf{X}^t))] \\
 1895 &\stackrel{\textcircled{4}}{\leq} \frac{2}{\alpha} \cdot \mathbb{E}_{\xi^t}[(\varphi_t - \varphi_{t+1}) \cdot \|\partial_{\mathcal{M}} F(\mathbf{X}^t)\|_{\mathbb{F}}] \\
 1896 &\stackrel{\textcircled{5}}{\leq} \frac{2}{\alpha} \cdot \mathbb{E}_{\xi^t}[(\varphi_t - \varphi_{t+1}) \gamma \|\partial_{\mathcal{M}} \mathcal{K}(\mathbf{I}_k; \mathbf{X}^t, \mathbb{B}^t)\|_{\mathbb{F}}] \\
 1897 &\stackrel{\textcircled{6}}{\leq} \frac{2}{\alpha} \cdot \mathbb{E}_{\xi^{t-1}}[(\varphi_t - \varphi_{t+1}) \gamma \phi \|\bar{\mathbf{V}}^{t-1} - \mathbf{I}_k\|_{\mathbb{F}}] \\
 1898 &\stackrel{\textcircled{7}}{=} \underbrace{\frac{2}{\alpha} \cdot \gamma \phi \cdot (\varphi_t - \varphi_{t+1})}_{\triangleq \kappa} \cdot E_t,
 1899 \\
 1900 \\
 1901 \\
 1902 \\
 1903 \\
 1904 \\
 1905 \\
 1906
 \end{aligned}$$

1907 where step $\textcircled{1}$ uses the sufficient decrease condition as shown in Theorem 4.2; step $\textcircled{2}$ uses Inequality
1908 (60); step $\textcircled{3}$ uses Inequality (59); step $\textcircled{4}$ uses Lemma A.7; step $\textcircled{5}$ uses Inequality (58); step $\textcircled{6}$ uses
1909 Lemma 4.4; step $\textcircled{7}$ uses the definitions of $\{\kappa, \varphi_t, E_t\}$.

1910 **Part (b).** Applying Lemma A.9 with $p_t = \kappa \varphi_t$ with $p_t \geq p_{t+1}$, for all $i \geq 1$, we have:
1911

$$1912 \quad \sum_{j=i}^{\infty} E_{j+1} \leq E_i + 2p_i.$$

1913 Using the definition of $D_t \triangleq \sum_{j=t}^{\infty} E_{j+1}$ and letting $i = t$, we obtain:
1914

$$1915 \quad D_t \leq E_t + 2p_t \stackrel{\textcircled{1}}{=} E_t + 2\kappa \varphi_t \stackrel{\textcircled{2}}{\leq} E_t + 2\kappa \varphi_1 \stackrel{\textcircled{3}}{\leq} 2\sqrt{k} + 2\kappa \varphi_1,$$

1916 where step $\textcircled{1}$ uses $p_t = \kappa \varphi_t$; step $\textcircled{2}$ uses $\varphi_t \leq \varphi_1$; step $\textcircled{3}$ uses $E_t \triangleq \mathbb{E}_{\xi^{t-1}}[\|\bar{\mathbf{V}}^{t-1} - \mathbf{I}_k\|_{\mathbb{F}}] \leq$
1917 $\mathbb{E}_{\xi^{t-1}}[\|\bar{\mathbf{V}}^{t-1}\|_{\mathbb{F}}] + \|\mathbf{I}_k\|_{\mathbb{F}} \leq \sqrt{k} + \sqrt{k}$. We conclude that $D_t \triangleq \sum_{j=t}^{\infty} E_{j+1}$ is always upper-bounded.
1918

1919 Using the fact that $\|\mathbf{X}^{t+1} - \mathbf{X}^t\|_{\mathbb{F}}^2 \leq \|\bar{\mathbf{V}}^t - \mathbf{I}_k\|_{\mathbb{F}}^2$ as shown in Lemma 2.2(c), we conclude that
1920 $\sum_{i=1}^{\infty} \mathbb{E}_{\xi^i}[\|\mathbf{X}^{i+1} - \mathbf{X}^i\|_{\mathbb{F}}]$ is also always upper-bounded.
1921

1922 \square

1923 F.5 PROOF OF THEOREM 4.11

1924 *Proof.* We define $\varphi_t \triangleq \varphi(s^t)$, where $s^t \triangleq F(\mathbf{X}^t) - F(\mathbf{X}^\infty)$.
1925

1926 We define $E_{t+1} \triangleq \mathbb{E}_{\xi^t}[\|\bar{\mathbf{V}}^t - \mathbf{I}_k\|_{\mathbb{F}}]$, and $D_i = \sum_{j=i}^{\infty} E_{j+1}$.
1927

1928 We have: $D_{t-1} - D_t = E_t \leq 2\sqrt{k} \triangleq \bar{r}$.
1929

1930 First, we have:
1931

$$\begin{aligned}
 1932 \quad \|\mathbf{X}^T - \mathbf{X}^\infty\|_{\mathbb{F}} &\stackrel{\textcircled{1}}{\leq} \sum_{j=T}^{\infty} \|\mathbf{X}^j - \mathbf{X}^{j+1}\|_{\mathbb{F}} \\
 1933 &\stackrel{\textcircled{2}}{\leq} \sum_{j=T}^{\infty} \|\bar{\mathbf{V}}^j - \mathbf{I}_k\|_{\mathbb{F}} \\
 1934 &\stackrel{\textcircled{3}}{=} \sum_{j=T}^{\infty} E_{j+1} \\
 1935 &\stackrel{\textcircled{4}}{=} D_T,
 1936 \\
 1937 \\
 1938 \\
 1939 \\
 1940 \\
 1941
 \end{aligned}$$

1942 where step $\textcircled{1}$ uses the triangle inequality; step $\textcircled{2}$ uses $\|\mathbf{X}^{t+1} - \mathbf{X}^t\|_{\mathbb{F}}^2 \leq \|\bar{\mathbf{V}}^t - \mathbf{I}_k\|_{\mathbb{F}}^2$, as shown in
1943 Lemma 2.2(c); step $\textcircled{3}$ uses the definition of E_{t+1} ; step $\textcircled{4}$ uses the definition of D_T . Therefore, it
1944 suffices to establish the convergence rate of D_T .

1944 Second, we obtain the following results:
1945

$$\begin{aligned}
1946 \quad \frac{1}{\varphi'(s^t)} &\stackrel{\textcircled{1}}{\leq} \|\text{dist}(\mathbf{0}, \partial F_t(\mathbf{X}^t))\|_{\mathbb{F}} \\
1947 &\stackrel{\textcircled{2}}{\leq} \|\partial \mathcal{M}F(\mathbf{X}^t)\|_{\mathbb{F}} \\
1948 &\stackrel{\textcircled{3}}{\leq} \mathbb{E}_{\xi^t} [\gamma \|\partial \mathcal{M}\mathcal{K}(\mathbf{I}_k; \mathbf{X}^t, \mathbf{B}^t)\|_{\mathbb{F}}] \\
1949 &\stackrel{\textcircled{4}}{\leq} \mathbb{E}_{\xi^t} [\gamma \phi \|\bar{\mathbf{V}}^{t-1} - \mathbf{I}_k\|_{\mathbb{F}}] \\
1950 &\stackrel{\textcircled{5}}{\leq} \gamma \phi E_t,
\end{aligned}$$

1955 where step $\textcircled{1}$ uses Proposition 4.9 that $\text{dist}(\mathbf{0}, \partial F_t(\mathbf{X}')) \varphi'(F_t(\mathbf{X}') - F_t(\mathbf{X}^\infty)) \geq 1$; step $\textcircled{2}$
1956 uses Lemma A.7; step $\textcircled{3}$ uses Inequality (58); step $\textcircled{4}$ uses the Riemannian subgradient lower bound
1957 for the iterates gap in Lemma 4.4; step $\textcircled{5}$ uses the definition of $E_t \triangleq \mathbb{E}_{\xi^{t-1}} [\|\bar{\mathbf{V}}^{t-1} - \mathbf{I}_k\|_{\mathbb{F}}^2]$.

1958 Third, using the definition of D_t , we derive:
1959

$$\begin{aligned}
1960 \quad D_t &\triangleq \sum_{i=t}^{\infty} E_{i+1} \\
1961 &\stackrel{\textcircled{1}}{\leq} E_t + 2\kappa \varphi_t \\
1962 &\stackrel{\textcircled{2}}{=} E_t + 2\kappa c \cdot \{[s^t]^\sigma\}^{\frac{1-\sigma}{\sigma}} \\
1963 &\stackrel{\textcircled{3}}{=} E_t + 2\kappa c \cdot \{c(1-\sigma) \cdot \frac{1}{\varphi'(s^t)}\}^{\frac{1-\sigma}{\sigma}} \\
1964 &\stackrel{\textcircled{4}}{=} E_t + 2\kappa c \cdot \{c(1-\sigma) \cdot \gamma \phi E_t\}^{\frac{1-\sigma}{\sigma}} \\
1965 &\stackrel{\textcircled{5}}{=} D_{t-1} - D_t + 2\kappa c \cdot \{c(1-\sigma) \cdot \gamma \phi (D_{t-1} - D_t)\}^{\frac{1-\sigma}{\sigma}} \\
1966 &= D_{t-1} - D_t + \underbrace{2\kappa c \cdot [c(1-\sigma) \gamma \phi]^{\frac{1-\sigma}{\sigma}}}_{\triangleq \ddot{\kappa}} \cdot \{D_{t-1} - D_t\}^{\frac{1-\sigma}{\sigma}}, \quad (61)
\end{aligned}$$

1972 where step $\textcircled{1}$ uses $\sum_{i=t}^{\infty} E_{i+1} \leq E_t + 2\kappa \varphi_t$, as shown in Theorem 4.10(b); step $\textcircled{2}$ uses the definitions that $\varphi_t \triangleq \varphi(s^t)$, and $\varphi(s) = cs^{1-\sigma}$; step $\textcircled{3}$ uses $\varphi'(s) = c(1-\sigma) \cdot [s]^{-\sigma}$, leading to $[s^t]^\sigma = c(1-\sigma) \cdot \frac{1}{\varphi'(s^t)}$; step $\textcircled{4}$ uses Inequality (61); step $\textcircled{5}$ uses the fact that $E_t = D_{t-1} - D_t$.

1976 We consider three cases for $\sigma \in [0, 1)$.
1977

1978 **Part (a).** We consider $\sigma = 0$. We have from Inequality (61):

$$\begin{aligned}
1979 \quad 0 &\leq -\frac{1}{\varphi'(s^t)} + \gamma \phi E_t \\
1980 &\stackrel{\textcircled{1}}{=} -\frac{1}{c(1-\sigma) \cdot [s^t]^{-\sigma}} + \gamma \phi E_t \\
1981 &\stackrel{\textcircled{2}}{=} -\frac{1}{c} + \gamma \phi E_t, \quad (62)
\end{aligned}$$

1984 where step $\textcircled{1}$ uses $\varphi'(s) = c(1-\sigma) \cdot [s]^{-\sigma}$; step $\textcircled{2}$ uses $\sigma = 0$ and $E_t = D_{t-1} - D_t$.

1985 Since $E_t \rightarrow 0$, and $\gamma, \phi, c > 0$, Inequality (62) results in a contradiction $E_t \geq \frac{1}{c\gamma\phi} > 0$. Therefore,
1986 there exists t' such that $D_t = 0$ for all $t > t'$, ensuring that the algorithm terminates in a finite
1987 number of steps.
1988

1989 **Part (b).** We consider $\sigma \in (0, \frac{1}{2}]$. We define $w \triangleq \frac{1-\sigma}{\sigma} \geq 1$. We have from Inequality (61):
1990

$$\begin{aligned}
1991 \quad D_t &\leq D_{t-1} - D_t + (D_{t-1} - D_t)^w \cdot \ddot{\kappa} \\
1992 &\stackrel{\textcircled{1}}{\leq} D_{t-1} - D_t + (D_{t-1} - D_t) \cdot \bar{r}^{w-1} \cdot \ddot{\kappa} \\
1993 &\leq D_{t-1} \cdot \frac{\bar{r}^{w-1} \cdot \ddot{\kappa} + 1}{\bar{r}^{w-1} \cdot \ddot{\kappa} + 2}, \quad (63)
\end{aligned}$$

1995 where step $\textcircled{1}$ uses the fact that $x^w \leq x \cdot \bar{r}^{w-1}$ for all $\sigma \in (0, \frac{1}{2}]$, and $x = D_{t-1} - D_t \in [0, \bar{r}]$.
1996 Therefore, we have:
1997

$$D_T \leq D_1 \cdot \left(\frac{\bar{r}^{w-1} \cdot \ddot{\kappa} + 1}{\bar{r}^{w-1} \cdot \ddot{\kappa} + 2} \right)^{T-1}.$$

1998 **Part (c).** We consider $\sigma \in (\frac{1}{2}, 1)$. We define $w \triangleq \frac{1-\sigma}{\sigma} \in (0, 1)$, and $\tau \triangleq 1/w - 1 \in (0, \infty)$. We
 1999 have from Inequality (61):
 2000

$$\begin{aligned} D_t &\leq D_{t-1} - D_t + \ddot{\kappa} \cdot (D_{t-1} - D_t)^{\frac{1-\sigma}{\sigma}} \\ &\stackrel{\textcircled{1}}{=} \ddot{\kappa} (D_{t-1} - D_t)^w + (D_{t-1} - D_t)^w \cdot (E_t)^{1-w} \\ &\stackrel{\textcircled{2}}{\leq} \ddot{\kappa} (D_{t-1} - D_t)^w + (D_{t-1} - D_t)^w \cdot \bar{r}^{1-w} \\ &= (D_{t-1} - D_t)^w \cdot \underbrace{(\ddot{\kappa} + \bar{r}^{1-w})}_{\triangleq \dot{\kappa}}, \end{aligned}$$

2008 where step $\textcircled{1}$ uses the definition of w and the fact that $D_{t-1} - D_t = E_t$; step $\textcircled{2}$ uses the fact that
 2009 $\max_{x \in (0, \bar{r}]} x^{1-w} \leq \bar{r}^{1-w}$ if $w \in (0, 1)$. We further obtain:
 2010

$$\underbrace{[D_t]^{1/w}}_{=[D_t]^{\tau+1}} \leq (D_{t-1} - D_t) \cdot \dot{\kappa}^{1/w}.$$

2014 Applying Lemma A.10 with $a = \dot{\kappa}^{1/w}$, we have:
 2015

$$D_T \leq \mathcal{O}(T^{-1/\tau}) \stackrel{\textcircled{1}}{=} \mathcal{O}(T^{-\frac{1}{1/w-1}}) \stackrel{\textcircled{2}}{=} \mathcal{O}(T^{-\frac{1}{\frac{\sigma}{1-\sigma}-1}}) = \mathcal{O}(T^{-\frac{1-\sigma}{2\sigma-1}}),$$

2016 where step $\textcircled{1}$ uses $\tau \triangleq 1/w - 1$; step $\textcircled{2}$ uses $w \triangleq \frac{1-\sigma}{\sigma}$.
 2017 \square

G ADDITIONAL EXPERIMENT DETAILS AND RESULTS

2024 This section provides additional experimental details and results for our proposed methods. We
 2025 first introduce nonnegative PCA as an additional application, describe the datasets and experimental
 2026 settings, and specify the compared baselines for ℓ_1 -regularized SPCA and nonnegative PCA. We
 2027 then report extended results on ℓ_0 -regularized SPCA, ℓ_1 -regularized SPCA, and nonnegative PCA,
 2028 demonstrating the effectiveness and robustness of our algorithms across these settings.
 2029

G.1 ADDITIONAL APPLICATION: NONNEGATIVE PCA

2032 Nonnegative PCA is an extension of PCA that imposes nonnegativity constraints on the principal
 2033 vector (Zass & Shashua, 2006; Qian et al., 2021). This constraint leads to a nonnegative representation
 2034 of loading vectors and it helps to capture data locality in feature selection. Nonnegative PCA
 2035 can be formulated as: $\min_{\mathbf{X} \in \text{St}(n, r)} -\frac{1}{2} \langle \mathbf{C}\mathbf{X}, \mathbf{X} \rangle$, s.t. $\mathbf{X} \geq \mathbf{0}$, where $\mathbf{C} \in \mathbb{R}^{n \times n}$ is the covariance
 2036 matrix of the data.

G.2 DATA SETS

2039 To generate the data matrix $\mathbf{A} \in \mathbb{R}^{m \times n}$, we consider 10 publicly available real-world or randomly
 2040 generated data sets: ‘w1a’, ‘TDT2’, ‘20News’, ‘sector’, ‘E2006’, ‘MNIST’, ‘Gisette’, ‘Caltech’,
 2041 ‘Cifar’, ‘randn’. We randomly select a subset of examples from the original data set. The size
 2042 of $\mathbf{A} \in \mathbb{R}^{m \times n}$ is chosen from the following set $(m, n) \in \{(2477, 300), (500, 1000), (8000, 1000),$
 2043 $(6412, 1000), (2000, 1000), (60000, 784), (3000, 1000), (1000, 1000), (500, 1000)\}$. We scale the
 2044 matrix \mathbf{A} to have unit Frobenius norm by setting $\mathbf{A} = \frac{\mathbf{A}}{\|\mathbf{A}\|_F}$ and let $\mathbf{C} = \mathbf{A}^T \mathbf{A} \in \mathbb{R}^{n \times n}$.
 2045

G.3 ADDITIONAL EXPERIMENT SETTINGS

2048 ▶ **Compared Methods on L_1 -Regularized SPCA.** We benchmark **OBCD** against the following
 2049 state-of-the-art algorithms: (i) Randomized Submanifold Subgradient Method (RSSM) (Cheung
 2050 et al., 2024); (ii) Linearized Alternating Direction Method of Multiplier (LADMM) (He & Yuan,
 2051 2012); (iii) Riemannian Subgradient Method (RSubGrad) (Li et al., 2021); (iv) ADMM (Lai &
 Osher, 2014); (v) Manifold Proximal Gradient Method (ManPG) (Chen et al., 2020). For RSSM

2052 and RSubGrad, the subgradient $\mathbf{G}^t \in \partial F(\mathbf{X}^t)$ at iterate \mathbf{X}^t is taken as $\mathbf{G}^t = -\mathbf{C}\mathbf{X}^t + \lambda \text{sign}(\mathbf{X}^t)$,
 2053 since $\text{sign}(\mathbf{X})$ is a valid subgradient of $\|\mathbf{X}\|_1$. All competing methods are initialized with a random
 2054 matrix, producing five variants: RSSM(rnd), LADMM(rnd), RSubGrad(rnd), ADMM(rnd), and
 2055 ManPG(rnd). For **OBCD**, we employ a random working-set rule with identity initialization, denoted
 2056 by **OBCD-R(id)**.

2057 **► Compared Methods on Nonnegative PCA.** For Nonnegative PCA, we compare **OBCD** with
 2058 two leading infeasible approaches: *(i)* Linearized ADMM (LADMM) (He & Yuan, 2012; Lai &
 2059 Osher, 2014), *(ii)* Penalty-based Splitting Method (PSM) (Yuan, 2024; Chen, 2012), and *(iii)* Rie-
 2060 mannian ADMM (RADMM) (Li et al., 2024a). Since LADMM, PSM, and RADMM are infeasible
 2061 methods and may violate the nonnegativity constraints, we evaluate the quality of intermediate solu-
 2062 tions using a surrogate objective, $f(\mathbf{X}) + 1000\|\min(\mathbf{0}, \mathbf{X})\|_F$ with $\mathbf{X} \in \text{St}(n, r)$, which penalizes
 2063 any violation of feasibility.

2064

2065 G.4 ADDITIONAL EXPERIMENT RESULTS

2066

2067 **► Results on L_0 -Regularized SPCA.** For $\lambda \in \{10, 50, 100, 500\}$, Figures 3-6 present the
 2068 convergence curves of the compared methods on L_0 -regularized SPCA. Across all setting, **OBCD-R**
 2069 consistently achieves lower objective values than competing methods, further reinforcing the con-
 2070 clusions drawn in the main paper.

2071

2072 **► Results on L_1 -Regularized SPCA.** For $\lambda \in \{10, 50, 100, 500\}$, Table 2 and Figures 7-10 report
 2073 objective values obtained by all methods with $r = 20$. Two observations follow. *(i)* ManPG is
 2074 generally faster than LADMM, ADMM and RSubGrad, which aligns with the findings reported
 2075 in (Chen et al., 2020). *(ii)* **OBCD-R** consistently achieves lower objective values compared with
 {LADMM, ADMM, RSubGrad, ManPG}, demonstrating its superior solution quality.

2076

2077 **► Results on Nonnegative PCA.** For $r \in \{10, 20, 40, 80\}$, Table 3 reports objective values and
 2078 feasibility violations measured by $\|\min(\mathbf{0}, \mathbf{X})\|_F$, while Figures 11-14 show the surrogate objective
 2079 $f(\mathbf{X}) + 1000\|\min(\mathbf{0}, \mathbf{X})\|_F$. Two key conclusions can be drawn. *(i)* The proposed methods gener-
 2080 ally achieve the best overall performance, and **OBCD-R** often substantially outperforms LADMM,
 PSM, and RADMM by locating stronger stationary points.

2081

2082

2083

2084

2085

2086

2087

2088

2089

2090

2091

2092

2093

2094

2095

2096

2097

2098

2099

2100

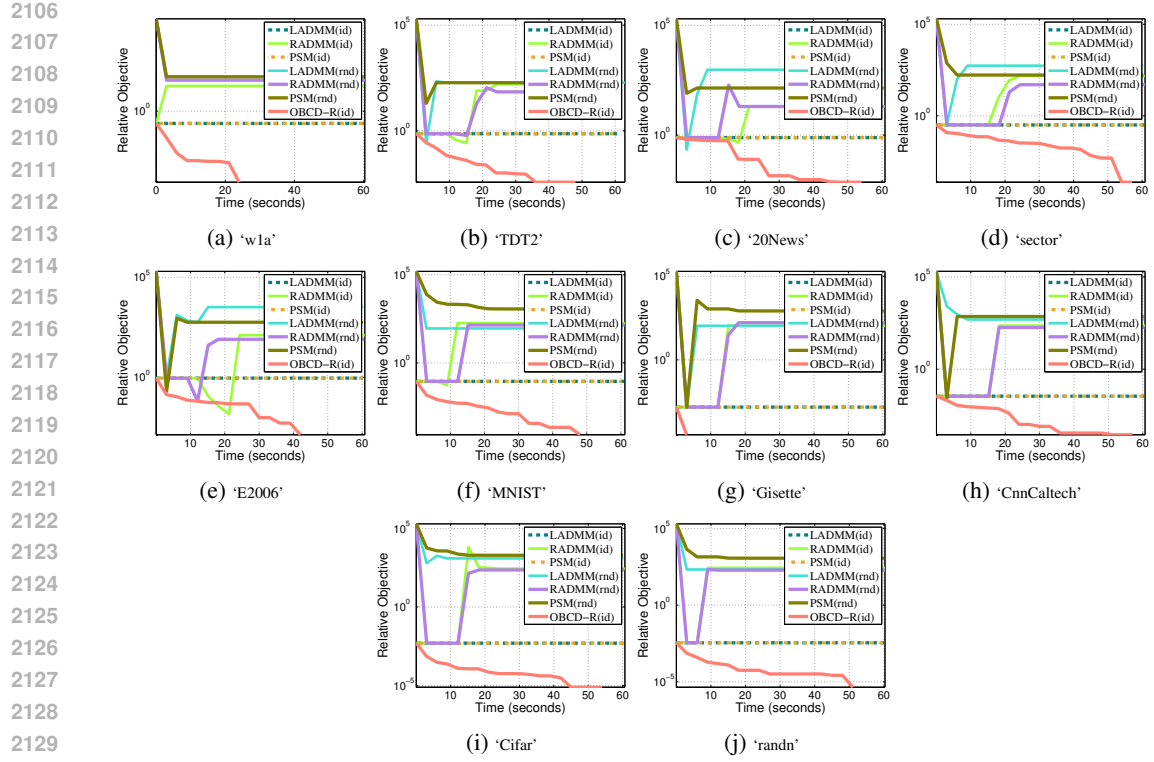
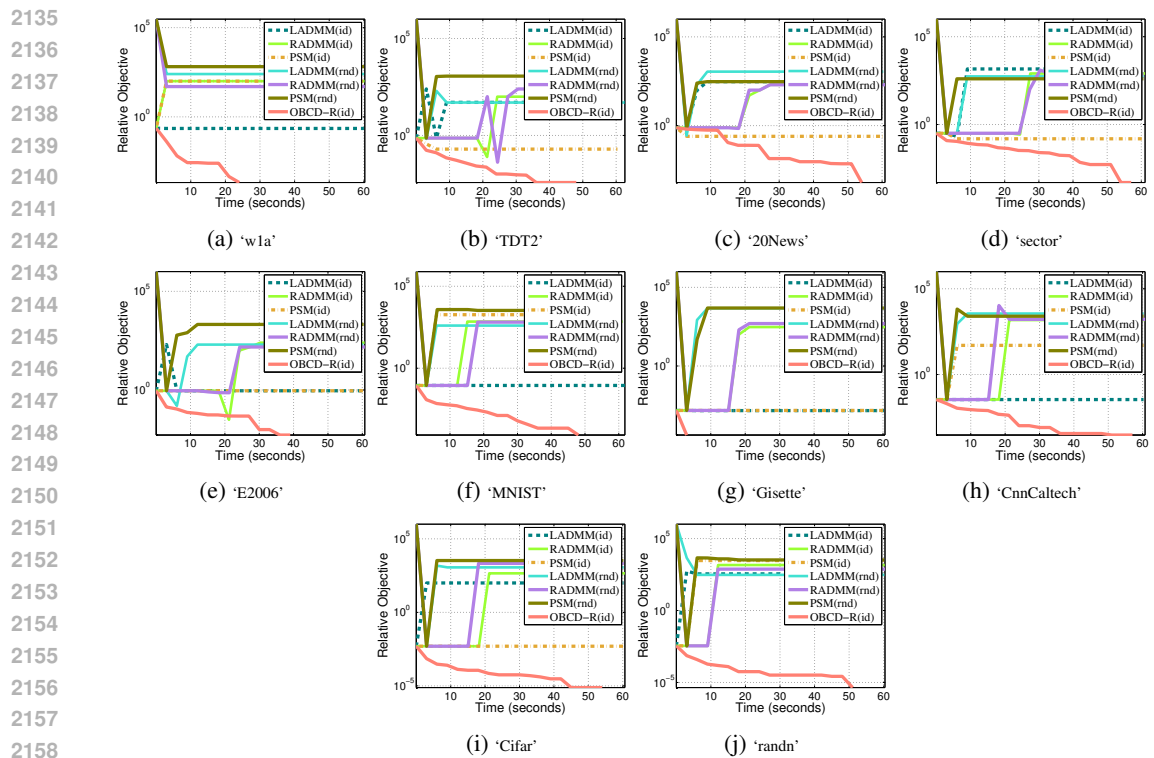
2101

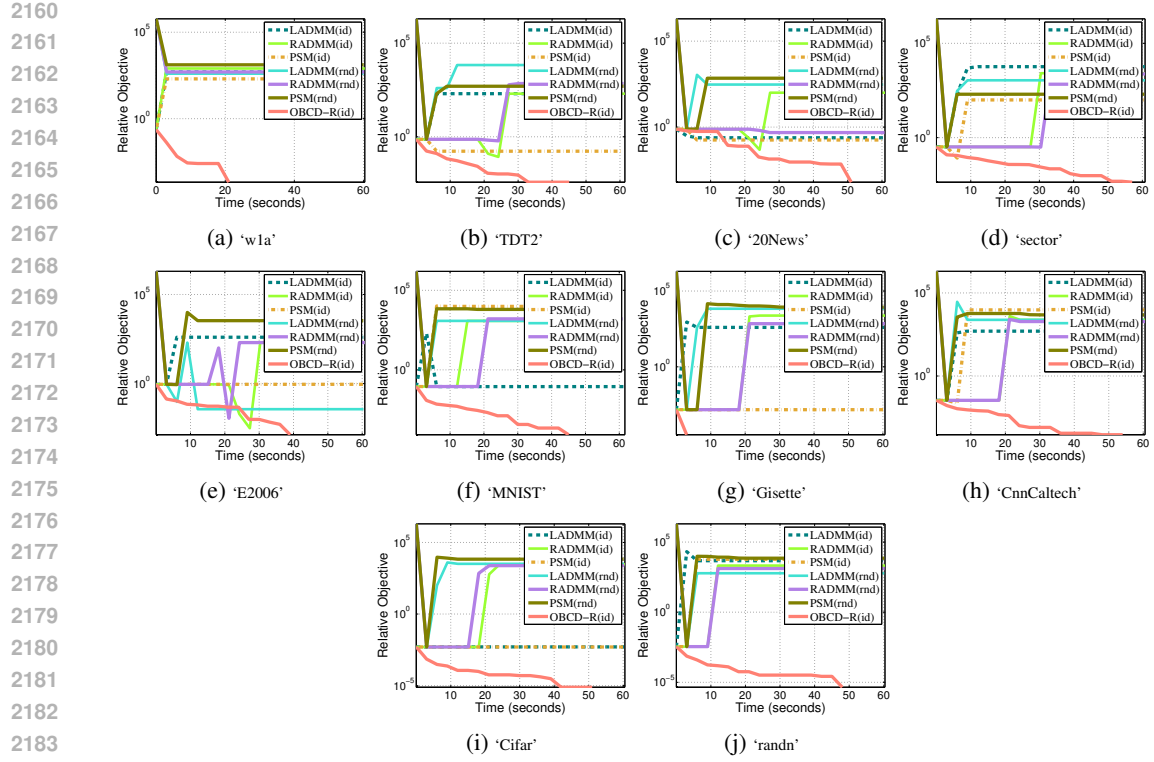
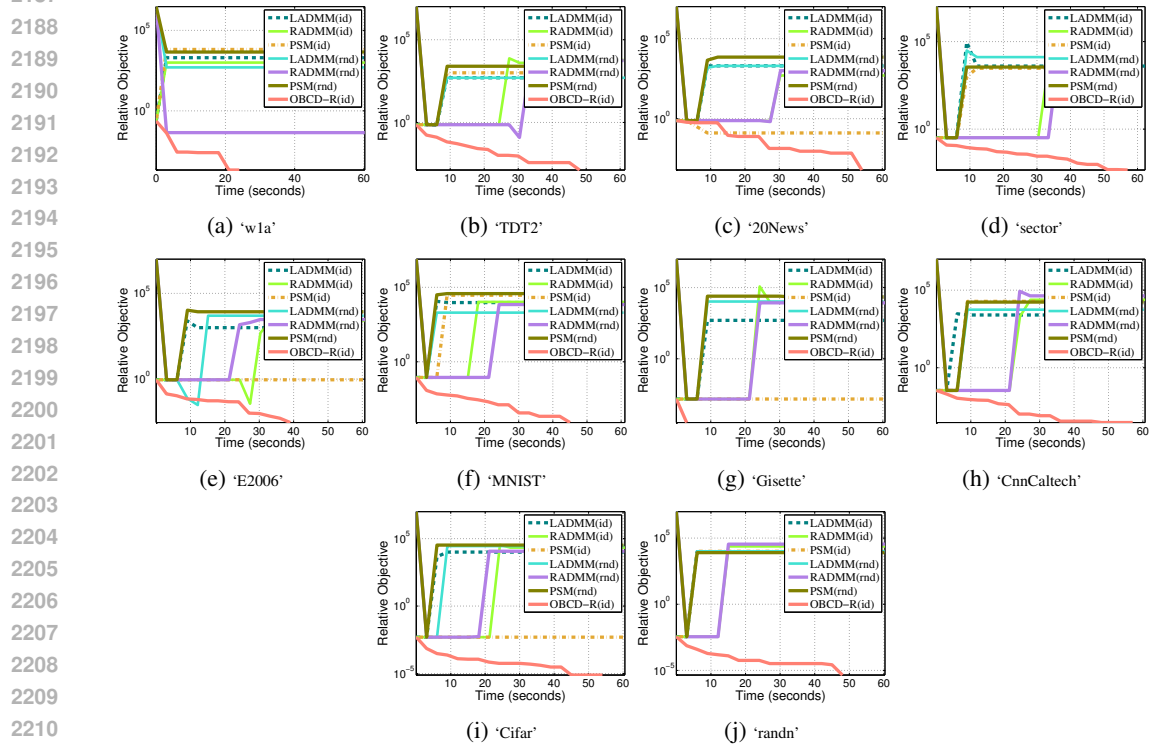
2102

2103

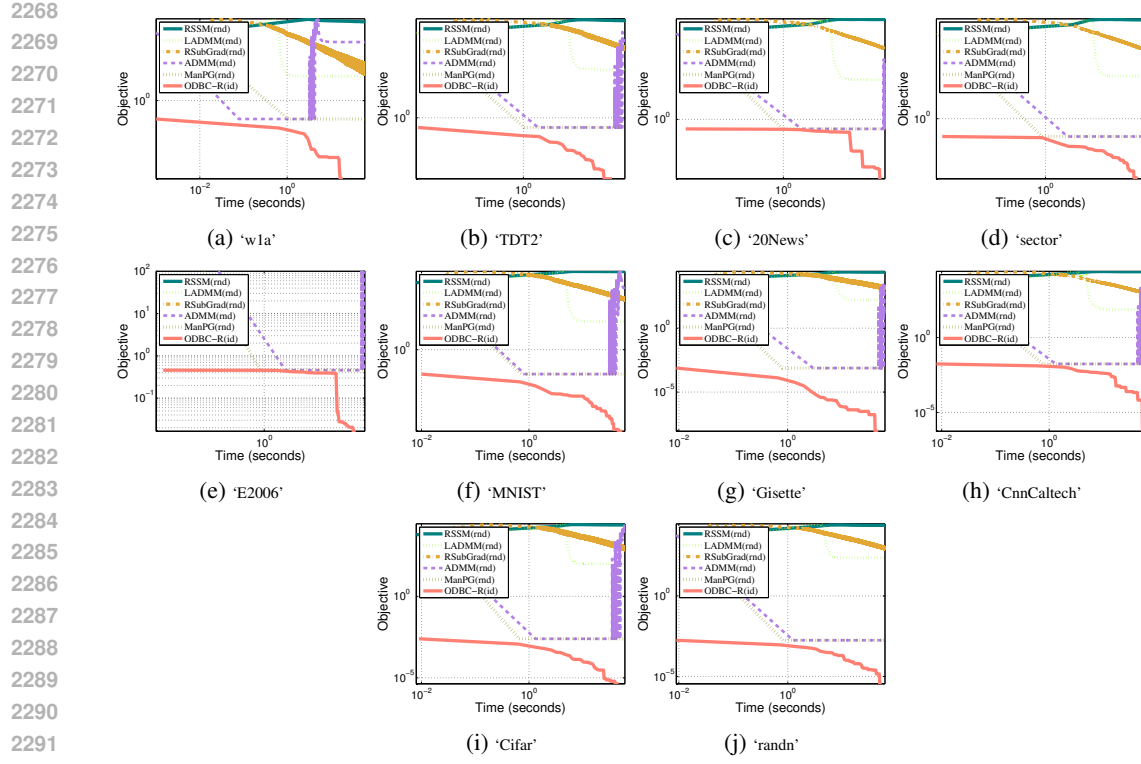
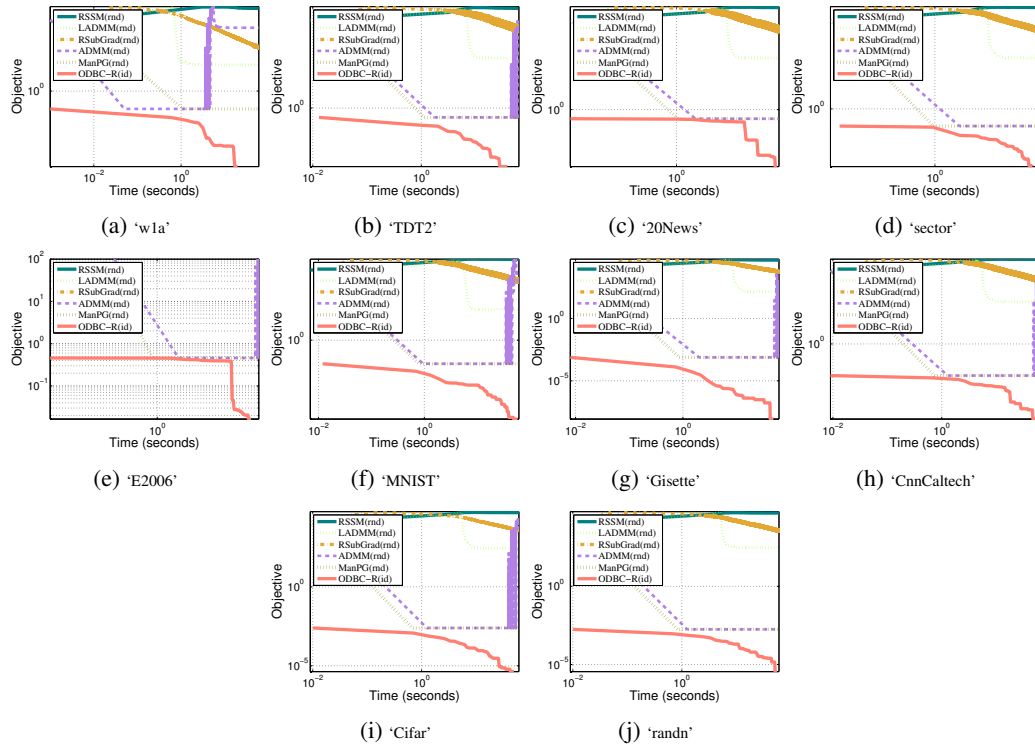
2104

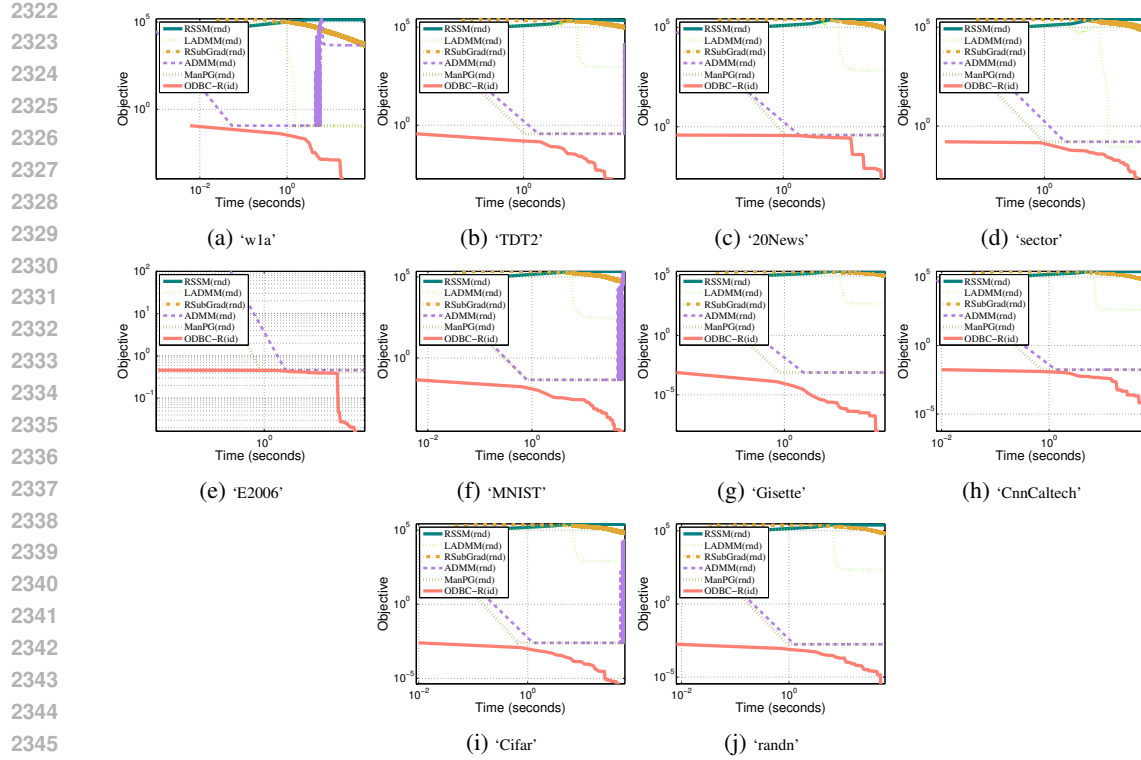
2105

Figure 3: The convergence curve for solving L_0 -regularized SPCA with $\lambda = 10$.Figure 4: The convergence curve for solving L_0 -regularized SPCA with $\lambda = 50$.

Figure 5: The convergence curve for solving L_0 -regularized SPCA with $\lambda = 100$.Figure 6: The convergence curve for solving L_0 -regularized SPCA with $\lambda = 500$.

2214	data-m-n	RSSM (rnd)	LADMM (rnd)	RSubGrad (rnd)	ADMM (rnd)	ManPG (rnd)	OBCD-R (id)	data-m-n	RSSM (rnd)	LADMM (rnd)	RSubGrad (rnd)	ADMM (rnd)	ManPG (rnd)	OBCD-R (id)	
$r = 20, \lambda = 10, \text{time limit}=60$															
2215	w1a-2477-300	16780.362	199.961	207.918	648.546	199.949	199.833	w1a-2477-300	11896.991	1017.039	1014.312	1948.020	999.949	999.833	
2216	TDT2-500-1000	4798.905	199.997	376.695	2756.315	199.999	199.636	TDT2-500-1000	24811.350	1142.577	5689.161	13596.188	999.999	999.643	
2217	20News-8000-1000	5099.667	203.159	458.525	2076.634	199.997	199.673	20News-8000-1000	25660.045	1085.026	4852.847	15234.296	999.997	999.673	
2218	sector-6412-1000	5088.999	211.558	257.937	2645.919	199.990	199.848	sector-6412-1000	25685.661	1076.243	5056.712	13985.491	999.990	999.834	
2219	E2006-2000-1000	4791.094	201.933	240.895	2873.292	200.000	199.541	E2006-2000-1000	23945.851	1085.356	4102.980	13800.413	1000.000	999.933	
2220	MNIST-60000-784	4491.492	199.990	304.146	3077.644	199.992	199.950	MNIST-60000-784	22829.255	1036.685	3035.519	15166.857	999.992	999.949	
2221	Gisette-3000-1000	5096.530	203.597	361.631	3054.472	199.990	199.989	Gisette-3000-1000	25696.928	1125.509	4866.266	15083.925	999.990	999.989	
2222	CnnCaltech-3000-1000	5274.750	203.177	287.583	2952.906	199.990	199.977	CnnCaltech-3000-1000	26443.995	1075.923	5648.585	14435.979	999.990	999.977	
2223	Cifar-1000-1000	5326.610	199.990	452.860	3007.068	199.990	199.987	Cifar-1000-1000	26174.415	1101.272	6080.349	1482.673	999.990	999.987	
2224	randn-500-1000	5299.246	207.757	267.307	2908.559	199.990	199.988	randn-500-1000	25917.437	1237.580	4616.156	14999.881	999.990	999.988	
$r = 20, \lambda = 100, \text{time limit}=60$															
2225	data-m-n	RSSM (rnd)	LADMM (rnd)	RSubGrad (rnd)	ADMM (rnd)	ManPG (rnd)	OBCD-R (id)	data-m-n	RSSM (rnd)	LADMM (rnd)	RSubGrad (rnd)	ADMM (rnd)	ManPG (rnd)	OBCD-R (id)	
2226	w1a-2477-300	25212.531	2024.330	2142.546	4172.640	1999.949	1999.833	w1a-2477-300	144765.556	9999.940	26452.425	14711.906	9999.949	9999.834	
2227	TDT2-500-1000	49303.568	2210.215	13770.257	27221.640	1999.999	1999.632	TDT2-500-1000	243550.365	1100.292	177896.188	137815.999	9999.999	9999.636	
2228	20News-8000-1000	52028.247	2204.356	12741.678	30561.467	1999.997	1999.673	20News-8000-1000	257513.893	10188.884	193633.121	152343.022	9999.997	9999.675	
2229	sector-6412-1000	51434.623	2222.105	17521.188	27816.620	1999.990	1999.834	sector-6412-1000	260801.229	9999.919	199887.443	138927.601	9999.990	9999.834	
2230	E2006-2000-1000	48063.148	2140.058	11120.402	27411.269	20000.000	1999.933	E2006-2000-1000	236514.992	10535.514	135563.372	143898.385	10000.000	9999.933	
2231	MNIST-60000-784	469090.059	2057.976	11107.393	30906.421	1999.992	1999.944	MNIST-60000-784	228035.432	10306.371	146677.724	145588.796	9999.992	9999.948	
2232	Gisette-3000-1000	51396.503	2202.300	15971.871	30698.736	1999.990	1999.981	Gisette-3000-1000	261983.906	10313.107	202913.351	152724.051	9999.990	9999.988	
2233	CnnCaltech-3000-1000	53046.484	2230.728	9917.898	29326.239	1999.990	1999.977	CnnCaltech-3000-1000	259056.451	10418.351	166856.613	149325.559	9999.990	9999.977	
2234	Cifar-1000-1000	52183.021	2282.490	16736.350	30070.764	1999.990	1999.987	Cifar-1000-1000	262528.151	10874.860	195776.730	150353.857	9999.990	9999.987	
2235	randn-500-1000	52275.431	2309.568	14891.818	30522.549	1999.990	1999.988	randn-500-1000	257825.619	10219.431	8081.264	137050.323	9999.990	9999.988	
$r = 20, \lambda = 500, \text{time limit}=60$															
2236	data-m-n	RSSM (rnd)	LADMM (rnd)	RSubGrad (rnd)	ADMM (rnd)	ManPG (rnd)	OBCD-R (id)	data-m-n	RSSM (rnd)	LADMM (rnd)	RSubGrad (rnd)	ADMM (rnd)	ManPG (rnd)	OBCD-R (id)	
2237	w1a-2477-300	25212.531	2024.330	2142.546	4172.640	1999.949	1999.833	w1a-2477-300	144765.556	9999.940	26452.425	14711.906	9999.949	9999.834	
2238	TDT2-500-1000	49303.568	2210.215	13770.257	27221.640	1999.999	1999.632	TDT2-500-1000	243550.365	1100.292	177896.188	137815.999	9999.999	9999.636	
2239	20News-8000-1000	52028.247	2204.356	12741.678	30561.467	1999.997	1999.673	20News-8000-1000	257513.893	10188.884	193633.121	152343.022	9999.997	9999.675	
2240	sector-6412-1000	51434.623	2222.105	17521.188	27816.620	1999.990	1999.834	sector-6412-1000	260801.229	9999.919	199887.443	138927.601	9999.990	9999.834	
2241	E2006-2000-1000	48063.148	2140.058	11120.402	27411.269	20000.000	1999.933	E2006-2000-1000	236514.992	10535.514	135563.372	143898.385	10000.000	9999.933	
2242	MNIST-60000-784	469090.059	2057.976	11107.393	30906.421	1999.992	1999.944	MNIST-60000-784	228035.432	10306.371	146677.724	145588.796	9999.992	9999.948	
2243	Gisette-3000-1000	51396.503	2202.300	15971.871	30698.736	1999.990	1999.981	Gisette-3000-1000	261983.906	10313.107	202913.351	152724.051	9999.990	9999.988	
2244	CnnCaltech-3000-1000	53046.484	2230.728	9917.898	29326.239	1999.990	1999.977	CnnCaltech-3000-1000	259056.451	10418.351	166856.613	149325.559	9999.990	9999.977	
2245	Cifar-1000-1000	52183.021	2282.490	16736.350	30070.764	1999.990	1999.987	Cifar-1000-1000	262528.151	10874.860	195776.730	150353.857	9999.990	9999.987	
2246	randn-500-1000	52275.431	2309.568	14891.818	30522.549	1999.990	1999.988	randn-500-1000	257825.619	10219.431	8081.264	137050.323	9999.990	9999.988	
$r = 20, \lambda = 1000, \text{time limit}=60$															
2247	data-m-n	RSSM (rnd)	LADMM (rnd)	RSubGrad (rnd)	ADMM (rnd)	ManPG (rnd)	OBCD-R (id)	data-m-n	RSSM (rnd)	LADMM (rnd)	RSubGrad (rnd)	ADMM (rnd)	ManPG (rnd)	OBCD-R (id)	
2248	w1a-2477-300	25212.531	2024.330	2142.546	4172.640	1999.949	1999.833	w1a-2477-300	144765.556	9999.940	26452.425	14711.906	9999.949	9999.834	
2249	TDT2-500-1000	49303.568	2210.215	13770.257	27221.640	1999.999	1999.632	TDT2-500-1000	243550.365	1100.292	177896.188	137815.999	9999.999	9999.636	
2250	20News-8000-1000	52028.247	2204.356	12741.678	30561.467	1999.997	1999.673	20News-8000-1000	257513.893	10188.884	193633.121	152343.022	9999.997	9999.675	
2251	sector-6412-1000	51434.623	2222.105	17521.188	27816.620	1999.990	1999.834	sector-6412-1000	260801.229	9999.919	199887.443	138927.601	9999.990	9999.834	
2252	E2006-2000-1000	48063.148	2140.058	11120.402	27411.269	20000.000	1999.933	E2006-2000-1000	236514.992	10535.514	135563.372	143898.385	10000.000	9999.933	
2253	MNIST-60000-784	469090.059	2057.976	11107.393	30906.421	1999.992	1999.944	MNIST-60000-784	228035.432	10306.371	146677.724	145588.796	9999.992	9999.948	
2254	Gisette-3000-1000	51396.503	2202.300	15971.871	30698.736	1999.990	1999.981	Gisette-3000-1000	261983.906	10313.107	202913.351	152724.051	9999.990	9999.988	
2255	CnnCaltech-3000-1000	53046.484	2230.728	9917.898	29326.239	1999.990	1999.977	CnnCaltech-3000-1000	259056.451	10418.351	166856.613				

Figure 8: The convergence curve for solving L_1 -regularized SPCA with $\lambda = 50$.Figure 9: The convergence curve for solving L_1 -regularized SPCA with $\lambda = 100$.

Figure 10: The convergence curve for solving L_1 -regularized SPCA with $\lambda = 500$.

data-m-n	ADMM (rnd)	PSM (rnd)	RADMM (rnd)	OBCD-R (id)	data-m-n	ADMM (rnd)	PSM (rnd)	RADMM (rnd)	OBCD-R (id)
<i>r</i> = 10, time limit=60									
w1a-2477-300	-4.08e-02 , 0e+00	-4.71e-02 , 0e+00	-1.11e-02 , 0e+00	-1.67e-01 , 7e-15	w1a-2477-300	-3.73e-02 , 0e+00	-5.36e-02 , 0e+00	-3.68e-02 , 0e+00	-2.17e-01 , 3e-15
TDT2-500-1000	-1.64e-01 , 0e+00	-6.70e-02 , 0e+00	-2.82e-03 , 0e+00	-3.32e-01 , 4e-15	TDT2-500-1000	-1.73e-03 , 0e+00	-9.53e-02 , 0e+00	-5.01e-03 , 0e+00	-3.71e-01 , 2e-15
20News-8000-1000	-4.82e-02 , 0e+00	-9.14e-02 , 0e+00	-8.43e-03 , 0e+00	-3.49e-01 , 2e-14	20News-8000-1000	-1.31e-03 , 0e+00	-3.14e-02 , 0e+00	-7.71e-03 , 0e+00	-3.78e-01 , 4e-15
sector-6412-1000	-5.70e-03 , 0e+00	-5.84e-03 , 0e+00	-3.30e-03 , 0e+00	-1.21e-01 , 1e-15	sector-6412-1000	-9.91e-03 , 0e+00	-1.55e-02 , 0e+00	-1.17e-02 , 0e+00	-1.67e-01 , 4e-15
E2006-2000-1000	-3.13e-01 , 0e+00	-3.39e-01 , 0e+00	-6.71e-03 , 0e+00	-4.42e-01 , 1e-14	E2006-2000-1000	-1.20e-03 , 0e+00	-3.56e-01 , 0e+00	-1.55e-03 , 0e+00	-4.62e-01 , 1e-14
MNIST-60000-784	-3.57e-02 , 0e+00	-9.10e-02 , 0e+00	-3.00e-02 , 0e+00	-2.78e-01 , 2e-14	MNIST-60000-784	-1.70e-02 , 0e+00	-9.40e-02 , 0e+00	-3.47e-02 , 0e+00	-2.95e-01 , 2e-14
Gisette-3000-1000	-1.41e-01 , 0e+00	-2.34e-01 , 0e+00	-6.84e-02 , 0e+00	-3.72e-01 , 2e-18	Gisette-3000-1000	-2.23e-02 , 0e+00	-2.31e-01 , 0e+00	-6.05e-02 , 0e+00	-3.80e-01 , 7e-19
CnnCaltech-3000-1000	-1.73e-01 , 0e+00	-2.91e-01 , 0e+00	-7.86e-02 , 0e+00	-4.47e-01 , 0e+00	CnnCaltech-3000-1000	-1.05e-02 , 0e+00	-6.87e-02 , 0e+00	-3.34e-02 , 0e+00	-1.52e-01 , 2e-26
Cifar-1000-1000	-1.73e-01 , 0e+00	-2.91e-01 , 0e+00	-7.86e-02 , 0e+00	-4.47e-01 , 0e+00	Cifar-1000-1000	-2.37e-02 , 0e+00	-2.87e-01 , 0e+00	-1.12e-01 , 0e+00	-4.54e-01 , 0e+00
randn-500-1000	-4.91e-03 , 0e+00	-5.10e-03 , 0e+00	-4.77e-03 , 0e+00	-1.24e-02 , 2e-14	randn-500-1000	-1.00e-02 , 0e+00	-9.90e-03 , 0e+00	-9.55e-03 , 0e+00	-2.11e-02 , 3e-14
data-m-n	ADMM (rnd)	PSM (rnd)	RADMM (rnd)	OBCD-R (id)	data-m-n	ADMM (rnd)	PSM (rnd)	RADMM (rnd)	OBCD-R (id)
<i>r</i> = 40, time limit=60									
w1a-2477-300	-6.45e-02 , 0e+00	-1.07e-01 , 0e+00	-8.56e-02 , 0e+00	-3.00e-01 , 7e-15	w1a-2477-300	-1.28e-01 , 0e+00	-1.70e-01 , 0e+00	-1.34e-01 , 0e+00	-3.90e-01 , 1e-16
TDT2-500-1000	-3.50e-02 , 0e+00	-9.89e-02 , 0e+00	-3.57e-02 , 0e+00	-4.09e-01 , 6e-15	TDT2-500-1000	-9.80e-02 , 0e+00	-4.97e-02 , 0e+00	-4.55e-02 , 0e+00	-4.49e-01 , 2e-14
20News-8000-1000	-1.92e-02 , 0e+00	-3.43e-02 , 0e+00	-1.11e-01 , 0e+00	-4.14e-01 , 2e-14	20News-8000-1000	-2.93e-02 , 0e+00	-3.04e-02 , 0e+00	-2.23e-02 , 0e+00	-4.47e-01 , 3e-14
sector-6412-1000	-8.70e-03 , 0e+00	-2.38e-03 , 0e+00	-1.11e-01 , 0e+00	-4.14e-01 , 2e-14	sector-6412-1000	-7.09e-02 , 0e+00	-3.82e-02 , 0e+00	-3.39e-02 , 0e+00	-2.96e-01 , 5e-15
E2006-2000-1000	-8.36e-03 , 0e+00	-3.64e-01 , 0e+00	-2.68e-02 , 0e+00	-4.75e-01 , 2e-14	E2006-2000-1000	-3.09e-03 , 0e+00	-3.31e-01 , 0e+00	-1.39e-01 , 0e+00	-4.89e-01 , 2e-14
MNIST-60000-784	-2.09e-02 , 0e+00	-1.09e-01 , 0e+00	-4.67e-02 , 0e+00	-2.89e-01 , 3e-14	MNIST-60000-784	-5.06e-02 , 0e+00	-9.95e-02 , 0e+00	-8.13e-02 , 0e+00	-3.03e-01 , 3e-14
Gisette-3000-1000	-2.59e-02 , 0e+00	-2.63e-01 , 0e+00	-1.47e-01 , 0e+00	-3.69e-01 , 6e-20	Gisette-3000-1000	-6.51e-02 , 0e+00	-2.64e-01 , 0e+00	-2.35e-01 , 0e+00	-3.56e-01 , 0e+00
CnnCaltech-3000-1000	-2.03e-02 , 0e+00	-8.75e-02 , 0e+00	-4.74e-02 , 0e+00	-1.49e-01 , 0e+00	CnnCaltech-3000-1000	-4.77e-02 , 0e+00	-1.02e-01 , 0e+00	-8.91e-02 , 0e+00	-1.61e-01 , 0e+00
Cifar-1000-1000	-2.65e-02 , 0e+00	-3.25e-01 , 0e+00	-1.60e-01 , 0e+00	-4.43e-01 , 0e+00	Cifar-1000-1000	-6.69e-02 , 0e+00	-3.21e-01 , 0e+00	-2.29e-01 , 0e+00	-4.24e-01 , 0e+00
randn-500-1000	-2.01e-02 , 0e+00	-2.03e-02 , 0e+00	-2.00e-02 , 0e+00	-3.08e-02 , 5e-16	randn-500-1000	-4.03e-02 , 0e+00	-4.02e-02 , 0e+00	-3.95e-02 , 0e+00	-5.31e-02 , 3e-14

Table 3: Comparisons of objective values and the violation of the nonnegative constraints ($\|\min(\mathbf{0}, \mathbf{X})\|_F$) for nonnegative PCA for all the compared methods. The 1st, 2nd, and 3rd best results are colored with red, green and blue, respectively.

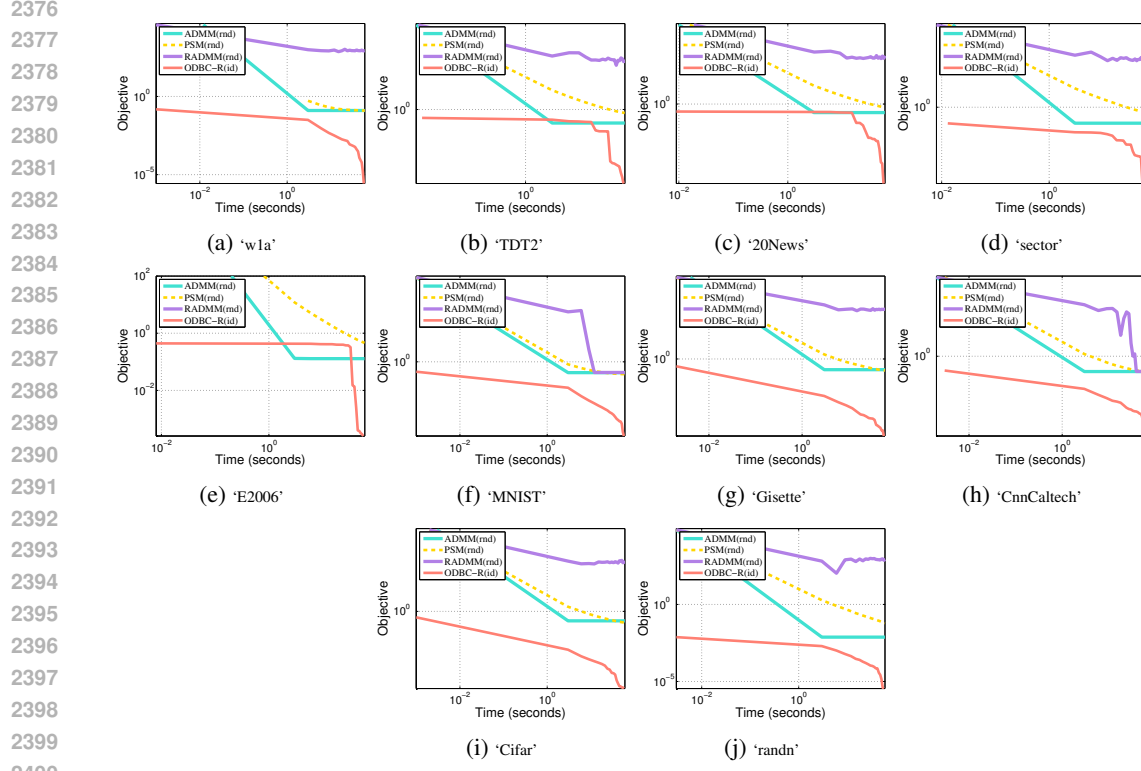


Figure 11: The convergence curve of the surrogate objective $f(\mathbf{X}) + 1000\|\min(\mathbf{0}, \mathbf{X})\|_F$ with $\mathbf{X} \in \text{St}(n, r)$ for solving the nonnegative PCA problem with $r = 10$.

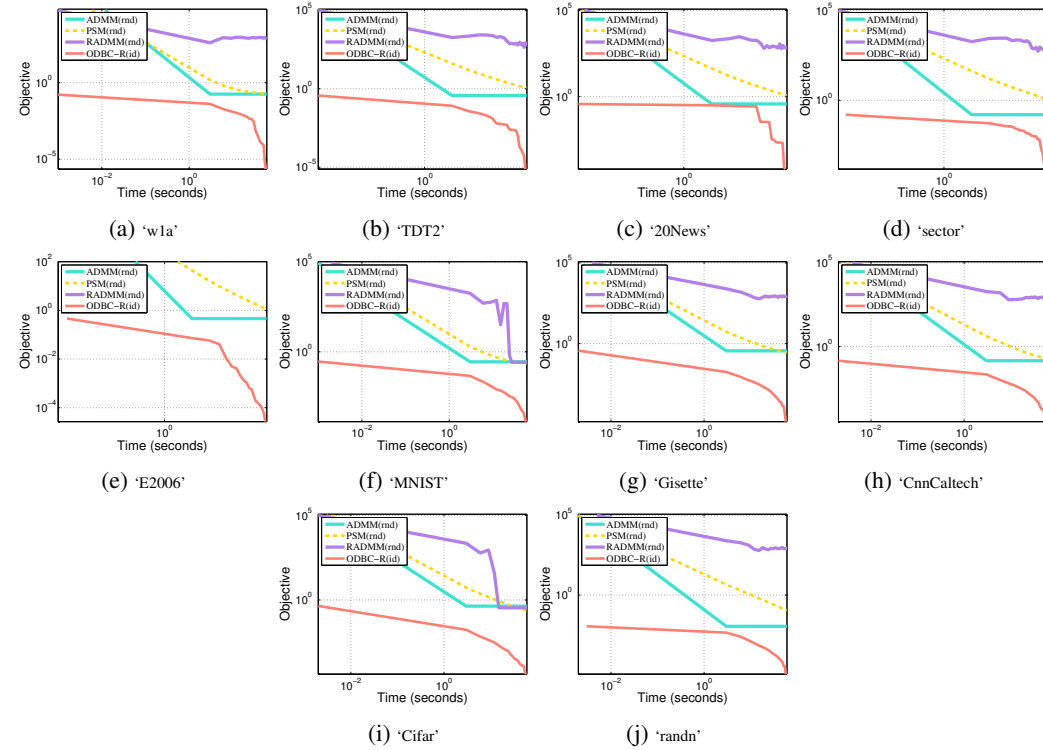


Figure 12: The convergence curve of the surrogate objective $f(\mathbf{X}) + 1000\|\min(\mathbf{0}, \mathbf{X})\|_F$ with $\mathbf{X} \in \text{St}(n, r)$ for solving the nonnegative PCA problem with $r = 20$.

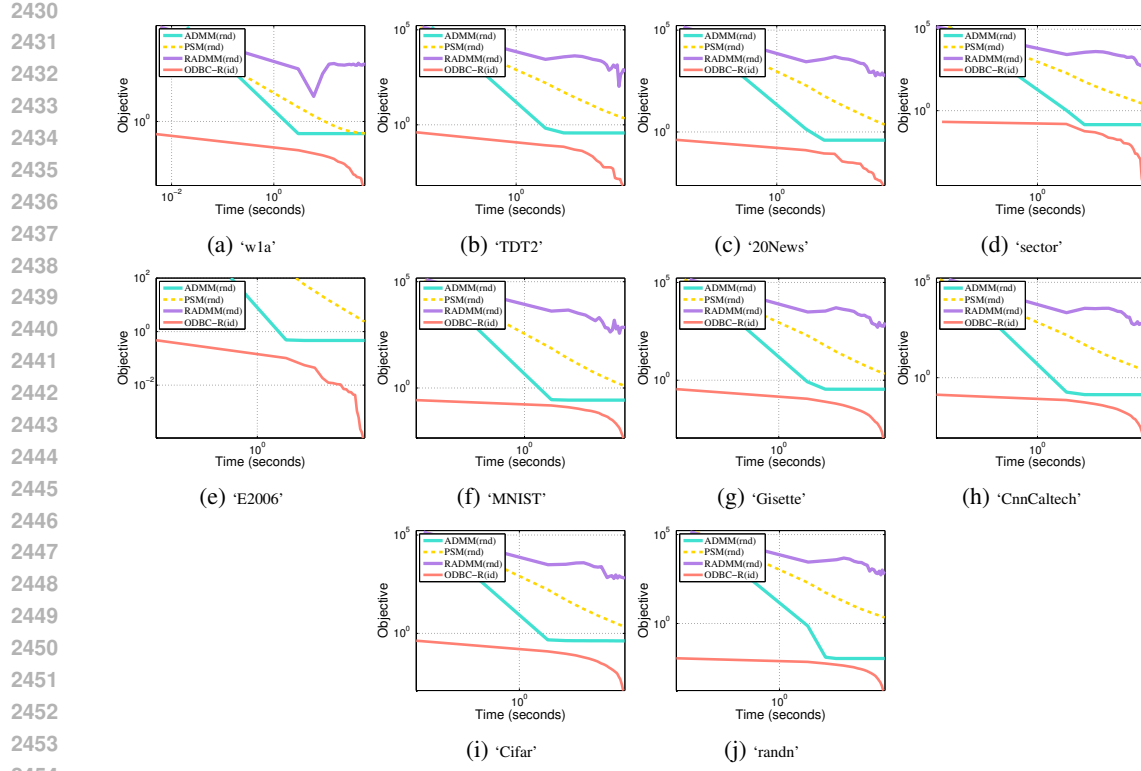


Figure 13: The convergence curve of the surrogate objective $f(\mathbf{X}) + 1000\|\min(\mathbf{0}, \mathbf{X})\|_F$ with $\mathbf{X} \in \text{St}(n, r)$ for solving the nonnegative PCA problem with $r = 40$.

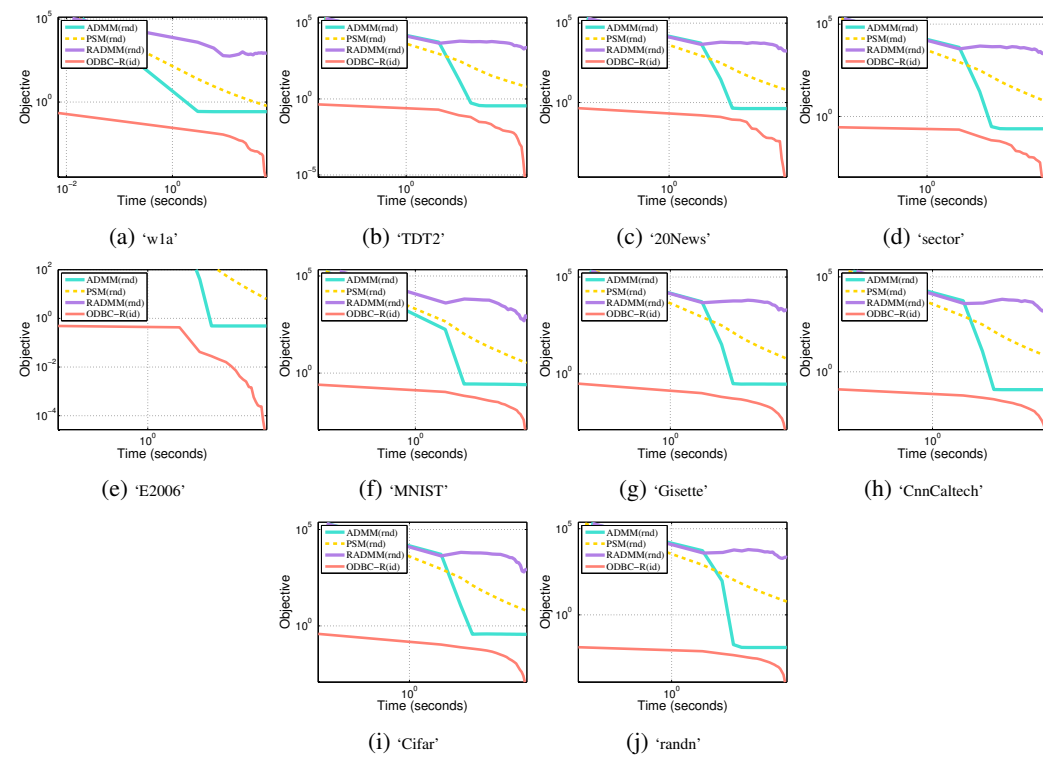


Figure 14: The convergence curve of the surrogate objective $f(\mathbf{X}) + 1000\|\min(\mathbf{0}, \mathbf{X})\|_F$ with $\mathbf{X} \in \text{St}(n, r)$ for solving the nonnegative PCA problem with $r = 80$.